RETINAL ELECTROPHYSIOLOGICAL CHARACTERISTICS OF THE MYOPIC EYE

HO WING CHEUNG

Ph.D

The Hong Kong Polytechnic University

2012

The Hong Kong Polytechnic University

School of Optometry

Retinal Electrophysiological Characteristics of the Myopic Eye

Ho Wing Cheung

A thesis submitted in partial fulfilment of the requirements for the Degree of Doctor of Philosophy

March 2012

CERTIFICATE OF ORIGINALITY

I hereby declare that this thesis is my own work and that, to the best of my knowledge and belief, it reproduces no material previously published or written, nor material that has been accepted for the award of any other degree or diploma, except where due acknowledgement has been made in the text.

_____ (Signed)

HO WING CHEUNG (Name of student)

ABSTRACT

Introduction

Myopia is a common refractive error in the Chinese population. About 50% of the children in Hong Kong are myopic. Anatomically, myopia is usually characterized by an increase in axial length of the eyeball, leading to an optical focus in front of the retina. Although myopia can be simply corrected by optical aids to solve the vision problem, the elongated eyeball has been found to influence the retinal structure and physiology. Clinically, high myopes are at greater risk of developing retino-choroidal degeneration.

Numerous studies have demonstrated reduced and delayed multifocal electroretinogram (mfERG) response in myopic adults. About 40% delayed mfERG response in myopic adults has been attributed to the effect of both refractive error and axial length, and the remaining variance of implicit time has been proposed to be related to attenuation of inner retinal function.

In contrast, the mfERG response in myopic children is only delayed without significant change in amplitude. The reasons of underlying difference in retinal function between children and adults with myopia are still not clear.

It has been shown that the retina can detect defocus signals locally in chicks. Inducing optical defocus in different retinal regions has profound effects on the compensatory response of the whole globe. However, there is still a lack of knowledge on the regional retinal activity in the presence of positive and negative optical defocus.

In this study, we aimed to investigate the retinal function in myopic eyes of both children and young adults. In addition, we also studied the changes of retinal activity to the defocus signals in different regions.

Objectives:

1. To investigate the changes in adaptive circuitry of the inner retina in myopic adults by using the global flash mfERG at different contrast levels (Experiment 1).
2. To compare the retinal functions of myopic children versus young adults using global flash mfERG (Experiment 2).
3. To examine the retinal electrophysiological changes during myopia progression over a 1-year period in children (Experiment 3).
4. To study the effect of positive and negative optical defocus on changes of electrical response as a function of retinal region in adults (Experiment 4).

Methods

The mfERG measured with conventional stimulation mainly reflects the activity of the outer retina. The global flash mfERG, which incorporates the global flash screen response within conventional stimulation, can enhance inner retinal activity, in addition to outer retinal activity. So, this special paradigm of mfERG recording was used in this study. There are two components, the direct component (DC) and the induced component (IC), which reflect the activity from outer retina and inner retina respectively, recorded in the global flash mfERG paradigm.

In Experiment 1, fifty-four adults (aged from 19 to 29 years) with various magnitudes of refractive error received the global flash mfERG at different levels of contrast, i.e. 29%, 49%, 65% and 96%. Cycloplegic subjective refraction and axial length were measured. Hierarchical multiple regression models were used to evaluate the effect of refractive error and the combined effects of refractive error and axial length on the mfERG responses.

In Experiment 2, fifty-two children (aged from 9 to 14 years) and nineteen young adults (aged from 21 to 28 years) with refractive errors ranging from plano to -5.50 D were recruited for the global flash mfERG at both 49% and 96% contrasts. Refraction and axial length were measured. The analyses were the

same as for Experiment 1.

In Experiment 3, twenty-six children (aged from 9 to 13 years) received the global flash mfERG at both 49% and 96% contrasts and refraction in two visits 1-year apart. Pearson's correlation was used to study the association between change in refraction and change in mfERG response in different retinal regions over the 1-year period.

In Experiment 4, twenty-three subjects (aged from 19 to 25 years) with normal ocular health were recruited for global flash mfERG measures at 96% contrast under the condition of control (in-focus), positive defocus (+2 D and +4 D) and negative defocus (-2 D and -4 D) conditions. Repeated-measures ANOVA was used to investigate the effect of defocus on the mfERG response in different retinal regions.

Results

In Experiment 1, myopic adults had a significant reduction in the paracentral DC amplitudes for both 29% and 49% contrasts and in the paracentral IC amplitudes at all contrasts measured. The peripheral IC amplitudes for 49% contrast were also reduced. Refractive error explained about 14% and 16% of the reduction in paracentral DC and IC amplitudes respectively, but axial length could not

account for further change in either paracentral DC or IC amplitude in the hierarchical regression models used. Neither refractive error nor axial length contributed to any change in implicit time for either DC or IC response.

In Experiment 2, myopic children had a significant reduction in central DC amplitude at 96% contrast and unaffected IC responses at both contrasts for all regions. In contrast, myopic adults showed a significant reduction in paracentral IC amplitudes at 49% contrast but not at 96% contrast. The DC amplitudes at both contrasts of all regions examined were virtually unaffected. Implicit times for DC and IC responses were unaffected for either group.

In Experiment 3, children with progressing myopia showed significant reduction of central DC and IC amplitudes, and mild attenuation of paracentral DC and IC amplitudes at 49% contrast as myopia progressed.

In Experiment 4, the mfERG responses were found to have more significant changes in the paracentral retinal region than in the central region under defocused conditions. The paracentral DC amplitudes showed a significant reduction under negative defocused conditions. In contrast, the paracentral IC amplitudes showed a significant increment under positive defocused conditions. Interestingly, the central IC response showed significant reduction in amplitude

only to negative defocus, while the response increased in amplitude to positive defocus. However, the DC and IC implicit times were virtually unchanged under defocused conditions.

Conclusions

This study shows that the effect of myopia mainly affected the inner retinal function in myopes. Retinal function was generally unaffected in myopic children, except for the outer retinal function in the central region. As myopia progressed, the inner retinal function from central to paracentral regions was reduced, especially in the central region. The retinal function in myopic adults differed from myopic children in terms of regions and retinal components being affected. The inner retinal function from paracentral to mid-peripheral regions was significantly impaired in myopic adults, whereas the outer retinal function in these regions was only mildly reduced due to myopia. There was also a progressive change of retinal impairment from central to mid-peripheral regions from children to adults with myopia. Moreover, paracentral retina in the human eye reacted more strongly to optical defocus than central retina did; paracentral retina also differentiated the sign of defocus. Therefore, we speculate that the regional deterioration in retinal function in adults with myopia is probably related to the effect of peripheral defocus on the myopic eye growth.

PUBLICATIONS ARISING FROM THE THESIS

1) Ho, W.C., Ng, Y.F., Chu, P.H., Fong, Y.Y., Yip, K.S., Kee, C.S., and Chan, H.H. (2011). Impairment of retinal adaptive circuitry in the myopic eye. *Vision Research*, 51, 367-375.
2) Ho, W.C., Wong, O.Y, Chan, Y.C., Wong, S.W., Kee, C.S., and Chan, H.H. (2012). Sign-dependent changes in retinal electrical activity with positive and negative defocus in the human eye. *Vision Research*, 52, 47-53.
3) Ho, W.C., Kee, C.S., and Chan, H.H. (2012). Myopic children have central reduction in high contrast multifocal ERG response while adults have paracentral reduction in low contrast response. *Investigative Ophthalmology and Visual Science*, 53, 3695-3702.
4) Ho, W.C., Kee, C.S., and Chan, H.H. (2012). Myopia progression in children is linked with reduced foveal function, *Investigative Ophthalmology and Visual Science*, 53, 5320-5325.

Conference Presentations

1) Ho, W.C., Ng, Y.F., Chu, P.H., Fong, Y.Y., Yip, K.S., and Chan, H.H. (2008). Changes of retinal adaptation in myopic eye. XLVI International Society for Clinical Electrophysiology of Vision Symposium. Morgantown, USA. Poster Presentation.
2) Ho, W.C., Wong, O.Y, Chan, Y.C., Wong, S.W., Kee, C.S., and Chan, H.H. (2009). Regional changes of electrical activity in human retina in response to optical defocus. The 17th Asia Pacific Optometric Congress. Hong Kong SAR, China. Oral Presentation.
3) Ho, W.C., Kee, C.S., and Chan, H.H. (2010). Characteristics of multifocal electroretinogram (mfERG) in children with low to moderate myopia. The 13th International Myopia Conference. Tubingen, German. Poster Presentation.
4) Ho, W.C., Kee, C.S., and Chan, H. H. (2011). Myopia progression in children is associated with regional changes in retinal function: a multifocal electroretinogram study. The Asia-Pacific Conference on Vision 2011. Hong Kong SAR, China. Oral Presentation.

ACKNOWLEDGEMENTS

I would like to thank

my chief supervisor, Dr. Henry Chan, for his professional guidance and advice on my research work, and his initiation of my research interest.

my co-supervisor, Dr. Chea-su Kee, for his valuable comments on my work and his guidance on all my manuscripts with great patience.

Prof. Brian Brown, for giving me so many critical comments on all my manuscripts and thesis.

my labmates, Dr. Patrick Chu and Dr. Forrest Ng for teaching me lots of electrophysiological technique and for their useful suggestions on my work.

my colleague Dr. Gordon Tang, for assisting me with statistics.

all research students and research staff at the School of Optometry giving me such a warm and wonderful environment, and also for their emotional support and encouragement.

my parents and family members for their support.

TABLE OF CONTENTS

ABBREVIATIONS

Adjusted R^2	Adjusted coefficient of determination
AL	Axial length
ANOVA	Analysis of variance
D	Dioptre
DC	Direct component
DS	Dioptre sphere
DTL	Dawson-Trick-Litzkow
ERG	Electroretinogram
GABA	Gamma-aminobutyric acid
IC	Induced component
m-sequence	"Maximum-length" sequence
mfERG	Multifocal electroretinogram
N1	First negative trough response in conventional mfERG
N2	Second negative trough response in conventional mfERG
NMDA	N-methyl-D-aspartic acid
P1	First positive peak response in conventional mfERG
r	Pearson's correlation coefficient
R^2	Coefficient of determination
RE	Refractive error
SD	Standard deviation
SE	Spherical-equivalent
SEM	Standard error of the mean
SPSS	Statistical Package for the Social Sciences
VERIS	Visual Evoked Response Imaging System

LIST OF FIGURES

Chapter 2

Chapter 3

inferior nasal retina.

Figure B.2. The percentage change (mean ± SEM) in (a) DC and (b) IC amplitudes with respect to control condition at different retinal quadrants, for various defocused conditions. Those marked with an asterisk "*" are statistically different from the in-focus (0 D) condition. The error bars indicate the standard error of the mean (SEM).

Figure B.3. The percentage change (mean ± SEM) in (a) DC and (b) IC implicit times with respect to control condition at different retinal quadrants, for various defocused conditions. Those marked with an asterisk "*" are statistically different from the in-focus (0 D) condition. The error bars indicate the standard error of the mean (SEM).

LIST OF TABLES

Chapter 6

Chapter 7

PART I – INTRODUCTION AND LITERATURE REVIEW

Chapter 1 - Introduction

About 50% of the Hong Kong children (aged from 6 to 12 years) are myopic (Lam et al., 2012). Although there has been no significant change in prevalence of myopia in Hong Kong children over the past two decades (Lam et al., 2012), the prevalence of myopia in Hong Kong children is much higher than that in Caucasian populations (He et al., 2004; Ip et al., 2008; Jobke et al., 2008; Lam et al., 2012; Ostadimoghaddam et al., 2012; Rezvan et al., 2012; Rudnicka et al., 2010; Zadnik, 1997). The possibility of a genetic influence on the generation of myopia cannot be ignored (Chew and Ritch, 1994; Liang et al., 2004; Pacella et al., 1999; Yap et al., 1993), especially among those of Chinese ethnicity (Lam et al., 1994). Rose et al. (2001) reported that hundreds of millions dollars has been spent on optical corrections as well as medical treatment for high myopes, making it one of the major public health problems in Australia.

Axial elongation is the major change in ocular parameter during myopia development (Lam et al., 1999; Lin et al., 1996). This structural alteration causes retinal thinning in the myopic eye, affecting the macular region (Lam et al., 2007; Lim et al., 2005; Luo et al., 2006) and mid-peripheral retina up to an eccentricity of about 40° (Cheng et al., 2010). Clinically, it is quite common to find retinal lesions such as lattice degeneration, macular holes, retinal tears and posterior

vitreous detachment in high myopes (Akiba, 1993; Morita et al., 1995; Pierro et al., 1992). Other clinical signs, for example, lacquer crack, Förster-Fuch's spots, posterior staphyloma and choroidal neovascularization are sometimes found in degenerative myopes (Baker and Pruett, 2004).

In addition to retinal thinning, retinal physiology and function are also altered. Clinically, the myopic eye usually shows poorer visual performance including deficits in contrast sensitivity (Liou and Chiu, 2001), visual acuity (Subbaram and Bullimore, 2002), peripheral visual acuity (Chui et al., 2005), visual sensitivity (Aung et al., 2001; Jaworski et al., 2006; Rudnicka and Edgar, 1995; Rudnicka and Edgar, 1996), dark adaptation and colour vision (Mantyjarvi and Tuppurainen, 1995), as well as critical flicker frequency and modulation transfer function (Chen et al., 2000). Hence, investigating the effect of myopia on retinal function and physiology can improve our understanding and management of myopia development.

Chapter 2 - Fundamentals of the electroretinogram

The electroretinogram (ERG) is a recording of the retinal electrical signals in response to a flash of light received at the retina. The retinal electrical activity can be recorded indirectly by placing a corneal electrode (as the active electrode) and another electrode at the ipsilateral outer canthus of the tested eye (as the reference electrode). A third electrode can be placed at either the forehead or earlobe (as the ground electrode) to minimize and stabilize the influence of background noise. Usually, the retinal signal is measured with a dilated pupil.

2.1. Full-field (Ganzfeld) electroretinogram

Different protocols can be used to trigger the ERG responses from different types of retinal cells by presenting appropriate diffuse light stimulation protocols; these have been documented in the International Society for Clinical Electrophysiology of Vision guidelines (Marmor et al., 2009). Three scotopic responses and two photopic responses are suggested in the guidelines, including scotopic rod responses, scotopic combined rod-cone responses, scotopic oscillatory potentials, cone single-flash responses and cone 30-Hz flicker responses. In addition, there is a suggested high-intensity ERG under scotopic conditions.

2.1.1. Origins of different ERG responses

2.1.1.1. Scotopic rod response

This response is triggered by a very dim white flash of 0.01 cds/m^2, with a flash interval of at least 2 seconds and involves mainly rod responses (Marmor et al., 2009). The a-wave, which is generated from rod photoreceptors, is barely visible as the response is triggered with a very dim stimulus, and the b-wave represents the activity from rod-bipolar cells (Lam, 2005).

2.1.1.2. Scotopic combined rod-cone response

The stimulus is produced by a white flash of 3.0 cds/m^2, with a minimum flash interval of 10 seconds (Marmor et al., 2009). This response consists of a- and b-waves. The a-wave originates from the activity of photoreceptors (Penn and Hagins, 1969) and the b-wave activity arises from bipolar cells and Müller cells (Gurevich and Slaughter, 1993; Miller and Dowling, 1970; Newman and Odette, 1984; Stockton and Slaughter, 1989).

2.1.1.3. Scotopic oscillatory potentials

The stimulus is the same as that used for the scotopic combined rod-cone responses recording (Marmor et al., 2009). The bandpass was set from 75 to 300

Hz (Marmor et al., 2009) to isolate the responses. The oscillatory potentials consist of several oscillatory wavelets superimposed on the ascending phase of the b-wave. It is believed that the cellular origins of these oscillatory wavelets are the bipolar cells and amacrine cells (Wachtmeister, 1998).

2.1.1.4. Cone single-flash response

The stimulus is made up of a white light of 3.0 cds/m^2, with a minimum flash interval of 0.5 second; and the background luminance is set at 30 cd/m^2 on the surface of the stimulus bowl (Marmor et al., 2009). This response contains a- and b-waves. Under a rod-suppressing background light, the a-wave is mainly generated from cone photoreceptors (Hood and Birch, 1993; Hood and Birch, 1995) and the b-wave originates from activity of ON- and OFF-bipolar cells and horizontal cells (Sieving et al., 1994).

2.1.1.5. Cone 30-Hz flicker response

The stimulus, which is set at 3.0 cds/m^2, presents at about 30 flickering per second. This response is a series of several repetitive b-waves. The response primarily represents the activity from postreceptoral level(s) including ON- and OFF-bipolar cells (Kondo and Sieving, 2002).

2.2. Multifocal electroretinogram (mfERG)

Full-field ERG measures the electrical signals from the whole retina in response to a light stimulus. The weakness of the full-field ERG is that it cannot provide topographical information regarding the functional integrity of the retina and cannot detect subtle functional defects. The response is dominated by the peripheral retina due to its predominance of retinal cells (Hood et al., 1997). The focal ERG can examine the local response of a particular retinal locus by varying the size and location of the stimulating beam. It provides a retinal response from different locations but requires multiple measurements. It is less effective in terms of clinical use, if measurement of multiple retinal loci is needed. It is usually limited to measurement of the macular response.

2.2.1. Basic concepts

The multifocal electroretinogram (mfERG) examines the retinal response of multiple loci within a short period of time (usually 5 to 10 minutes), which is similar to multiple measurements of focal ERGs. The mfERG measurement provides topographical responses of the retina (Sutter and Tran, 1992). The stimulus is usually made up of a 61- or 103- (Figure 2.1) scaled hexagonal array. The extent of retinal area being tested depends on the size of the stimulator

(monitor) used and the viewing distance between stimulator and subject. The scaling of hexagons follows the retinal magnification and is used to maintain similar signal-to-noise ratios across the whole stimulated area (Sutter and Tran, 1992).

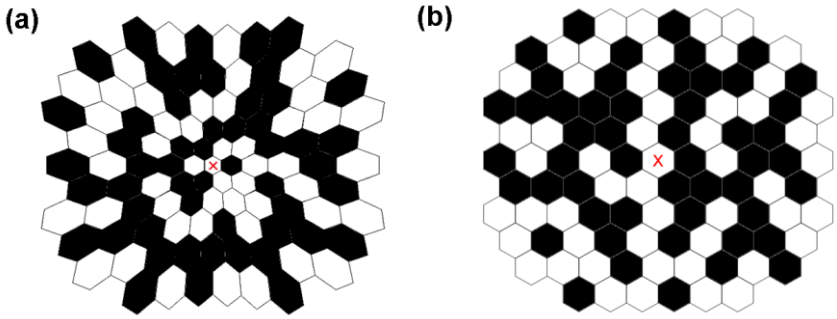

Figure 2.1. A typical pattern of mfERG stimulus consists of 103 (a) scaled (left) and (b) non-scaled (right) hexagonal array.

The mfERG uses a multi-input stimulation protocol to examine the response of multiple retinal loci simultaneously. For each hexagonal area, the stimulus is temporally flickered between dark (no flash) and bright (flash) presentations, according to a pseudo-random binary m-sequence stimulation (or "maximum-length" sequence) (Sutter, 2000; Sutter and Tran, 1992), in which each region has equal chance of receiving either a bright or dark presentation at each frame. In fact, the stimulus sequence of each hexagon is the same according to the selected m-sequence but is lagged by different amounts of time in the series compared with the others (Sutter, 2000; Sutter and Tran, 1992). The time

lag makes the sequence of stimulation of each region independent of each other, so as to facilitate the derivation of each local response through cross-correlation in the multifocal ERG measurement (Sutter and Tran, 1992). The topographical response can be presented as a ring-averaged response (Figure 2.2a), traces array (Figure 2.2b), and three-dimensional plot (Figure 2.2c).

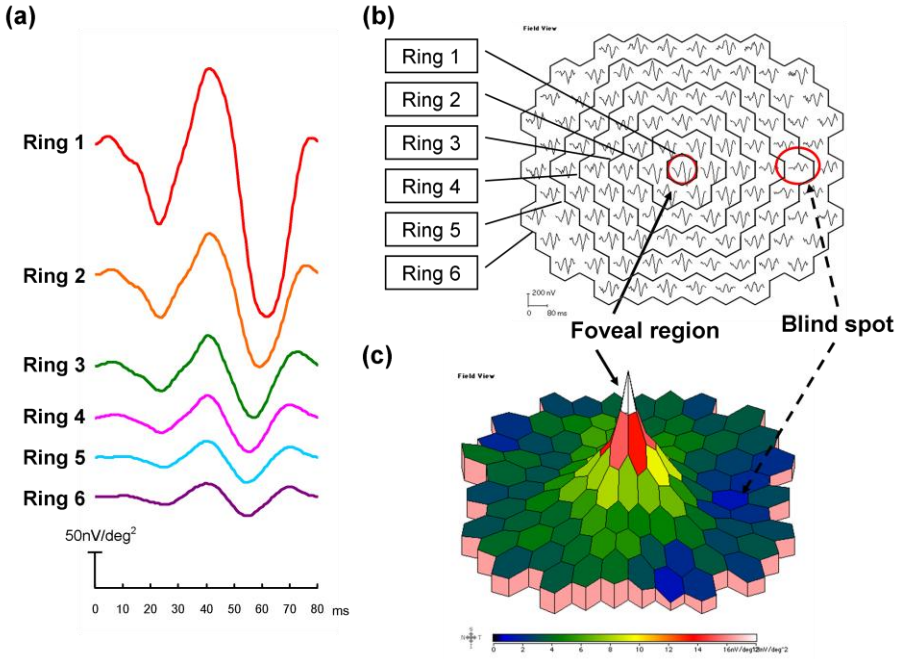

Figure 2.2. Topographical presentation of the retinal response by using (a) a ring-averaged response from central (Ring 1) to mid-peripheral (Ring 6) regions, (b) traces array and (c) three-dimensional plot.

2.2.2. Derivation of first and second order kernels

Each local mfERG response is a mathematical computation of the response through cross-correlation and so is not a real biological response from retinal cells. The first order kernel is derived by averaging all the responses to dark stimulation,

and subtracted this from the average of all the responses to bright stimulation, within the m-sequence stimulations (Sutter, 2000) (Figure 2.3a). In short, the first order kernel represents the averaged response of the retina to a light stimulus. On the other hand, the second order kernel represents the interactive response between the preceding frame and current frame and thus reflects the adaptive response to consecutive stimulation (Sutter, 2000). The first slice of the second order kernel, is derived by subtracting the response with change of stimuli between two frames (i.e. either bright-to-dark or dark-to-bright) from the response without change of stimuli (i.e. bright-to-bright or dark-to-dark). This represents the response due to interaction between the previous frame and the current frame (Figure 2.3b).

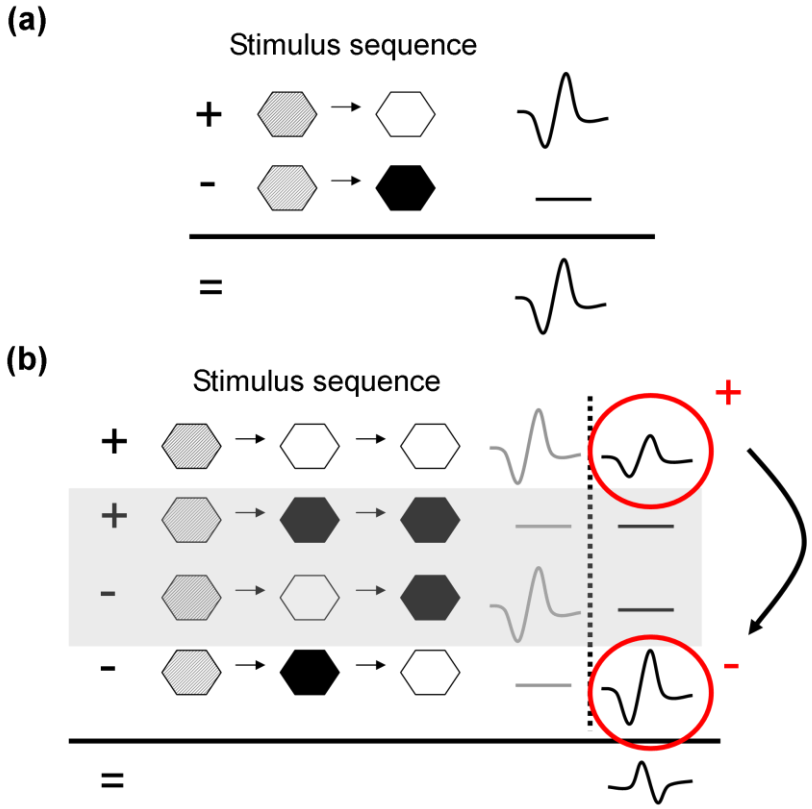

Figure 2.3. A schematic diagram illustrates the mathematical derivation of the first and second order kernels. The white and dark hexagons represent the bright (flash) and dark (no flash) presentations respectively. The hexagon shaded in grey represents the frame not under consideration for the computation of the response. (a) The first order kernel is obtained by averaging the responses to all dark presentations, and subtracting the averaged responses from all bright presentations within the m-sequence. (b) The first slice of the second order kernel is achieved by adding all the responses with different stimuli between preceding and current frames (i.e. either bright-to-dark or dark-to-bright), and subtracted from all the responses with the same stimulus between two continuous frames (i.e. bright-to-bright or dark-to-dark) (Figure is adapted from Sutter (2000) with modification).

2.2.3. Response density

Since the pattern of mfERG stimulation (as it is usually used) contains hexagons of different sizes (scaled hexagonal array), the strength of the response will definitely be affected by the size of the stimulus. Therefore, the response is

usually expressed as response (amplitude) density, which is equal to the response magnitude divided by the area (i.e. response amplitude/stimulating area). This represents the response amplitude per unit area for easy comparison across different parts of retina. The unit is nV/deg^2.

2.2.4. Origins of first order kernel mfERG components: N1, P1 and N2 responses

The appearance of a typical first order kernel response consists of an initial negative trough (N1), a second positive peak (P1), and a negative trough (N2) (Figure 2.4), which is similar to the photopic cone single-flash response in full-field ERG waveform. It has been thought that the cellular origins of first order kernel mfERG response resembled the origins of photopic cone single-flash ERG response (Hood et al., 1997).

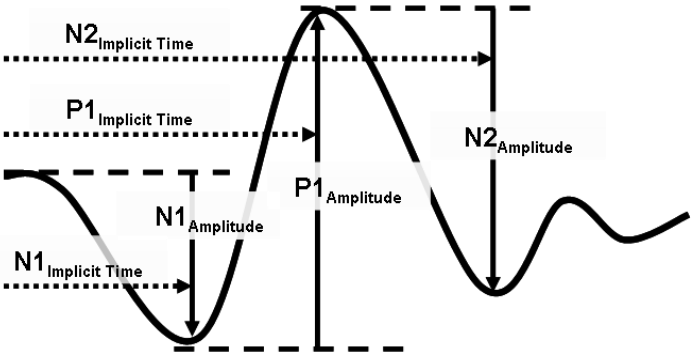

Figure 2.4. A schematic diagram showing a typical first order kernel mfERG response. The amplitude of individual component is measured using peak-to-peak measurement and the implicit time is the time taken from the onset of stimulus to its peak response.

The understanding of the cellular contribution to each component of mfERG responses is enhanced by sequential removal of the responses of retinal cells using a pharmaceutical dissection technique in studies on animals (Hood, 2000; Hood et al., 2002; Ng et al., 2008a; Ng et al., 2008b). The first order kernel response involves major contribution from outer retinal activity and minor contribution from inner retinal activity (Hood, 2000; Hood et al., 2002; Ng et al., 2008a; Ng et al., 2008b). Specifically, the N1 response originates from both cone photoreceptors and OFF-bipolar cells (Hood, 2000; Hood et al., 2002; Ng et al., 2008a; Ng et al., 2008b). However, the central (visual angle less than 13°) and peripheral (visual angle greater than 13°) regions of the N1 response are dominated by cone and OFF-bipolar cells respectively in the monkey eye (Hood, 2000; Hood et al., 2002). For both central and peripheral regions, the P1 response, on the other hand, originates from ON-bipolar cells (Hood, 2000; Hood et al., 2002; Ng et al., 2008a; Ng et al., 2008b). The N2 response consists of both ON- and OFF-bipolar cells and the N-methyl-D-aspartic acid (NMDA) sensitive retinal components such as amacrine cells in pig eye (Ng et al., 2008a; Ng et al., 2008b).

In the human, eye diseases affecting the outer retina, such as central serous chorioretinopathy (Bearse et al., 1995), retinitis pigmentosa (Chan and Brown,

1998; Seeliger et al., 1998), Stargardt's disease (Kretschmann et al., 1996) and choroidal atrophy (Kretschmann et al., 1996) also produce a reduced first order kernel response.

2.2.5. Origins of second order kernel mfERG components

The second order kernel represents the temporal adaptive response of retina. There are some discrepancies in the waveform of the second order kernel response between humans and animals (Chan and Mohidin, 2003; Hood, 2000; Hood et al., 2002; Ng et al., 2008a; Ng et al., 2008b). In general, the second order kernel response involves major contributions from inner retinal cells and small contributions from outer retinal cells such as ON- and OFF-bipolar cells (Hood, 2000; Hood et al., 2002; Ng et al., 2008a; Ng et al., 2008b).

Chapter 3 - Retinal electrophysiological characteristics of the myopic eye

3.1. Full-field ERG response

The retinal function of the myopic eye was first studied using the full-field electroretinogram in 1966. It is not unexpected that the a- and b-waves of the scotopic combined rod-cone response were reduced in degenerative and pathological myopes (Blach et al., 1966). However, the ERG response was also reduced in the myopic eye, even in the absence of any signs of pathological myopia. The b-wave of the scotopic rod response, and both a- and b-waves of scotopic combined rod-cone response and photopic cone single-flash response were reduced with increasing refractive error but the implicit times of these components were not significantly affected (Chen et al., 1992; Perlman et al., 1984; Westall et al., 2001). Hence, the reduced ERG responses under these stimulation protocols suggest that the retinal function in myopes, most likely at outer retinal level, was weaker than in non-myopes. Moreover, the oscillatory potentials in myopes were also reduced, indicating a functional deterioration of the interplexiform layer (Westall et al., 2001).

3.2. mfERG response

3.2.1. First order kernel

There are several studies investigating the mfERG responses in the myopic eye. All of these studies showed that the N1, P1 and N2 responses were reduced and delayed in the myopic eye within about central 40° of retina, even if the refractive errors of the subjects were corrected during mfERG measurement (Chan and Mohidin, 2003; Chen et al., 2006a; Kawabata and Adachi-Usami, 1997; Luu et al., 2006). On regional analysis of response topography, most of the studies generally supported the idea that the functional loss in the paracentral retina (eccentricities from ~ 9 to 13°) was greater than that in the central retina (Chan and Mohidin, 2003; Chen et al., 2006a; Kawabata and Adachi-Usami, 1997). However, a single study suggested a uniform reduction of retinal function within the central 40° of retina (Luu et al., 2006). Interestingly, the mfERG responses, including both amplitudes and implicit times of the N1, P1 and N2 responses, were significantly affected by magnitude of refractive error in adults but were virtually unaffected in children (Luu et al., 2006). These results imply that there may be some age-related changes in retinal function between children and adults with myopia.

3.2.2. Second order kernel

Chan and Mohidin (2003) explored the inner retinal function in myopes by analyzing the second order kernel mfERG responses. They found that the n1p1 response amplitude at retinal eccentricities from 5 to 13° and from 18 to 25°, and the n2p2 amplitude at retinal eccentricities from 5 to 25°, decreased linearly with increasing axial length. The amplitude was reduced by about 5 to 10% per millimeter elongation of axial length. The time domain of the second order kernel response, however, was generally unaffected.

3.2.2.1. Possible factors affecting the mfERG response measured in the myopic eye as a result of enlarged eyeball

All of these studies have excluded the pathological form of myopia as a potential confounding factor for the attenuated mfERG response (Chan and Mohidin, 2003; Chen et al., 2006a; Kawabata and Adachi-Usami, 1997; Luu et al., 2006). However, it has been argued that the reduction in mfERG response in the myopic eye is due to changes in physiological factors such as ocular resistance, cell density, or optical factors such as retinal illuminance, retinal image size (induced by corrective lenses) and peripheral defocus.

3.2.2.1.1. Ocular resistance

Perlman and his-colleagues (1984) proposed that the reduction in ERG amplitude was associated with an increase in ocular resistance due to the enlarged eyeball in the myopic eye. However, Chen and her co-workers (1992) rejected this resistance theory because it disobeys Ohm's law.

According to Ohm's law,

$$V = IR$$

where V, I and R represent the ERG amplitude, strength of electrical signal and ocular resistance respectively.

They explained that the increase in ocular resistance should lead to an increase in the ERG response measured, which is the product of the retinal electrical signals and the ocular resistance (between active and reference electrode). However, the ERG response amplitude was reduced in the myopic eye. Therefore, the increase in ocular resistance could not account for the attenuated response in myopes.

3.2.2.1.2. Reduced cell density

High myopia is linked to decreased cell density in both psychophysical (Chui et al., 2005; Coletta and Watson, 2006) and histological studies (Beresford et al., 1998). The effect of axial elongation on retinal cell density varies with

eccentricity, in which the cell density in myopes was reduced more at the central region, especially the fovea, than at the peripheral region (Chui et al., 2008; Chui et al., 2005). The mfERG response, presented as response density, represents the retinal electrical signal from a particular area. The coarse distribution of photoreceptors in the myopic eye may have considerable effect on the measured mfERG response due to the decline in cell density.

Chen and her co-workers (1992) have proposed the “low responsivity” hypothesis and “stretched retina” hypotheses. The low responsivity hypothesis assumes a decline in function of the retinal elements, but not increased spacing between photoreceptors, and this leads to a lower saturated amplitude. Hence, the sensitivity remained unchanged but the saturated amplitude was reduced. The “stretched retina” hypothesis stated that the number of photoreceptors per unit area (cell density) decreased and the spacing between photoreceptors increased as axial length increased. The chance of a photon stimulating the photoreceptors, therefore, reduced. In other words, sensitivity decreased while the saturated amplitude remained the same. Consequently, the stimulus intensity needed to achieve the same amplitude of ERG response as in the emmetropic eye should be increased in the myopic eye.

Kawabata and Adachi-Usami (1997) investigated the stimulus-response

function of the mfERG responses in low (Range of refractive errors: +1.00 to -3.00D; mean = -0.78 ± 0.89 D) and high myopes (Range of refractive errors: ≥ -6.25D; mean = -10.33 ± 3.38 D) with best corrected visual acuity of 1.0, normal colour vision, clear ocular media and normal fundus, except mild myopic cresent around optic disc. High myopes showed much lower saturated mfERG response amplitudes. On the other hand, the stimulus response curves of low myopes and high myopes were extracted and re-analyzed, according to the strategy of Chen et al. (1992). The sensitivity (log σ, defined as intensity of stimulus to produce 50% of saturated response) for both the N1 and P1 responses of low and high myopic groups were about 1.6 td·s (Figure 3.1). These findings indicate that the sensitivity was almost unchanged but the saturated amplitude was reduced in high myopes. Hence, the reduced mfERG response in high myopes was more likely to be due to a functional change of retinal cells, rather than increased spacing between cells (cell density).

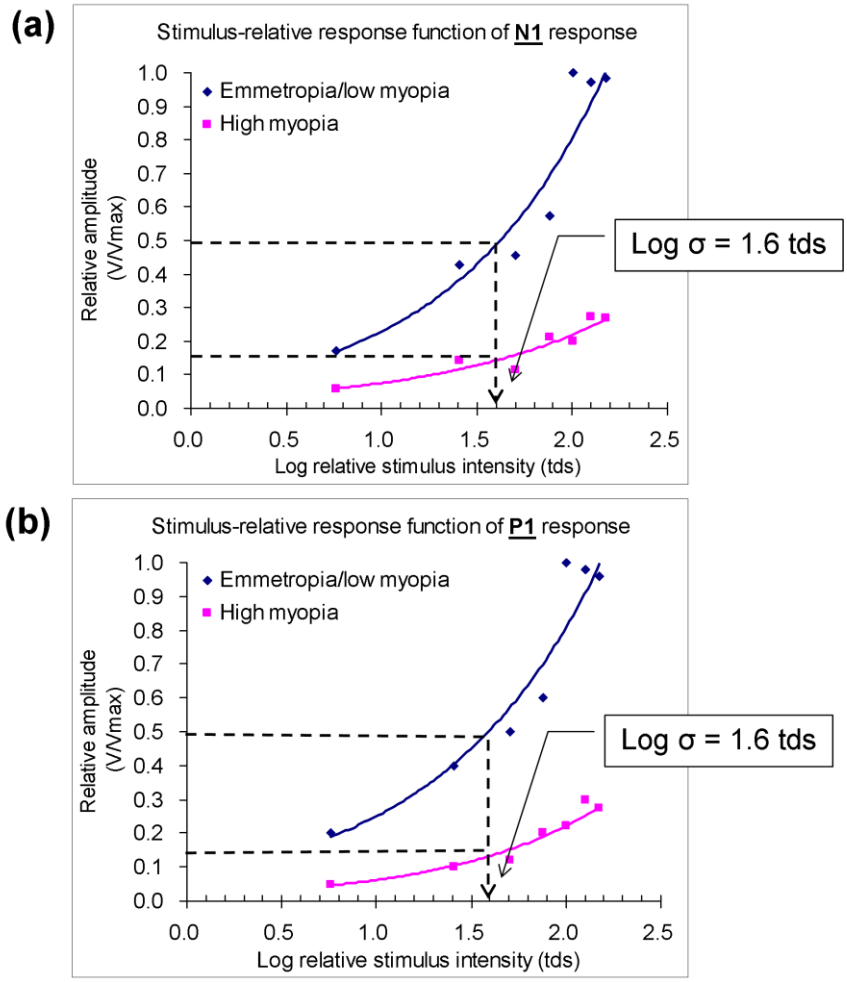

Figure 3.1. The stimulus-response functions of the (a) N1 and (b) P1 amplitudes of mfERG response in low and high myopes. The second order best-fit line shows the exponential relationship between (log) stimulus intensity and relative response amplitude ($R^2 \geq 0.90$ for all trend lines). Sensitivity (log σ, defined as the 50% of its saturated response) for both N1 and P1 responses are shown (Data from Kawabata and Adachi-Usami (1997) was adapted and re-analyzed).

3.2.2.1.3. Retinal illuminance

The mfERG response density represents the response per unit area of retina (Sutter and Tran, 1992). The light flux reached per unit retinal area is reduced in the myopic eye due to the elongated eyeball. Kawabata and Adachi-Usami (1997) examined the stimulus-response curve of low and high myopes. They found that

the low myopic group showed rapid increase in response amplitude with increasing luminance (intensity) of the mfERG stimulus. In contrast, the high myopic group only demonstrated a subtle increment in amplitude, even though there was tremendous increase in luminance of the stimulus. In addition, the mfERG response of both low and high myopic groups saturated at a certain luminance level. However, high myopes saturated at much lower amplitude compared to low myopes. If the attenuated response in high myopes was related to the decreased light flux reached per unit area in the enlarged eyeball, the increase in luminance of the stimulus should trigger a stronger response. According to the study of Kawabata and Adachi-Usami (1997), the mean P1 response amplitude across six concentric rings in low and high myopic groups, with corresponding axial length of 24.51 mm and 27.45 mm, was 27.04 and 11.17 nV/deg^2 respectively. The retinal surface area in high myopes increases by 25% and then the light energy per unit retinal area is decreased by 20%. Brown and Yap (1996) found a minimum of 0.4 log unit (~ 60%) reduction in luminance of the stimulus to produce a significant reduction in mfERG response amplitude. Due to subtle change in luminance, the reduced mfERG response in high myopes may be associated with impaired retinal function, instead of a reduction of light energy per unit area in the enlarged eyeball of the myopic eye.

3.2.2.1.4. Change of retinal image size

The use of spectacle lenses to compensate for the refractive error causes different retinal image size among myopes with various magnitudes of refractive error. The hexagonal array of the mfERG stimulus projected onto the retina in myopes is smaller than the uncorrected image due to minification of the image caused by the divergent lens, and this could lead to a reduction in mfERG response in myopes. According to Knapp's law, the image size of the stimulus pattern in high myopes is similar to that of emmetropes if the corrective lens is placed at the anterior focal plane of the eye. There are only two studies that have considered retinal image size (Chan and Mohidin, 2003; Kawabata and Adachi-Usami, 1997) while other studies have not taken the effect of spectacle magnification into consideration. The mfERG amplitude in the myopic eye was still reduced even the retinal image size was maintained among all myopic subjects by placing the corrective lens at the anterior focal plane of the eye (Chan and Mohidin, 2003; Kawabata and Adachi-Usami, 1997). These results suggest that the reduced mfERG response in highly myopic eyes, whose refractive error was as high as -9 D, was not likely to be due to the minified image of the mfERG stimulus.

3.2.2.1.5. Peripheral defocus at mid-peripheral retina

Myopic eyes are more frequently prolate in shape (Deller et al., 1947). It has been found that the peripheral retina at 30° eccentricity in the myopic eye suffers from relative hyperopic refraction (spherical-equivalent) (SE) of about 2 D with the correction of full distant prescription (Lin et al., 2010). The mfERG response in the mid-peripheral retina (eccentricity of 25°) is not affected by up to 3 D of optical defocus (Chan and Siu, 2003). Some researchers have reported that the mfERG response at 25° peripheral retina does not change significantly even with 6 D of optical defocus (Palmowski et al., 1999). Thus, it seems unlikely that optical defocus would contribute to the change of paracentral to mid-peripheral mfERG responses in the myopic eye because the mfERG responses in these regions seem relatively insensitive to optical defocus.

3.2.2.2. Origins of reduced and delayed first order kernel mfERG responses

The change in optical factors or uncorrected peripheral refractive error in myopic eye may explain for subtle reduction in mfERG response. We believed that the attenuated and delayed mfERG response in the adult myopes was probably due to the intrinsic physiological change in retina.

Kawabata and Adachi-Usami (1997) explained that the attenuation of mfERG response might be attributable to the functional losses of cones in the myopic eye. However, their explanation assumes that the origins of the mfERG response are similar to that of the full-field ERG (Hood et al., 1997). Recent studies have clarified that the N1 and P1 components in the mfERG response originate from the activity of photoreceptors and OFF-bipolar cells, and ON-bipolar cells respectively (Hood, 2000; Hood et al., 2002; Ng et al., 2008a), which are different from the sources of a- and b-waves in photopic cone single-flash response in the full-field ERG. Therefore, the delayed and reduced N1 and P1 responses may not only relate to impaired cone function but also involve postreceptoral cells.

Chen and her co-workers (2006a) have investigated the effect of myopia on the mfERG in detail. They studied the effects of both axial length and refractive error on mfERG, while the previous studies had only studied either one of these two factors (Chan and Mohidin, 2003; Kawabata and Adachi-Usami, 1997; Luu et al., 2006). After adjusting the variance of axial length on mfERG response, the mfERG response amplitude did not show significant difference between emmetropes and myopes. However, the P1 implicit time was significantly delayed by about 3 ms in myopes, in which axial length and refractive error

accounted for, respectively, 15% and 27% of the variance in implicit time. According to Hood (2000), the delayed mfERG response with normal amplitude was related to impairment of the inner plexiform layer. Chen and her colleagues (2006a) proposed that the remaining variance of delayed response could be the cause of impaired retinal function at the inner plexiform layer.

3.2.2.3. Origins of reduced second order kernel mfERG responses

The second order kernel response, which represents the temporal interaction (adaptation) between continuous flashes, reflects activity from inner retina layers (Hood, 2000; Hood et al., 2002; Ng et al., 2008a; Ng et al., 2008b). The reduction in the first slice of the second order kernel response in the myopic eye indicates impaired temporal adaptive function in the neurons of inner retinal layers. Thus, the reduction of the second order kernel, as shown in Chan and Mohidin (2003)'s study, supports the hypothesis from Chen and her colleagues (2006a), that the inner retinal function is impaired in the myopic eye.

3.3. Characteristics of mfERG response in progressing myopes

Study of the mfERG response in progressing myopes gives information regarding the retinal regions and components that are primarily affected during

myopia development. However, there is no longitudinal study investigating the retinal functional changes during myopia progression. There are only two studies trying to characterize the mfERG response in adults with progressing myopia (Chen et al., 2006a; Chen et al., 2006b). The myopia progression was obtained by comparing the past clinical record of the subjects and the refractive status on the date of experiment. Progressing myopes, whose myopia increased by -0.50 D or more over past 2-year period showed smaller P1 amplitude of the mfERG response in the paracentral region (eccentricities from 3.8 to 15.0°) than stable myopes in adults (Chen et al., 2006a). Similarly, progressing myopes also had shorter implicit time of oscillatory potentials (measured with slow flash paradigm of mfERG) in the paracentral region (eccentricities from 4.5 to 22.0°) than stable myopes (Chen et al., 2006b). Regardless of the mfERG stimulation protocols used, progressing myopes showed altered mfERG responses in the paracentral region, in agreement with previous cross-sectional studies showing significant reduction of mfERG response in paracentral region of the myopic eye (Chan and Mohidin, 2003; Chen et al., 2006a; Kawabata and Adachi-Usami, 1997).

Contradictory findings were reported by Luu and his co-workers (2007) when they attempted to characterize the retinal electrophysiology in a prospective study. They found that the P1 response of the foveal region

(eccentricities within 2.5°) was reduced more in children who had greater myopia progression (Luu et al., 2007). Their study gives new insights into the early retinal electrophysiological changes which occur prior to myopia progression.

The discrepancy in findings may be related to differences in study design and subject selection. Chen and her co-workers (2006a; 2006b) classified the subjects into either stable or progressing myopes according to pre-existing clinical records. The result of their studies showed the functional loss after myopia progressed. However, the study of Luu et al. (2007) examined retinal function before myopia progressed. In addition, the discrepancy in findings may be related to the intrinsic characteristics in the retinal physiology between adults and children with myopia, as demonstrated in another study carried out by Luu and his colleagues (2006). Nevertheless, it is still necessary to investigate the underlying physiological changes in the retina during myopia development from childhood to adulthood, in order to understand the underlying cause of the regional difference in functional integrity between myopic children and adults.

Chapter 4 - Eye growth process in human and animals

4.1. Emmetropization during the postnatal period

Human infants are frequently born with high magnitudes of hyperopia and astigmatism. These magnitudes gradually reduce during the first few years of postnatal development, a process commonly referred to as “emmetropization” (Mayer et al., 2001). Although it has also been found that this process exists in a variety of animal species such as chicks (Wallman et al., 1981), guinea pigs (Howlett and McFadden, 2007), tree shrews (Norton and McBrien, 1992) and monkeys (Bradley et al., 1999; Smith et al., 1994), the time required to complete the emmetropization process varies from species to species.

4.2. Importance of visual stimulus during emmetropization

An appropriate visual stimulus is important for emmetropization. Human infants with congenital ptosis (Hoyt et al., 1981) or ocular opacity due to corneal scar (Gee and Tabbara, 1988; Meyer et al., 1999) or cataract (Nathan et al., 1985; Rabin et al., 1981; von Noorden and Lewis, 1987) may develop myopia.

In animal studies, it has been demonstrated that proper visual stimulation is important for emmetropization. The interruption of normal visual experience in animal studies through lid suture [cats (Kirby et al., 1982); tree shrews

(Marsh-Tootle and Norton, 1989; Norton et al., 1994; Sherman et al., 1977); monkeys (Wiesel and Raviola, 1977); chicks (Yinon et al., 1980); mice (Tejedor and de la Villa, 2003)] or wearing diffuser goggles [chicks (Hodos and Kuenzel, 1984; Wallman et al., 1987; Wallman et al., 1978); guinea pigs (Howlett and McFadden, 2006); fish (Shen et al., 2005); marmoset (Troilo and Judge, 1993); monkeys (Smith et al., 1999; Smith and Hung, 2000)] can lead to a myopic eye. The results of these studies indicate that visual experience has a significant impact on the refractive error development of the eye, in line with retrospective clinical studies in humans which show that proper visual stimulus is important for the emmetropization process (Hoyt et al., 1981; Nathan et al., 1985).

4.2.1. Monochromatic aberration

Since eye growth is influenced by a blurred retinal image (Smith and Hung, 2000), it has been hypothesized that eye growth is affected by blurred retinal images due to both on-axis (Buehren et al., 2007; Campbell et al., 2002; Collins et al., 1995; He et al., 2002) and off-axis (Hoogerheide et al., 1971) aberrations. However, there is no conclusive evidence of the relationship between monochromatic aberration and myopia development in the literature. Some studies suggested that higher order monochromatic aberration is associated with

development of myopia (Carkeet et al., 2002; Collins et al., 1995; He et al., 2002; Kwan et al., 2009; Paquin et al., 2002) but other studies do not (Cheng et al., 2003; Llorente et al., 2004; McLellan et al., 2001). Even though some studies supported the association of aberration with myopia, the magnitude of aberration reported in these studies was small, e.g., the spherical aberration was 0.20 D and 0.01 D in emmetropes and myopes, respectively, for a 5 mm pupil (Carkeet et al., 2002). A recent study in human showed that the peripheral aberration is dominated by off-axis oblique astigmatism (Jaeken and Artal, 2012). Higher order aberration like coma has subtle effect on the visual quality (Jaeken and Artal, 2012). However, it is still inconclusive if the myopic progression is affected by off-axis defocus (Thibos et al., 2002) or off-axis oblique astigmatism (Jaeken and Artal, 2012).

4.2.2. Chromatic aberration

Chromatic aberration is due to the fact that different wavelengths of light are refracted differently in an optical medium, e.g., light with shorter wavelength (blue) is refracted more strongly than light of longer wavelength (red). So, chromatic aberration has been suggested as a visual cue for eye growth. However, earlier study in chicks has shown that the removal of chromatic cues by using

monochromatic light does not affect the emmetropization process (Rohrer et al., 1992). Chicks incubated in red light showed insignificant difference in refractive status compared to chicks reared in blue light during emmetropization but the chromatic focus difference between red (wavelength = 665 nm) and blue (wavelength = 400) light has a magnitude of approximately 3 D in chicks. Conversely, later work in chicks demonstrated that a shorter range of wavelengths (Seidemann and Schaeffel, 2002) or simulated myopic and hyperopic defocus by adjusting the red, green and blue components of the stimulus (Rucker and Wallman, 2009) could influence the eye growth. Therefore, chromatic aberration may be one of the cues for eye growth during emmetropization.

4.2.3. Defocus

4.2.3.1. Animal eyes

In chicks, because the eye can compensate for imposed positive and negative defocus, respectively, by becoming hyperopic and myopic through adjusting its rate of axial eye growth (Irving et al., 1992; Schaeffel et al., 1988) (Figure 4.1), eye growth is thought to be a visually-regulated process. This compensatory eye growth to both positive and negative power lenses is also

found in a great diversity of animal species, e.g., marmosets (Graham and Judge, 1999), guinea pigs (Howlett and McFadden, 2009) and monkeys (Hung et al., 1995; Smith, 1998; Smith and Hung, 1999), suggesting that human eyes may also have similar properties.

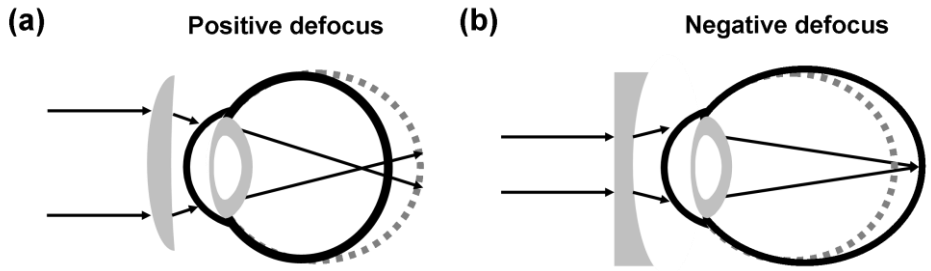

Figure 4.1. (a) Positive (convergent) lens moves the focal plane of the eye in front of the retina (positive defocus). The eye compensates for the defocus by reducing its rate of axial growth. (b) Negative (divergent) lens shifts the focal plane of the eye behind the retina (negative defocus). The eye eliminates the defocus by increasing its rate of axial growth. The dashed line indicates the rate of axial growth in an eye with plano lens (control eye).

To explore the role of sign of defocus on eye growth, Schaeffel and Diether (1999) reared chicks in a visually restricted environment to control the focal plane of the optical focus within the eye. All the chicks were cyclopleged in order to prohibit the use of accommodative cues. They induced optical defocus with equal magnitude but opposite sign in chicks to study the eye growth. The chicks showed compensatory eye growth in the appropriate direction for both positive and negative lenses, demonstrating that the eye can discriminate the sign of defocus signals (Schaeffel and Diether, 1999).

4.2.3.2. Human eye

Light is refracted through the cornea and then through the crystalline lens to focus on the retina. In the human, myopic, emmetropic and hyperopic eyes are frequently associated with, respectively, prolate, spherical and oblate eye shapes in both children (Mutti et al., 2000) and adults (Deller et al., 1947; Millodot, 1981; Seidemann et al., 2002). However, Stone and Flitcroft (2004) pointed out that the posterior contour of the eyeball among different kinds of ametrope showed great variations of curvature and so the type of posterior eye shape may not reflect the specific characteristic of a particular kind of ametropic eye. They reanalyzed the eye shape of ametropic subjects in Mutti et al. (2000)'s study and used more strict criteria to classify the shape of eyeball. They found that prolate eye shape is not a typical shape for myopic eyes, implying that eye shape is not a key predictor for myopia.

The myopic eye has been shown to have a relative hyperopic refraction in the peripheral retina in both children (Mutti et al., 2000; Schmid, 2003) and adults (Millodot, 1981). The optical defocus in the peripheral retina has been proposed to trigger myopic eye growth. A longitudinal study on young pilots showed that individuals with relative hyperopic refraction in the peripheral retina were more likely to later become myopic (Hoogerheide et al., 1971). In addition,

emmetropic children were also shown to develop relative hyperopic refraction in the peripheral retina before becoming myopic (Mutti et al., 2007). All these findings demonstrate that peripheral defocus may affect the development of axial refraction in humans.

4.3. Retina as detector of eye growth signals

The retina is the first site in the visual pathway to receive light stimulation. The signals are then transmitted to lateral geniculate body for further processing and finally reached the primary visual cortex for interpretation. However, partial deprivation of the vision using either defocussing lens (Diether and Schaeffel, 1997; Smith et al., 2010) or diffuser (McFadden, 2002; Wallman et al., 1987) triggers compensatory eye growth to the deprived or defocused region only, instead of a global compensatory response, suggesting that eye growth is locally regulated by the visual stimulus.

In chicks, the eye can still detect and grow to the altered focal plane of the eye, which is due to the defocussing lens, even if there is a breakdown of communication between eye and visual cortex produced through optic nerve section (Choh et al., 2006; Wildsoet, 2003) or removal of accommodative cues through ciliary nerve section (Schmid and Wildsoet, 1996) or lesions to

Edinger-Westphal nuclei (Schaeffel et al., 1990). These findings imply that the interpretation of the defocus signal in chick does not necessary rely on signal processing from higher visual centres or on accommodative cues. However, in guinea pig, the eye could not compensate to the imposed defocus without an intact optic nerve, suggesting that higher visual centres are involved in interpretation of defocus signals (McFadden and Wildsoet, 2009). The discrepancy in findings may indicate different underlying mechanism of detecting the eye growth signal among different animal species.

In addition to structural changes of the eye, there were several biochemical messengers identified in eye growth at the retinal level, e.g., glucagon (Buck et al., 2004; Feldkaemper et al., 2000), ZENK expression (Bitzer and Schaeffel, 2002; Fischer et al., 1999), retinoic acid (Mertz et al., 1999) and dopamine (Guo et al., 1995). These messengers show sign-dependent changes in concentration in response to opposite signs of defocus, suggesting that the eye can detect the signs of defocus at the retinal level.

4.3.1. Effect of peripheral vision on eye growth

The foveal region is of critical importance for vision because of its high spatial sensitivity. In studies using monkeys as subjects, however, removing

fovea with argon laser photo-ablation did not have significant impact on the emmetropization process (Smith et al., 2007) or compensatory ocular growth to a defocussing lens (Smith et al., 2009). These results indicate that normal foveal function was probably not essential during the emmetropization process and the peripheral retina was able to regulate the emmetropization process.

The effect of peripheral vision alone on eye growth has been examined using either spectacle lenses with a central aperture (Smith et al., 2009) or two-zone concentric bifocal lenses combining plano with either positive or negative power (Liu and Wildsoet, 2011). Even if clear central vision is allowed, imposing peripheral defocus with these special lenses was found to alter the axial growth of the eyeball in both chicks (Liu and Wildsoet, 2011) and monkeys (Smith et al., 2009), suggesting that peripheral vision could alter the central refractive error development of the eye.

Schippert and Schaeffel (2006) have also investigated the effect of peripheral defocus alone with different central aperture sizes of spectacle lenses on both central and peripheral refractive error development in chicks. Their study showed only subtle change in axial refractive error in chicks, but moderate change in peripheral refractive error. Smith and his co-workers (2009) suggested that the discrepancy of the effect of peripheral defocus on axial refractive error

was not directly related to the interspecies difference but was more likely to be related to methodological differences. The study of Schippert and Schaeffel (2006) induced localized defocus at more peripheral retina compared to the study of Smith and his colleagues (2009). It is likely that the chicks underwent defocus in the far peripheral retina only, leading to a more localized changes in refractive status. Their speculation has recently received some support from the study of eye growth using concentric bifocal lenses of varying size between central and peripheral zones in chicks (Liu and Wildsoet, 2011). Liu and Wildsoet (2011) showed that the effect of peripheral defocus on axial eye growth reduced when peripheral defocus was imposed beyond the paracentral retina.

Nevertheless, it seems that off-axis refraction would affect the refractive error development and fovea is not essential for detection of defocus signals. The dependence of higher visual centres for interpretation of signs of defocus is not conclusive because of the discrepancy of findings among different animal species. In case of conflicting vision between central and peripheral retina, peripheral vision dominates the overall eye growth.

Chapter 5 - Purpose of investigation

There is strong evidence suggesting that retinal function is impaired in the myopic eye, especially in the paracentral retina. Most of these previous studies have focused on outer retinal function without providing enough information about the functional integrity of inner retina. This gap of knowledge may be related to the weak inner retinal response derived from second order kernel of mfERG. Since the retina is the site for detecting the signal for eye growth, its functional integrity could have profound effect on the eye growth. Furthermore, most previous studies which focused on retinal function in the myopic eye were cross-sectional and aimed at providing insight about the retinal components and regions affected. Despite the fact that the retinal function varies between children and adults with myopia, there is still a lack of systematic investigation of the changes in retinal function from childhood to adulthood. We hypothesize that the retinal function is not the same at various age groups. On the other hand, the retina has been thought to be the site for detecting eye growth signal. Since most studies reporting the retinal response to defocus have been conducted on animals, it is uncertain that the findings can be extended to humans. The objectives of the current studies are to:

1) investigate the functional integrity of different retinal layers and attempt to

determine the key retinal components affected in myopic adults;

2) compare and contrast the functional integrity of the retina in myopic children and adults;

3) study the changes of retinal function during myopia progression (over a 1-year period) in children.

4) examine the retinal component(s) potentially involved in the detection of defocus signals and the regional retinal activity in response to the defocus signals in the human eye.

This study will help to deepen our understanding of the mechanisms producing retinal functional changes during myopia development, and enrich our knowledge of the retinal signalling in response to optical defocus.

PART II – EXPERIMENTS

Chapter 6 - Experiment I - Impairment of retinal adaptive circuitry in the myopic eye

(Adapted from the manuscript published in Vision Research 2011, 51, 367-375)

Abstract

Previous studies have proposed that the inner retina is affected in myopes. This study aimed to investigate the changes in adaptive circuitry of the inner retina in myopia, using the global flash mfERG with different levels of contrast.

Fifty-four myopes had global flash mfERG recorded with different contrasts. The direct component (DC) and the induced component (IC) of the mfERG response were pooled into six regions for analyses. The amplitudes and implicit times at different contrasts were also analysed.

Results showed that myopes had significant reduction in the paracentral DC amplitudes for the 29% and 49% contrasts and in the paracentral IC amplitudes at all contrasts measured. The peripheral IC amplitudes for the 49% contrast were also reduced. No significant change was found in implicit time for either DC or IC response. Refractive error explained about on average 14% and 16% of the variance in paracentral DC and IC amplitudes respectively; axial length could not account for additional variance in either paracentral DC or IC amplitude in the hierarchical regression models used.

We concluded that the paracentral retinal region in myopes showed signs of impaired temporal adaptive response, suggesting a functional loss at the inner retinal layer. In addition, functions attributed to the outer retinal layer showed

only small changes due to myopia.

6.1. Introduction

There is ample evidence that mfERG components were affected by myopia. The first order kernel response has been reported to be reduced and delayed with increasing myopic refractive error (Chen et al., 2006a; Kawabata and Adachi-Usami, 1997; Luu et al., 2007; Wolsley et al., 2008) or axial length (Chan and Mohidin, 2003) (See Section 3.2.1). Several studies have suggested that the attenuation of the mfERG response was due to axial elongation (Chen et al., 2006a; Kawabata and Adachi-Usami, 1997; Wolsley et al., 2008) and this functional loss was attributed to the outer retina (Chan and Mohidin, 2003; Kawabata and Adachi-Usami, 1997). Chen and her co-workers (2006a) found that axial length and refractive error could only account for, respectively, 15% and 27% of the total variance of the mfERG delay in the myopic eye. Since an increase in implicit time in ocular diseases may be related to a damage in the inner plexiform layer (Hood, 2000), Chen and her colleagues (2006a) proposed that the remaining variance of delayed mfERG response in the myopic eye might be caused by altered synaptic connections at the inner plexiform layer. On the other hand, the first slice of second order kernel response has also been found to

be reduced in amplitude by 5 to 10% for each millimetre of axial length elongation, indicating that the inner retinal function was probably impaired in the myopic eye (Chan and Mohidin, 2003).

Conventional mfERG, which measures the interactive response to continuous flashes, presents flashes at 13.3 ms intervals (75Hz), so that a second flash may be presented before the response elicited by the first focal flash has completed, resulting in a superimposition of the waveforms of successive flashes (Hood, 2000). Although the higher order kernel response probably represents the inner retinal activity (Hood, 2000; Hood et al., 2002; Ng et al., 2008a; Ng et al., 2008b), the use of higher order kernels is limited by poor signal-to-noise ratio.

The global flash mfERG measures the dynamics of the inner retinal processing by incorporating dark frames and a periodic full screen global flash stimulus within the m-sequence stimulation (Chu et al., 2006; Chu et al., 2008; Fortune et al., 2002; Shimada et al., 2005; Sutter et al., 1999). This paradigm involves a direct response to focal flash, called direct component (DC) (Shimada et al., 2005), and a larger non-linear component originating from the temporal interaction between focal flash and periodic global flash, called induced component (IC) (Bearse et al., 2000; Sutter et al., 1999). These DC and IC responses have been shown to reflect predominantly the outer (Chu et al., 2008)

and inner (Chu et al., 2008; Fortune et al., 2002; Shimada et al., 2005; Sutter et al., 1999) retinal activities, respectively. This stimulation paradigm has identified retinal defects in glaucoma patients (Chu et al., 2006; Fortune et al., 2002), which are presumed to originate in the inner retinal level.

Compared to emmetropes, myopes showed an attenuation in temporal vision including critical flicker frequency and temporal modulation sensitivity (Chen et al., 2000). It indicates that myopes take longer to recover from stimulations. Temporal adaptive responses are thought to take place mainly in the inner retina (Sutter et al., 1999). Several studies have suggested that the mfERG measurement with lower contrast stimulation can increase the relative contributions of inner retina cells to the mfERG response (Bearse and Sutter, 1998; Chan, 2005; Hood et al., 1999; Palmowski et al., 2000). This study was to investigate the temporal adaptive function at retina in the myopic eye using the global flash mfERG at different contrasts, in an attempt to examine the inner retinal function of the myopic eye.

6.2. Method

6.2.1. Subjects

Fifty-four subjects aged from 19 to 29 years (mean = 21.9 ± 1.9 years;

median = 22.0 years) with refractive errors (in SE) from plano to -8.13 D (mean = -4.00 ± 2.16 D; median = -3.75 D) and astigmatism equal to or less than 1.00 D were recruited from the Optometry Clinic of The Hong Kong Polytechnic University. All subjects received a thorough ophthalmic examination including subjective refraction and ocular health assessment by a registered optometrist. Subjective refraction was performed 30 minutes after the instillation of 1 drop of 0.4% Oxybuprocaine (Agepha Pharmaceuticals, Austria) and 2 drops of 1% Tropicamide (Alcon Laboratories, Inc., Fort Worth, TX, USA) at 5-minute intervals. The endpoint of the subjective refraction was the 'best visual acuity with the maximum plus' optical correction. Ocular health assessment included slit lamp examination and ophthalmoscopy. Colour vision was also examined with the 24-plate version of Ishihara colour vision test. The inclusion criteria were best corrected LogMAR visual acuity of 0.00 or better in both eyes, normal colour vision, cup-to-disc ratio of less than 0.5 with normal neuroretinal rim appearance, similar optic nerve head appearance in both eyes and myopic crescent of less than 0.5 disc diameter. Subjects with ocular pathological changes, clinically significant fundus degeneration, systemic disease, a history of epilepsy or a family history of pathological myopia or retinal disease were excluded from this study.

Subjects were informed of the nature and the risks of the experiment. Consent was obtained from each subject after the study had been explained and all enquiries had been answered. This study adhered to the tenets of the Declaration of Helsinki and was approved by the Human Ethics Committee of The Hong Kong Polytechnic University.

6.2.2. mfERG stimulation

The stimulus pattern, consisting of 103-hexagon array scaled with eccentricity (stretch factor = 10.46), was presented on a 19-inch RGB computer monitor (Model no.: GDM-500PS, Sony, Tokyo, Japan) using the Visual Evoked Response Imaging System (VERIS) (VERIS Science 4.1, Electro-Diagnostic Imaging, Inc., San Mateo, CA, USA). The hexagonal pattern subtended 44° vertically and 52° horizontally at a working distance of 33 cm. To maintain constant retinal image size among all subjects (Rabbetts, 2007), the spectacle corrective lenses were placed at the anterior focal plane of the tested eye during the mfERG recording to eliminate the variance of the image size among different magnitude of myopia.

The global flash paradigm, which contained four video frames, started with a multifocal flash frame, followed by a dark frame (3 cd/m^2), a full screen global

flash (162 cd/m^2) and a second dark frame for each of the m-sequence stimulations (2^{13}) (Chu et al., 2006; Fortune et al., 2002; Shimada et al., 2001). As illustrated in Figure 6.1a, in the frames containing multifocal flash, each hexagon was either a dark or bright stimulus according to the m-sequence with a stimulation rate of 75 video frames per second. To investigate the retinal temporal adaptive changes at different contrasts, the luminance-difference of the multifocal flash was set at 142, 89, 70 and 43 cd/m^2, corresponding to the stimulus contrasts of 96%, 65%, 49% and 29%, respectively. The mean luminance of the multifocal flash and the background was 73 cd/m^2 for all contrast levels. The total recording time for each condition was 7 minutes and 17 seconds. Each subject was tested four times, once with each contrast and the order of presentation of the contrasts was randomised across subjects.

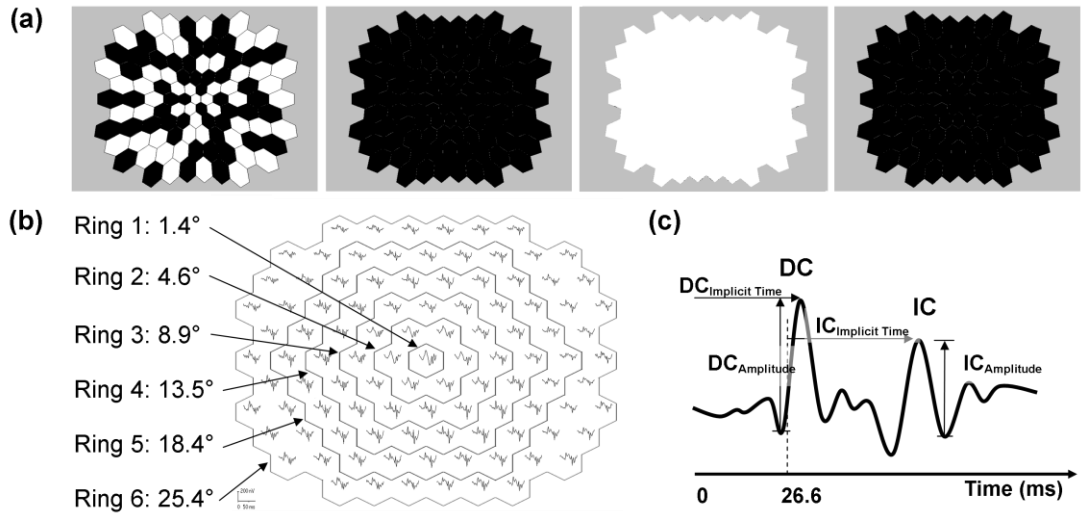

Figure 6.1. (a) Schematic diagram showing the video frame sequence of the global flash paradigm. The four frame sequence contained a multifocal flash frame, followed by a dark frame, a (full screen) global flash and a second dark frame. (b) Each local response was pooled into 6 rings and was averaged. The eccentricity boundaries of each pooled region are labelled by the arrows. (c) The first order kernel response waveform consisting of DC followed by IC response was shown (See text in details).

6.2.3. mfERG recording

Only one eye was randomly chosen for recording. The pupil of the tested eye of each subject was dilated to at least 7 mm before mfERG recording. A Dawson-Trick-Litzkow (DTL) thread electrode was used as the active electrode. Gold-cup surface electrodes were placed about 10 mm lateral to the outer canthus of the tested eye as reference and at the central forehead as ground electrode. An amplifier (Model: P511K, Grass-Telefactor, West Warwick, RI, USA) was used to amplify and filter the signals (gain: 100,000x; band pass: 10-300 Hz). The instantaneous compound ERG was monitored by the examiner using the VERIS program. The recording process for each contrast was separated into 32 slightly

overlapping segments and a short rest was provided between segments. If a segment was contaminated with artifacts such as blinks or small eye movement, the segment was discarded and re-recorded immediately.

6.2.4. Axial length measurement

The axial length of the tested eye was measured with a non-contact optical biometer (IOL master, V.4.08, Carl Zeiss Meditec, Inc., Dublin, CA, USA). Five readings were taken to obtain a mean value. The data were used if the signal-to-noise ratio for each reading was greater than 2.00 and the range of the five readings was less than 0.10 mm. Otherwise, the data was measured again. The axial length of the subjects was from 22.52 to 28.00 mm (mean = 25.33 ± 1.14 mm; median = 25.29 mm).

6.2.5. mfERG response analysis

Amplitudes and implicit times of the DC and IC responses were measured for each retinal region (Figure 6.1b). The amplitudes of DC and IC responses were evaluated by using peak-to-peak measurement. The DC amplitude was measured from the first negative trough to the first positive peak while the IC amplitude was calculated from the second distinct peak to the subsequent trough.

The implicit time of DC response was measured from the onset of the stimulus to the peak of the DC response while the implicit time of IC response was measured from the presentation of the global flash (i.e. 26.6 ms) to the IC response peak (Figure 6.1c).

6.2.6. Statistical analysis

Statistical Package for the Social Sciences (SPSS) (Version 15.0, SPSS Inc., Chicago, IL, USA) was used to perform the statistical analysis. Since both refractive error (Kawabata and Adachi-Usami, 1997; Luu et al., 2006) and axial length (Chan and Mohidin, 2003) were found to influence the mfERG response, hierarchical multiple regression was separately performed to investigate the contribution of axial length on the global mfERG responses for different regions, in addition to the effect of refractive error. This statistical method not only allowed assessment of sets of independent variables at various levels with the control of each factor at preceding levels, but also evaluated the contribution of each factor involved. Since refractive error had a greater effect on mfERG response than axial length (Chen et al., 2006a), refractive error was used in the first step of the hierarchical regression model and both refractive error and axial length were used in the second step. Bonferroni adjustment with level of

significance (α) set at 0.008 was used to correct for the multiple comparisons between different retinal regions.

6.3. Results

There was a strong correlation between refractive error and axial length indicating that the myopia was primarily axial in nature (Pearson's correlation, r = -0.803; $p < 0.001$) (Figure 6.2).

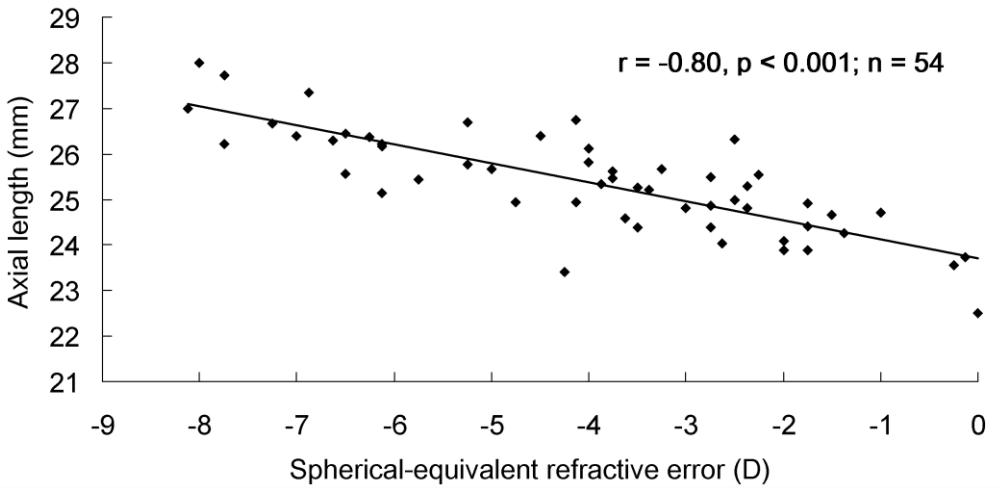

Figure 6.2. Correlation between refractive errors and axial length for our subjects.

Every subject had mfERG waveforms with distinct DC and IC responses at all the contrasts and regions. Figure 6.3 shows the typical global flash mfERG waveforms at 96% contrast measured from one of the subjects. At 96% contrast, the DC and IC responses reached their peaks at, respectively, 30 and 57 ms after

the onset of the stimulus. Both the DC and IC responses reached their peaks slightly later at central region (i.e. Rings 1 and 2). The waveforms of the mfERG responses at other contrasts shared similar characteristics but the implicit times of both DC and IC responses were reduced under lower contrasts compared to high contrasts (data not shown).

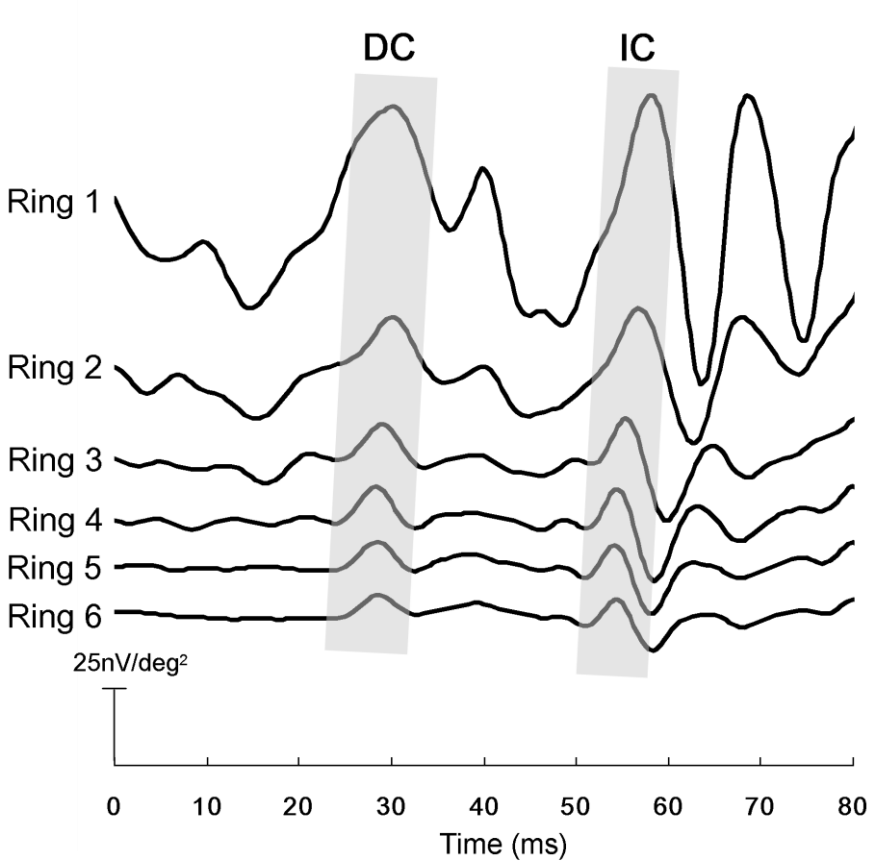

Figure 6.3. The waveforms of the ring-averaged responses from central (Ring 1) to peripheral (Ring 6) retina of a subject (SE = -1.38 D) at 96% contrast. The waveforms consist of two distinct peaks corresponding to the DC and IC responses as highlighted in the figure.

Table 6.1 summarizes the results from the hierarchical regression analysis in determining the independent effects of refractive error and the combined effects of refractive error and axial length on the DC and IC amplitudes. When refractive error was entered into the first step of this model, it explained 11 to 14% of the variance in DC amplitudes from Rings 2 to 4 at 29% contrast. At these regions, the DC response decreased significantly as myopia increased at this contrast (only the scatter plot for Ring 3 is shown) (Figure 6.4). In addition, about 19% of the variance in DC amplitude of Ring 3 at 49% contrast was attributed to refractive error (Table 6.1) and the amplitude also decreased with increasing myopic refractive error (Figure 6.4). The DC amplitudes were not affected by refractive error for the remaining contrasts or other retinal regions. When both refractive error and axial length were included in the second step of this model, only the DC amplitude of Ring 2 at 49% contrast made a further contribution to the model (Adjusted R^2 change = 0.17, F change = 12.08, $p = 0.001$). However, axial length did not account for any additional change of DC response in the remaining contrasts or other retinal regions (all $p > 0.05$). Both central (Ring 1) and peripheral DC (Rings 5 and 6) amplitudes were unaffected by either refractive error or axial length (Table 6.1).

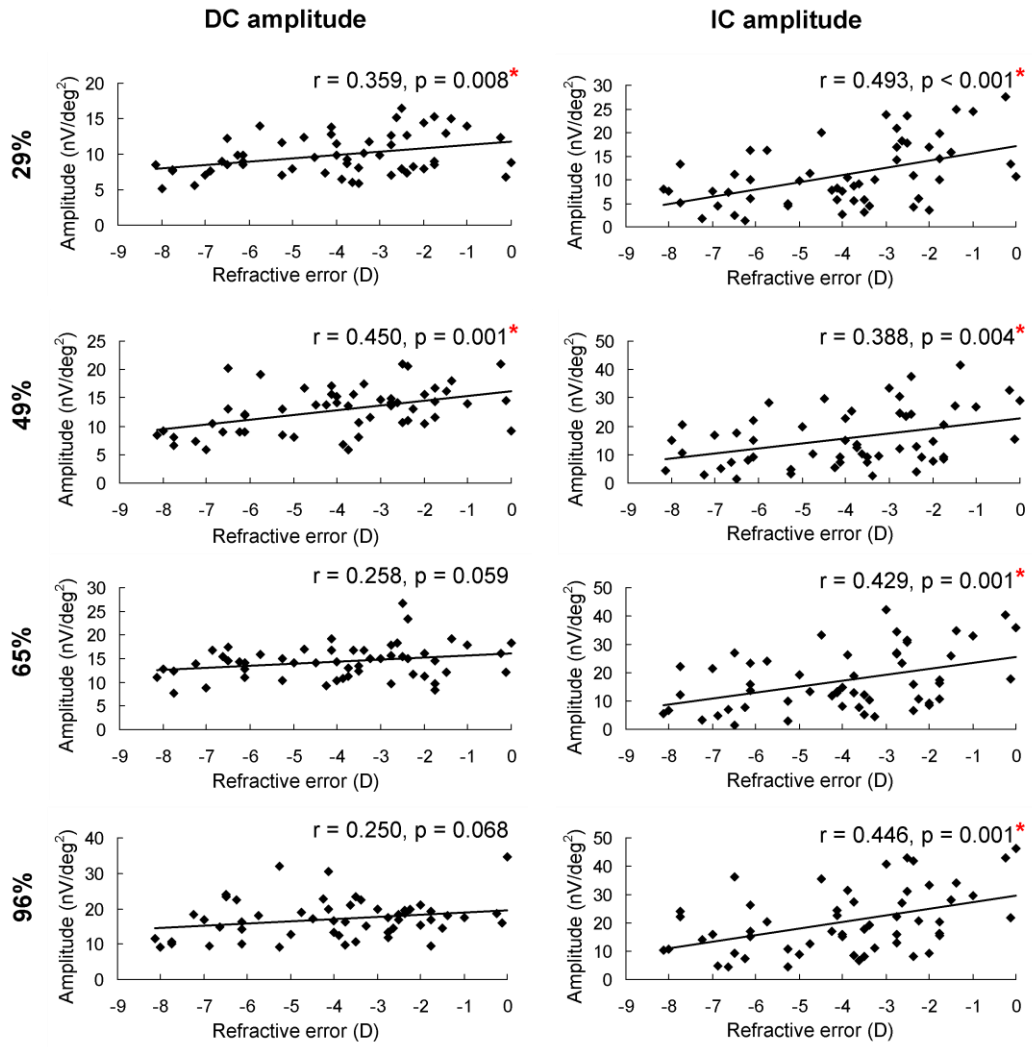

Figure 6.4. Scatter plots showing the relationship between global flash mfERG responses (Ring 3) and refractive errors at the four contrasts: 29% (top), 49% (second), 65% (third) and 96% (bottom). The DC response decreased significantly with increasing myopic refractive error at 29% and 49% contrasts (marked with "*") but this was not the case at 65% and 96% contrasts. In contrast, the IC response decreased significantly as a function of refractive error at all contrasts measured (marked with "*").

		Contrast (%)											
		29%			49%			65%			96%		
Region	Model	adjusted R^2	F	p	adjusted R^2	F	p	adjusted R^2	F	p	adjusted R^2	F	p
Direct Component (DC)													
Ring 1	RE	0.006	1.302	0.259	0.026	2.415	0.126	-0.008	0.576	0.451	0.015	1.780	0.188
	RE + AL	-0.014	0.643	0.530	0.098	3.863	0.027	-0.026	0.317	0.730	0.019	1.501	0.233
Ring 2	RE	**0.137**	**9.431**	**0.003**	0.055	4.098	0.048	-0.015	0.240	0.627	0.015	1.803	0.185
	RE + AL	0.137	5.200	0.009	**0.221**	**8.524**	**0.001**	-0.025	0.347	0.709	0.018	1.499	0.233
Ring 3	RE	**0.112**	**7.670**	**0.008**	**0.187**	**13.195**	**0.001**	0.049	3.722	0.059	0.045	3.474	0.068
	RE + AL	0.098	3.876	0.027	**0.174**	**6.572**	**0.003**	0.030	1.833	0.170	0.101	3.982	0.025
Ring 4	RE	**0.114**	**7.839**	**0.007**	0.026	2.430	0.125	-0.003	0.854	0.360	0.011	1.589	0.213
	RE + AL	0.110	4.271	0.019	0.032	1.881	0.163	0.001	1.019	0.368	0.023	1.624	0.207
Ring 5	RE	0.001	1.042	0.312	-0.019	<0.001	0.983	-0.014	0.273	0.603	<0.001	0.985	0.326
	RE + AL	0.008	1.225	0.302	-0.035	0.093	0.911	-0.034	0.134	0.875	0.036	1.985	0.148
Ring 6	RE	0.039	3.175	0.081	-0.013	0.304	0.584	0.023	2.227	0.142	-0.008	0.602	0.441
	RE + AL	0.065	2.843	0.068	-0.028	0.279	0.758	0.004	1.095	0.342	0.034	1.936	0.155

Table 6.1. A hierarchical regression analysis showing the effects of refractive error (RE) and the combined effects of refractive error and axial length (RE + AL) on DC amplitude. The table shows the adjusted R-square (adjusted R^2), F-value (F) and p-value (p) for each step of the models. Bold-face: Bonferroni-corrected statistically significant values ($p < 0.008$).

		Contrast (%)											
		29%			49%			65%			96%		
Region	Model	adjusted R^2	F	p	adjusted R^2	F	p	adjusted R^2	F	p	adjusted R^2	F	p
Induced Component (IC)													
Ring 1	RE	-0.018	0.062	0.804	0.015	1.795	0.186	-0.017	0.092	0.763	0.020	2.063	0.157
	RE + AL	-0.036	0.091	0.913	0.001	1.022	0.367	-0.037	0.046	0.955	0.013	1.340	0.271
Ring 2	RE	0.057	4.211	0.045	0.012	1.648	0.205	0.060	4.368	0.042	0.074	5.218	0.026
	RE + AL	0.039	2.065	0.137	-0.005	0.856	0.431	0.046	2.291	0.111	0.092	3.690	0.032
Ring 3	RE	**0.229**	**16.706**	**<0.001**	**0.134**	**9.208**	**0.004**	**0.169**	**11.759**	**0.001**	**0.183**	**12.877**	**0.001**
	RE + AL	**0.220**	**8.488**	**0.001**	0.123	4.705	0.013	**0.153**	**5.781**	**0.005**	**0.170**	**6.425**	**0.003**
Ring 4	RE	**0.124**	**8.523**	**0.005**	**0.121**	**8.280**	**0.006**	0.094	6.513	0.014	**0.173**	**12.116**	**0.001**
	RE + AL	0.112	4.342	0.018	0.117	4.498	0.016	0.088	3.568	0.035	**0.158**	**5.961**	**0.005**
Ring 5	RE	0.077	5.447	0.023	**0.144**	**9.945**	**0.003**	0.083	5.794	0.020	0.051	3.835	0.056
	RE + AL	0.096	3.812	0.029	**0.151**	**5.727**	**0.006**	0.100	3.943	0.026	0.032	1.884	0.162
Ring 6	RE	0.080	5.616	0.022	**0.150**	**10.333**	**0.002**	0.100	6.866	0.011	0.058	4.269	0.044
	RE + AL	0.090	3.633	0.034	**0.145**	**5.489**	**0.007**	0.100	3.953	0.025	0.040	2.112	0.132

Table 6.2. A hierarchical regression analysis showing the effects of refractive error (RE) and the combined effects of refractive error and axial length (RE + AL) on IC amplitude. The table shows the adjusted R-square (adjusted R^2), F-value (F) and p-value (p) for each step of the models. Bold-face: Bonferroni-corrected statistically significant values ($p < 0.008$).

With regards to the IC amplitude, refractive error accounted for 13 to 23% of the variance in IC amplitudes for Ring 3 at all contrasts, i.e., the IC amplitudes reduced significantly as the myopic refractive error increased (Table 6.2 and Figure 6.4). In addition, refractive error explained 12 to 17% of the variance in IC amplitudes for Ring 4 at all contrasts measured but not at 65% contrast. Similar findings were also observed at low to moderate contrasts (i.e. 29%, 49% and 65%) but not at high contrast for Rings 5 and 6. However, only the IC amplitudes of these two regions at 49% contrast reached the Bonferroni corrected significant level (Table 6.2). When axial length was added as a secondary explanatory variable in this model, it did not account for the extra variance in the IC amplitudes for all the contrasts (all $p > 0.05$) (data not shown).

Neither DC nor IC implicit time showed significant association with refractive error at all the contrasts tested (data not shown). The implicit time for both DC and IC responses remained virtually constant as refractive error increased. The addition of axial length as a secondary variable in the model could not account for extra variance in either DC or IC implicit time (all $p > 0.05$).

6.4. Discussion

Our findings showed that the paracentral (i.e. Ring 3, eccentricities from 4.6 to 8.9°) DC response of myopes reduced significantly as a function of the magnitude of myopia at low (29%) and moderate (49%) contrasts but not at high contrasts (Table 6.1 and Figure 6.4). The DC is the response to the focal flash and reflects the interactive response between focal flash and the periodic global flash in the preceding m-sequence stimulation. The DC thus reflects retinal temporal adaptive changes (Chu et al., 2006; Chu et al., 2008; Shimada et al., 2005; Sutter et al., 1999). This component involves a larger contribution from the outer retinal activity (Chu et al., 2008) and a smaller contribution from the inner retinal activity (Chu et al., 2008; Sutter et al., 1999). Decreasing stimulus contrast increases the contribution of the inner retinal activity to the mfERG response with conventional m-sequence stimulation (Bearse and Sutter, 1998; Chan, 2005; Hood et al., 1999; Palmowski et al., 2000). Furthermore, the cellular origin of the global flash mfERG response was investigated using porcine eye (Chu et al., 2008). Chu and co-workers (2008) have reported that some oscillatory-like wavelets originating from the inner retina are superimposed on the DC waveform under these stimulus conditions. One of these oscillatory wavelets contributed to the peak of DC response and saturated at moderate to

high contrasts, while the activities of the outer retinal components including photoreceptors, ON- and OFF-bipolar cells increased linearly as contrast increased. Thus, compared to higher contrasts, it is likely that the DC response at low contrasts involves a larger contribution from the inner retinal activity. Reduction of the DC response amplitude has also been reported in eye diseases affecting the inner retina (Chu et al., 2006; Shimada et al., 2001). Taken together, the attenuated DC response amplitudes in myopes at low and moderate contrasts are probably consequences of impaired temporal adaptive function at the inner retinal level.

The paracentral (i.e. Rings 3 and 4, eccentricities from 4.6 to 13.5°) IC responses of myopic eyes were reduced at all contrasts measured and similar effects were observed in the peripheral (Rings 5 and 6, eccentricities from 13.5 to 25.4°) IC responses at low and moderate contrasts (Table 6.2 and Figure 6.4). The IC response, which is a temporal adaptive response produced by the global flash in the concurrent m-sequence stimulation, predominantly reflects the activity of the inner retina (Chu et al., 2008; Fortune et al., 2002; Shimada et al., 2005; Sutter et al., 1999). It has been suggested that the IC response originates primarily from amacrine cells and retinal ganglion cells in porcine eyes (Chu et al., 2008). An attenuated IC response has also been identified in glaucoma

patients whose inner retina was impaired (Chu et al., 2006; Fortune et al., 2002). So, an attenuated IC response in this experiment provides further evidence of impaired temporal adaptive function of the inner retina in myopes.

In contrast to our findings, Chen and her colleagues (2006a), who also carried out global flash mfERG measurements at high contrast, found that both DC and IC amplitudes increased with increasing myopic refractive error but their findings did not reach statistical significance. In their study, the DC and IC amplitudes of subjects were statistically adjusted to compensate for the change in response due to the variance of axial length among different myopic subjects. However, the adjustment may not be applicable to each retinal region as previous studies have demonstrated that the effect of myopia and axial length on retinal function is different with changing eccentricities (Chan and Mohidin, 2003; Chen et al., 2006a; Kawabata and Adachi-Usami, 1997). This statistical manipulation has presumed a uniform effect of myopia/axial length on retinal function and might not be an ideal method to study retinal function in the myopic eye. Since a substantial relationship exists between refractive error and axial length, using axial length as a co-variate may remove the shared variance with refractive error and cannot really reflect the influence of refractive error on the mfERG response.

The mfERG measures the retinal response to the light stimuli (Sutter and

Tran, 1992) and the luminance of the stimulus would affect the retinal response (Brown and Yap, 1996). In myopes, the projected image of the stimulus onto the retina reduces because of the enlarged eyeball and may affect the retinal response. In this study, the retinal surface area in high myopes with axial length of 28.0 mm is increased by 54% compared to emmetropes with axial length 22.5 mm. The retinal illuminance will be reduced by 35% in high myopes. However, the mfERG response amplitude was reduced by 60% on average (Figure 6.4), which is greater than the calculated reduction of retinal illuminance. Therefore, the decrease in brightness in high myopes is not likely to be an important factor contributed to the response reduction.

The conventional mfERG is a measure of the temporal interactive response to successive flashes (Hood et al., 1998). The focal flash is presented before the response due to the preceding focal flash is fully developed. Thus, an adaptive response triggered by a sequential flash superimposes on the waveform of the previous flash (Hood, 2000). This response is an inverted second order kernel response, which was named the “induced component” by Sutter (2000), mainly overlapped the late portion of the first order waveform and led to an early and sharp P1 response (see Section 2.2.4 and Figure 2.4 in details for definition of P1 response) (Hood, 2000). Chen and her colleagues (2006a) investigated the

mfERG response in the myopic eye and found a delayed P1 response using the conventional mfERG without significant change in amplitude. Hood (2000) suggested that the delay in timing was likely to be caused by an attenuated "induced component" response, leading to a shift of the peak of the P1 response waveform. The attenuated "induced component" may presumably relate to altered synaptic transmission at the inner plexiform layer. The global flash paradigm separates the temporal adaptive response by inserting a dark frame between two flashes. So, the reduced IC response without a significant change in the DC response as found in our results, especially at the higher contrasts, supported the hypothesis that the delayed response may be caused by an altered synaptic connection in the inner plexiform layer.

The second order kernel response obtained with a conventional mfERG, which reflects the retinal temporal adaptive changes, mainly represents the activity from inner retina with small contributions from outer retina (see Sections 2.2.2 and 2.2.5). It is reduced in myopes not only at retinal eccentricities from 5 to 13° but also from 18 to 25° (Chan and Mohidin, 2003), which is consistent with our findings. The pattern electroretinogram response, which mainly represents the activity from the inner retina, is also reduced with longer eyeballs (Hidajat et al., 2003). Psychophysical measurements of temporal vision including

the critical fusion frequency and the temporal modulation sensitivity also showed poorer performance in the myopic eye (Chen et al., 2000). These results indicated that the myopic eye took longer to recover from temporal stimulation. All this evidence matches with our findings that the temporal adaptive function of the myopic eye was impaired.

In the myopic human eye, both the scotopic and photopic b-wave responses, as well as the oscillatory potentials, of the full-field ERG are reduced (Perlman et al., 1984; Westall et al., 2001). They are also reduced in animal models of myopia (Fujikado et al., 1997). Recent studies using primates have shown that the photopic b-wave is partially affected by the inner retinal activity such as amacrine cells and ganglions cells (Bui and Fortune, 2004; Mojumder et al., 2008), in addition to the outer retinal activity (Sieving et al., 1994) (see Section 2.1.1). In addition, the oscillatory potentials probably originate from inner plexiform cells (Wachtmeister, 1998). Thus, the attenuated response in the myopic eye does not relate simply to the decline in cell density or physiological change in the outer plexiform cells but may also include cells of the inner plexiform layer.

It is surprising to find that retinal function in the paracentral region is more affected in myopes, and that peripheral retina response is partially attenuated at

low contrasts, but central response appears unaffected. Light sensitivity is generally depressed in myopes (Aung et al., 2001; Chihara and Sawada, 1990; Rudnicka and Edgar, 1995; Rudnicka and Edgar, 1996) and is predominantly affected at eccentricities from 15 to 20° (Chihara and Sawada, 1990). Orientation discrimination in the myopic eye is mildly changed at the fovea but is markedly reduced at an eccentricity of 15°, suggesting non-uniform stretching of the posterior part of the globe (Vera-Diaz et al., 2005). The retinal thickness in the paracentral region at an eccentricity from 1.5 to 3 mm (i.e. ~ from 5 to 10°) has been found to be thinner in the myopic eye (Lam et al., 2007; Luo et al., 2006; Wu et al., 2008). Beyond the central region, the dendrites of secondary and tertiary neurons like bipolar cells, amacrine cells and ganglion cells synapse horizontally with several presynaptic retinal neurons (Curcio and Allen, 1990; Kolb and Dekorver, 1991; Kolb et al., 1992; Kolb and Marshak, 2003). It is likely that the dendrites of these neurons may be influenced as a result of retinal thinning, which in turn affects the physiological function of the retina. The results of this experiment are in agreement with all of these previous studies, confirming that the paracentral retinal region is vulnerable (see Section 3.2.1) and foveal function seems to be relatively preserved in the myopic eye.

The present results show that myopic refractive error predominantly affects

retinal function in the paracentral region from 5 to 14° of eccentricity. In contrast, common central retinal diseases such as age-related maculopathy and glaucoma mainly affected the parafoveal (eccentricities from 2.5 to 4°) (Maguire and Vine, 1986; Sarks et al., 1988) and mid-peripheral regions (beyond 20° of eccentricity) (Henson and Hobley, 1986), respectively, at the early stage of the disease. These results imply that more attention to potential functional deficits in the paracentral retina is needed in myopic patients.

Previous studies on chicks have demonstrated that the process of eye growth is regulated locally by visual stimuli (Diether and Schaeffel, 1997; Gottlieb et al., 1987; Troilo et al., 1987; Wallman et al., 1987) and the paracentral retina in higher primates has been shown to be involved in regulating eye growth (Smith et al., 2005; Smith et al., 2007). In humans, the myopic eye usually has a relative hyperopic peripheral refraction (Mutti et al., 2007; Mutti et al., 2000). In addition, a longitudinal study of a group of pilots indicated that individuals with hyperopic refraction in the peripheral retina were more prone to develop axial myopia (Hoogerheide et al., 1971). This implies that the paracentral retina of the human eye may have certain mechanism to detect defocus, even if it is not the site with the highest resolving power across the retina. We hypothesized that local hyperopic defocus in the peripheral retina would trigger retinal thinning, leading

to reduced retinal function and inferior visual performance in the paracentral retinal region.

6.5. Conclusions

In the myopic eye, the paracentral IC amplitudes at all contrasts measured were significantly reduced and paracentral DC amplitudes were significantly reduced at low and middle contrasts only. Refractive error attributed to about 16% and 14% of the variance in paracentral IC and DC amplitudes respectively, suggested that the temporal adaptive function of inner retina may be impaired in the myopic eye and the affected area was predominantly shown in the paracentral retina.

Chapter 7 - Experiment II - Myopic children have central reduction in high contrast mfERG response while young adults have paracentral reduction in low contrast response

(Adapted from the manuscript published in Investigative Ophthalmology and Visual Science 2012, 53, 3695-3702)

Abstract

This study compared the retinal function of myopic children and young adults using the global flash mfERG.

Fifty-two children (aged from 9 to 14 years) and nineteen young adults (aged from 21 to 28 years) with refractive errors (in SE) ranging from plano to -5.50 D were recruited. They were examined using the global flash mfERG at 49% and 96% contrasts. Each local mfERG response was pooled into five concentric rings for analysis. The amplitudes and implicit times of DC and IC responses from the global flash mfERG were analyzed. Hierarchical multiple regressions were used to evaluate the influence of refractive error and axial length on the DC and IC responses.

Compared to the emmetropes of the same age group, myopic children had a significant reduction in central macular DC response at 96% contrast while the IC response was unaffected. In contrast, myopic adults showed significant reductions in paracentral IC amplitudes at 49% contrast. Implicit times for DC and IC components were not affected for either group.

Retinal function was unaffected in myopic children, except for the outer retinal function in the central macular region. In contrast, the inner retinal function was substantially reduced in myopic adults, especially in the paracentral region. This

study provides further evidence for different retinal physiological characteristics in myopic children and myopic adults.

7.1. Introduction

Most previous studies have focused on investigating retinal function (Chan and Mohidin, 2003; Chen et al., 2006a; Kawabata and Adachi-Usami, 1997; Luu et al., 2006) or visual function (Aung et al., 2001; Chen et al., 2000; Chui et al., 2005; Jaworski et al., 2006; Liou and Chiu, 2001; Mantyjarvi and Tuppurainen, 1995; Rudnicka and Edgar, 1995; Rudnicka and Edgar, 1996; Subbaram and Bullimore, 2002) in myopic adults. Luu and his co-workers (2006) were first to study retinal function in myopic children; they found reduced and delayed first order kernel mfERG response in myopic adults, but only delayed response in myopic children, suggesting a difference in retinal physiology between myopic adults and myopic children. However, the investigation of only the first order kernel mfERG response, which primarily reflects the activity from the outer retina (Hood, 2000; Hood et al., 2002; Ng et al., 2008a; Ng et al., 2008b), without the assessment of the activity from the inner retina, is not sufficient for an understanding of the detailed functional integrity of the retina in the myopic eye. In Experiment 1 (Chapter 6), inner retinal function in adults was shown to

be more susceptible to effects of myopia than is outer retinal function. These findings are in agreement with a histological study which showed that inner retina was affected most when retina thinned in myopic tree shrews (Abbott et al., 2011).

The global flash mfERG measures both outer and inner retinal functions (see Section 6.1), in addition to providing response topography. It would appear to be a better protocol for examining different retinal layers in myopes. The primary purpose of the current study was to compare retinal function between myopic children and myopic adults. The secondary purpose was to investigate the functional integrity of the retina, especially the inner retinal function, in myopic children.

7.2. Methods

7.2.1. Subjects

Fifty-two children aged from 9 to 14 years (mean = 11.1 ± 1.2 years; median = 11.0 years) and nineteen adults aged from 21 to 28 years (mean = 23.4 ± 2.0 years; median = 23.0 years) were recruited as subjects. All subjects received a comprehensive eye examination including a cycloplegic subjective refraction, a colour vision test with 24-plate version of the Ishihara colour vision

test, and ocular biomicroscopy carried out by an optometrist. All subjects had best corrected visual acuity of logMAR 0.00 or better in both eyes, normal colour vision, and good ocular health. Using criteria from previous epidemiological studies, we classified children whose myopia developed after the age of 6 years as acquired myopia (Edwards, 1999; Edwards and Lam, 2004). Subjects with myopia developed before the age of 6 years (classified as congenital myopia) were excluded, as were subjects with ocular degenerative changes, any ocular disease, any known systemic disease, or history of epilepsy.

All children were accompanied by their parent(s) or guardian(s) throughout the experiment. Before the start of the experiment, the aim of this study was explained. Written consent was obtained from adult subjects, and parents gave consent for their children to participate. All research procedures followed the tenets of the Declaration of Helsinki. The study was reviewed and approved by the Human Ethics Committee of The Hong Kong Polytechnic University.

7.2.2. Refraction and axial length measurement

Before these measurements, each subject had 1 drop of 0.4% Oxybuprocaine (Agepha Pharmaceuticals, Vienna, Austria) and 2 drops of 1% Tropicamide (Alcon Laboratories, Inc., Fort Worth, TX, USA) instilled 5 minutes

apart, so as to achieve both mydriasis and cycloplegia. Subjective refraction was performed at least 30 minutes after the instillation of the cycloplegia. Axial length was measured using a non-contact optical biometer (IOL master, V.4.08, Carl Zeiss Meditec, Inc., Dublin, CA, USA). The axial length of each eye was measured five times to obtain a mean value.

7.2.3. mfERG stimulation

The stimulus pattern was presented on a 22-inch liquid crystal display (Model: 2232GW+, SAMSUNG, Tianjin, China) and was controlled with VERIS (VERIS Science 6.0.09d19, Electro-Diagnostic Imaging, Redwood City, CA, USA) run on an Apple Macintosh computer.

The pattern for the global flash mfERG paradigm was made up of 61-hexagon array, scaled with eccentricity (Stretch factor = 12.18), for both children and adults groups. The pattern subtended 39° horizontally and 37° vertically at a working distance of 40 cm. The stimulus sequence started with a multifocal flash frame followed by a dark frame, a global flash, and a second dark frame for each of the m-sequence stimulations; the video frame rate was 75 Hz (Figure 7.1(a)) (Chu et al., 2006; Fortune et al., 2002; Shimada et al., 2001). For the multifocal flash, each hexagon was temporally modulated between bright

and dark stimulation, according to a pseudorandom binary m-sequence. The global flash mfERG responses were measured at 49% and 96% contrasts in two separate examinations and the mean luminance was maintained at 50 cd/m^2; the background was set at 50 cd/m^2. High and low contrast tests were conducted in random order. The recording time for each stimulation sequence was 3 minutes and 40 seconds with a 2^{12} binary m-sequence, and the recording process was divided into 16 slightly overlapping segments.

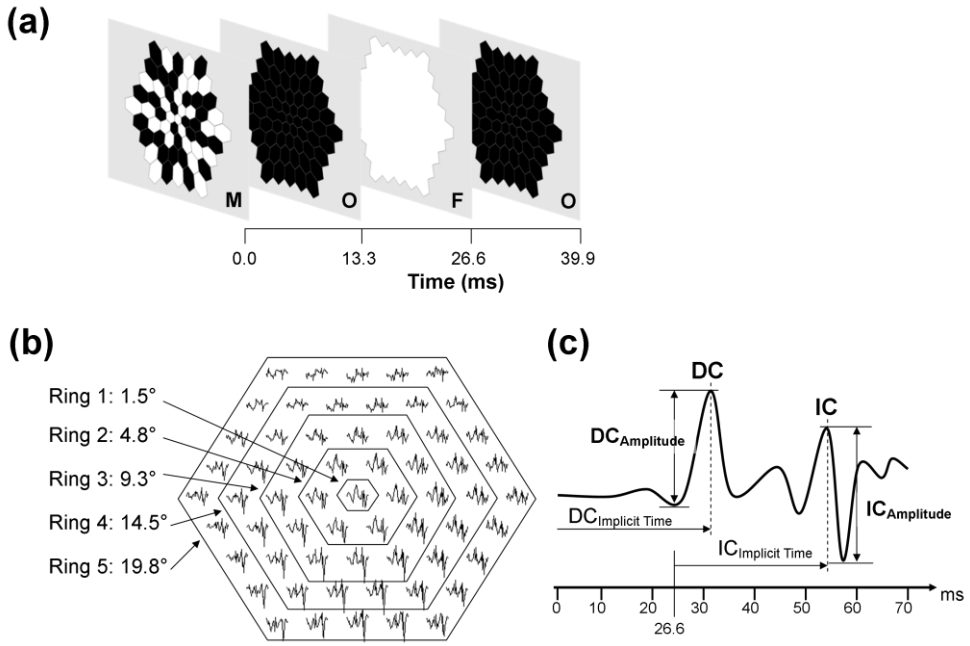

Figure 7.1. (a) Schematic diagram showing the video frames of the global flash mfERG paradigm. The stimulus consisted of four video frames in each of the m-sequence stimulations with this order: a multifocal flash frame ("M", 61-scaled hexagonal array), a dark frame ("O", 1 cd/m^2), a global flash ("F", 100 cd/m^2) and a second dark frame. The video frame rate was 75 frames per second, with a frame interval of 13.3 ms. (b) The 61 local responses were pooled into 5 concentric rings and were averaged. The eccentricity boundary of each ring is shown. (c) The typical waveform of the first order kernel global flash mfERG response, together with measured parameters (See text in details).

The 61-scaled hexagonal array used in this study covers the retinal areas which have been shown to be affected in adult myopes (i.e. from 9 to 27° of horizontal visual field) (Experiment 1; see Section 6.3). Using a 61-hexagon stimulus field increases signal-to-noise ratio, decreases the influence of fixation errors and is thus more suitable when recording from children.

7.2.4. mfERG recording

The eye to be measured was randomly selected. The mfERG examination started only after the pupil of the tested eye was dilated to at least 7 mm diameter. A DTL thread electrode was placed in the inferior fornix of the tested eye as the active electrode. Gold-cup surface electrodes were placed 10 mm lateral to the outer canthus of the tested eye and at the central forehead, as reference and ground, respectively. The refractive error of the tested eye was corrected for the working distance of the mfERG stimulator (i.e. 40 cm) with spectacle trial lenses of 35 mm diameter. The signal was amplified using a Physiodata Amplifier system (Model: 15A54, Grass Technologies, Astro-Med, Inc., West Warwick, RI, U.S.A.). The band pass was set at 10 to 200 Hz and the gain was 100,000 times. The measurement was monitored using the real-time response shown by the VERIS program, and any recording segments contaminated with blinks or small

eye movements were rejected and re-recorded immediately.

7.2.5. mfERG response analysis

The local mfERG responses were pooled into five concentric rings (Figure 7.1(b)) and averaged for analyses using the system software (VERIS 6.0.09d). Only the first order kernel response was analyzed. The first and second distinct peaks were defined as DC and IC responses respectively (Figure 7.1(c)). The DC amplitude was measured from the first distinct trough to the following peak whereas the IC amplitude was measured from the second distinct peak to the subsequent trough. The DC implicit time was measured from the onset of the multifocal flash frame to the first distinct peak. The IC implicit time was measured from the presentation of the global flash frame (i.e. 26.6 ms) to the second distinct peak.

7.2.6. Statistical analysis

Both refractive error (Kawabata and Adachi-Usami, 1997; Luu et al., 2006) and axial length (Chan and Mohidin, 2003) could affect the mfERG response in myopic adults. In essence, compared to axial length, refractive error was found to account for greater proportion of the variability in mfERG response measured

with conventional stimulation in myopic adults (Chen et al., 2006a). We hypothesized that these two factors would also operate similarly in children. Since refractive error had a greater impact than axial length on the mfERG response in adults (Chen et al., 2006a), a hierarchical regression model was used to first evaluate the effect of refractive error on the global flash mfERG response; then the total effects of refractive error and axial length on the global flash mfERG response were evaluated (see Section 6.2.6). Bonferroni correction was used to correct the level of significance due to multiple comparisons across different retinal regions, i.e. the level of significance was set at 0.01. SPSS (Version 15.0, SPSS Inc., Chicago, IL, USA) was used to perform all statistical testing.

7.3. Results

Table 7.1 summarizes the refractive error and axial length of two groups of subjects. There was no difference in refractive error (in SE) ($p > 0.05$) or axial length ($p > 0.05$) between adults and children. For both groups of subjects, there was a significant correlation between refractive error and axial length, with longer eyes being more myopic ($p < 0.001$ for children, $p < 0.01$ for adults) (Figure 7.2).

	Range		Mean	SD	Median	Unpaired t-test
	Minimum	Maximum				
Refractive error (in SE, D)						
Children	-5.50	-0.13	-2.43	1.47	-2.25	t < 0.01, p > 0.05
Adults	-5.50	-0.13	-2.43	1.75	-2.25	
Axial length (mm)						
Children	22.79	26.01	24.36	0.76	24.39	t = -0.01, p > 0.05
Adults	22.83	26.66	24.37	1.14	23.91	

Table 7.1. The characteristics of refractive error and axial length in children and adults.

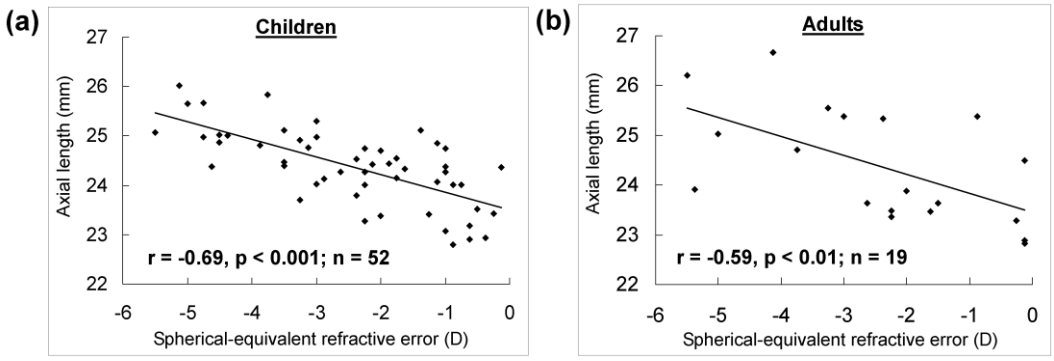

Figure 7.2. Correlation between refractive errors and axial length in (a) children and (b) adults.

Figure 7.3 shows the typical global flash mfERG waveforms recorded from a child and an adult subject with low magnitude of myopic refractive error (-0.25 - -0.50 DS). The waveforms have been normalized to facilitate comparisons of the contours of the waveforms at different eccentricities and between the two subjects. For all regions examined, the mfERG waveforms had a first positive peak at about 35 ms and a second positive peak at about 63 ms in both the child and adult. Also, there were some oscillatory wavelets between the two main

peaks in both subjects. The waveform recorded from both groups of subjects with higher magnitudes of myopia also demonstrated a similar pattern. The overall contour of the global flash mfERG waveforms at 49% contrast, which was similar to those recorded at 96% contrast, also consisted of two distinct peaks at about 35 and 63 ms, corresponding to the DC and IC responses respectively (waveform not shown).

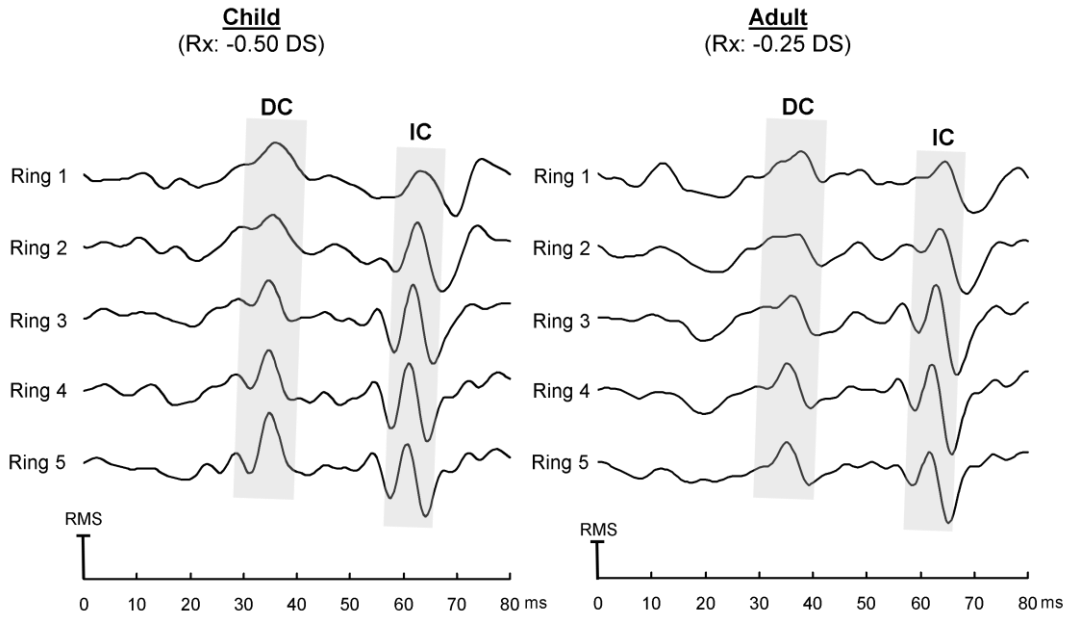

Figure 7.3. The typical ring-averaged global flash mfERG waveforms at 96% contrast recorded from a child (left) and an adult (right) with low myopia. The shaded areas indicate the DC (first distinct peak) and IC (second distinct peak) responses.

The global flash mfERG response data of both children and adults groups were log-transformed to meet the normality and linearity requirements of the hierarchical regression models applied to these findings. Table 7.2 summarizes

the results of the hierarchical regression model from the effect of refractive error, and the combined effects of refractive error and axial length on the log-DC amplitude in both child and adult groups. For the children, refractive error accounted for about 8% of the change in logarithm of DC amplitude of Ring 1 at 96% contrast ($p < 0.05$), but this just failed to reach statistical significance after Bonferroni correction. The addition of axial length as a second independent variable accounted for an extra 10% of the change in log-DC amplitude (F change = 6.16, $p < 0.05$). Thus refractive error and axial length combined accounted for 18% of the reduction in the log-DC amplitude of Ring 1 at 96% contrast ($p < 0.01$). Neither refractive error nor axial length contributed to any variance in log-DC amplitudes from Rings 2 to 5 at 96% contrast; they did not contribute to any change in log-DC amplitudes of any rings at 49% contrast in the group of myopic children (all $p > 0.05$).

For the myopic adults, refractive error accounted for 23 to 25% of reduction of log-DC amplitudes of Ring 5 at both 49% and 96% contrasts ($p < 0.05$) but it did not reach the statistically significant level after Bonferoni correction. The addition of axial length as a secondary independent variable failed to account for further changes at Ring 5. Refractive error contributed to 17 to 19% of reduction of the log-DC amplitudes at both contrasts at Ring 4, which were not statistically

significant (all $p > 0.05$). However, the addition of axial length as a secondary variable accounted for an additional 22% of reduction of log-DC amplitude at 49% contrast (F change = 5.83, $p < 0.05$). So, the combined effects of refractive error and axial length contributed to 39% of the reduction of response ($p < 0.05$) but it just failed to reach the Bonferroni corrected significance level. Neither refractive error nor axial length explained any significant changes in log-DC amplitudes at 49% or 96% contrast from Rings 1 to 3 (all $p > 0.05$).

Table 7.3 summarizes the results of the hierarchical regression model from the effect of refractive error alone and the combined effects of refractive error and axial length on log-IC amplitude for the myopic children and adults. For adults, refractive error contributed to 41 to 45% of the reduction in log-IC amplitudes from Rings 4 to 5 at 49% contrast (all $p < 0.01$) (Figure 7.4) but not the other regions examined. It did not account for any change in log-IC amplitudes at 96% contrast for any region examined. The addition of axial length did not explain additional variance in log-IC amplitudes of any region examined for either contrast (all $p > 0.05$). For the children, refractive error or axial length did not contribute to any change in log-IC amplitudes of any region examined at either 49 or 96% contrast (all $p > 0.05$).

Refractive error and refractive error combined with axial length made no

contribution to any statistical significant change in either DC or IC implicit time at either of the contrast levels examined in either group (all $p > 0.05$).

The second independent variable (i.e. axial length) had greater effect than the first independent variable (i.e. refractive error) on the DC amplitude at 96% contrast at Ring 1 in the hierarchical regression models of the children. This violated the basic assumption of this model, i.e. the impact of each independent variable at each level on the dependent variable reduced successively. Thus simple linear regression models for refractive error and axial length on the response were also performed separately for further verification. Refractive error and axial length accounted for, respectively, 8% and 18% of the reduction of log-DC amplitude respectively at 96% contrast for this region (Figure 7.5), indicating that axial length had a greater effect than refractive error on the DC amplitude in the myopic children.

	Group	Children						Adults					
	Contrast	49%			96%			49%			96%		
Region	Model	R^2	F	p	R^2	F	p	R^2	F	p	R^2	F	p
Ring 1	RE	0.04	1.93	0.17	0.08	4.15	0.05	0.05	0.90	0.36	0.07	1.26	0.28
	RE + AL	0.06	1.41	0.25	**0.18**	**5.37**	**<0.01**	0.18	1.75	0.21	0.13	1.24	0.32
Ring 2	RE	0.06	2.91	0.09	0.03	1.72	0.20	0.05	0.89	0.36	0.01	0.19	0.67
	RE + AL	0.06	1.43	0.25	0.06	1.47	0.24	0.16	1.53	0.25	0.02	0.15	0.86
Ring 3	RE	0.02	0.80	0.38	0.01	0.63	0.43	0.04	0.64	0.44	<0.01	0.02	0.89
	RE + AL	0.02	0.54	0.59	0.07	1.89	0.16	0.16	1.50	0.25	0.02	0.16	0.86
Ring 4	RE	<0.01	0.10	0.75	<0.01	0.09	0.77	0.17	3.40	0.08	0.19	3.90	0.07
	RE + AL	0.07	1.86	0.17	0.08	2.08	0.14	0.39	5.10	0.02	0.21	2.17	0.15
Ring 5	RE	0.01	0.48	0.49	0.02	1.24	0.27	0.25	5.59	0.03	0.23	4.99	0.04
	RE + AL	0.05	1.21	0.31	0.10	2.83	0.07	0.25	2.63	0.10	0.30	3.47	0.06

Table 7.2. Hierarchical regression analysis was conducted to study the effects of refractive error (RE) and the combined effects of refractive error and axial length (RE + AL) on $\log_{10}$ of DC amplitude at 49% and 96% contrasts in myopic children and adults. The table shows the R^2, F-value and p-value for each step of the models. Values in bold-face are Bonferroni-corrected statistically significant ($p < 0.01$).

	Group	Children						Adults					
	Contrast	49%			96%			49%			96%		
Region	Model	R^2	F	p	R^2	F	p	R^2	F	p	R^2	F	p
Ring 1	RE	<0.01	0.05	0.83	<0.01	0.03	0.87	0.07	1.35	0.26	<0.01	0.04	0.84
	RE + AL	<0.01	0.07	0.93	0.02	0.48	0.62	0.09	0.78	0.49	<0.01	0.05	0.95
Ring 2	RE	0.01	0.56	0.46	0.02	0.99	0.32	0.06	1.01	0.33	0.01	0.24	0.63
	RE + AL	0.02	0.52	0.60	0.10	2.74	0.07	0.21	2.06	0.16	0.01	0.12	0.89
Ring 3	RE	<0.01	0.15	0.70	0.02	0.98	0.33	0.06	1.07	0.32	0.09	1.62	0.22
	RE + AL	<0.01	0.09	0.91	0.06	1.61	0.21	0.22	2.27	0.14	0.09	0.77	0.48
Ring 4	RE	<0.01	0.62	0.44	0.03	1.66	0.20	**0.45**	**13.76**	**<0.01**	0.10	1.86	0.19
	RE + AL	<0.03	0.80	0.45	0.05	1.26	0.29	**0.50**	**7.92**	**<0.01**	0.10	0.93	0.41
Ring 5	RE	<0.02	0.78	0.38	0.05	2.64	0.11	**0.41**	**11.66**	**<0.01**	0.15	3.06	0.10
	RE + AL	<0.03	0.61	0.55	0.08	2.26	0.12	**0.51**	**8.44**	**<0.01**	0.16	1.51	0.25

Table 7.3. Hierarchical regression analysis was conducted to study the effects of refractive error (RE) and the combined effects of refractive error and axial length (RE + AL) on $\log_{10}$ of IC amplitude at 49% and 96% contrasts in myopic children and adults. The table shows the R^2, F-value and p-value for each step of the models. Values in bold-face are Bonferroni-corrected statistically significant ($p < 0.01$).

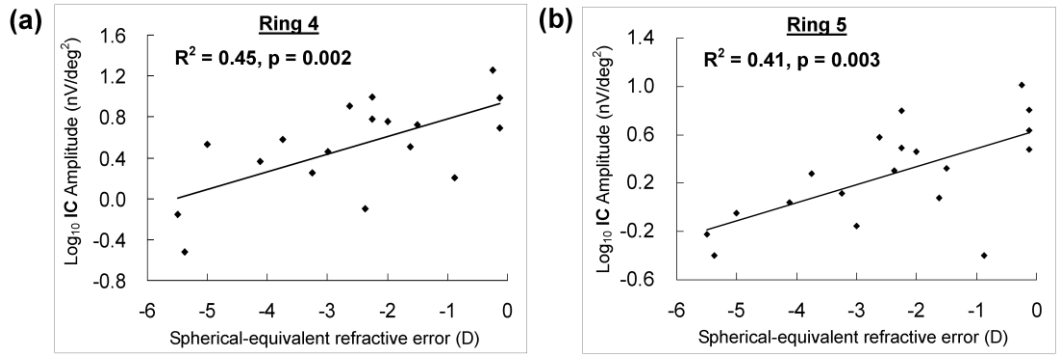

Figure 7.4. The scatter plots show the change in logarithm of IC amplitudes as a function of refractive error for (a) Ring 4 and (b) Ring 5 at 49% contrast in the adults.

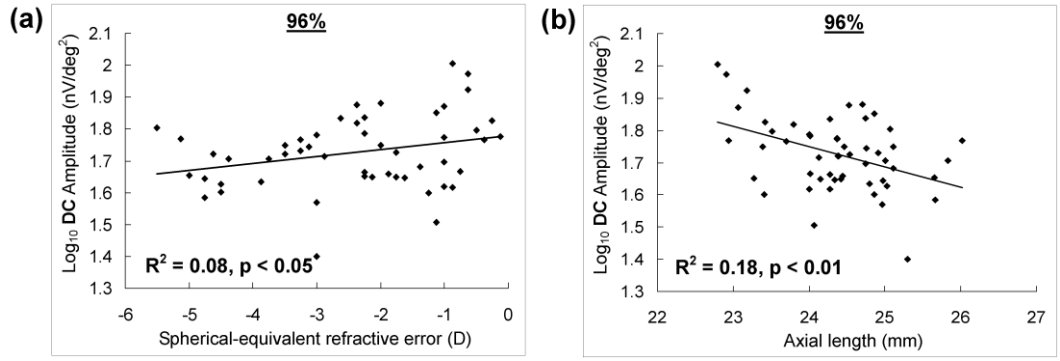

Figure 7.5. The logarithm of DC amplitudes at 96% contrast reduced with increasing (a) refractive error and (b) axial length for Ring 1 in the children.

7.4. Discussion

Unlike myopic adults, who showed reduced mfERG response in the paracentral region (i.e. Rings 4 to 5, eccentricities from 9.3 to 19.8°), myopic children showed attenuated mfERG responses in the central retina (i.e. Ring 1, within 1.5° eccentricity) (Tables 7.2 and 7.3). In addition to results shown in Experiment 1 (Chapter 6), several studies performed on myopic adults have noted reduced retinal function measured electrophysiologically (Chan and

Mohidin, 2003; Chen et al., 2006a; Kawabata and Adachi-Usami, 1997) (see Section 3.2.1) and reduced visual function examined psychophysically (Aung et al., 2001; Chen et al., 2000; Chui et al., 2005; Jaworski et al., 2006; Liou and Chiu, 2001; Mantyjarvi and Tuppurainen, 1995; Rudnicka and Edgar, 1995; Rudnicka and Edgar, 1996; Subbaram and Bullimore, 2002). However, there is a paucity of data in the literature regarding retinal or visual function in myopic children. Luu and his co-workers (2006) reported that the mfERG response measured with conventional mfERG stimulation is generally reduced and delayed in myopic adults but is only delayed in myopic children. We have found a reduction in central, high contrast, DC response amplitude of mfERG in myopic children, but have found no effect on implicit time of the response.

Depending on the age groups, various parameters (i.e. refractive error and axial length) showed different effects on the mfERG responses. In myopic adults, refractive error contributed more to the delay in conventional mfERG response when compared to axial length (Chen et al., 2006a). Our study showed that refractive error contributed 41 to 45% of reduction in IC amplitude in adults but axial length did not account for an additional change in children; this substantiates the findings of Experiment 1 (Chapter 6). Both Chen et al. (2006a) and Experiment 1 showed that refractive error had a strong effect on the mfERG

response in myopic adults. However, in children, axial length explained a greater amount of the reduction of the DC response at 96% contrast than did refractive error in both the hierarchical regression (Table 7.2) and simple regression analyses (Figure 7.5). So, the investigation of the effect of refractive error on the mfERG response alone may not be sufficient to explain the characteristics of retinal electrophysiology in myopic children; axial length needs to be taken into consideration, since it is an important determinant of retinal illuminance. Our study shows that the effect of increases in both refractive error and axial length on the mfERG response was different between children and adults with myopia.

Luu and his colleagues (2006) did not find any reduction in central mfERG response in myopic children whereas our study detected a retinal functional change in the central region with the global flash mfERG paradigm. The discrepancy in results may be associated with the difference in the mfERG stimulation sequence as well as with differences in the analytical method. Firstly, the global flash mfERG paradigm incorporates a dark frame between the multifocal flash frame and the global flash. It allows a better separation of the retinal responses from outer and inner retinal activities, without overlapping of those responses due to subsequent flashes (Shimada et al., 2005; Sutter et al., 1999). Secondly, we used a scaled 61-hexagon array, while Luu et al. (2006) used

a scaled 37-hexagon array as the stimulus; the 61-hexagon array provides better resolution of response topography for identifying localized functional changes. Thirdly, our regression analyses showed that axial length explained a significant reduction of the DC response in myopic children, while refractive error did not, which probably explains why Luu and his co-workers (2006) could not find any reduction in mfERG response.

The paracentral (i.e. Rings 4 to 5, eccentricities from 9.3 to 19.8°) IC amplitudes at middle contrast (i.e. 49% contrast) were reduced in myopic adults (Figure 7.4) while the IC responses of all regions were unaffected in myopic children. The IC amplitudes at 96% contrast of all regions were not changed over the range of refractive errors examined in either the children or adults. The IC response primarily reflects the inner retinal activities (i.e. retinal ganglion cells and amacrine cells) (see Section 6.4; Paragraph 2). The current experiment suggests that the inner retinal function in the paracentral region was weakened in myopic adults, which matches with the findings of Experiment 1 (Chapter 6), but inner retinal function within the central region (~40° of visual angle) was virtually unaffected in myopic children.

The effect of myopia on the mfERG response varied in terms of the regions and retinal components affected between children and adults. The central (i.e.

Ring 1, within 1.5° eccentricity) DC amplitude at high contrast was reduced in myopic children but the DC responses of all regions examined were almost unaffected in myopic adults (Table 7.2). The DC response at high contrast reflected activity from outer retina, and that at middle contrast consisted of greater contribution from inner retina (see Section 6.4; Paragraph 1). The central macular DC amplitude was reduced at high contrast but was unchanged at middle contrast in myopic children, indicating that the functional change mainly occurred at an outer retinal level.

On the other hand, the reduced DC amplitude at high contrast found only in myopic children but not in adults is in need of further study. It may be a cause of ocular growth during progression of myopia. Intact retinal function is essential for emmetropization. Early disruption of normal retinal function with neurotoxic agents during postnatal development in animal studies have been reported to cause myopia development (Fischer et al., 1998a; Fischer et al., 1997; Wildsoet and Pettigrew, 1988). Furthermore, a reduction in foveal mfERG response has also been associated with subsequent higher rates of myopia progression in children (Luu et al., 2007). We therefore speculate that the reduced central macular DC amplitude at high contrast in myopic children may be related to the process of ocular development, and may be associated with myopia progression

in this age group (Edwards, 1999). Additionally, the difference in the central mfERG response between children and adults with myopia may be related to the age-related physiological changes at macular region. Further study is necessary to investigate the changes in mfERG response during myopia development in order to understand the underlying cause of regional changes in retinal function between myopic children and adults.

The stretch factor chosen for the hexagonal array was the same in both children and adults groups. The scaling of the hexagon follows the change of photoreceptor cell density across the retina (Sutter and Tran, 1992). To date, it is still lack of study related to the age-related change in cell density and cell number from childhood to adulthood. If there is a variation in cell density between children and adults, the difference in mfERG response amplitude between two groups may attribute to both the age-related retinal functional change and the variance of cell density.

7.5. Conclusions

Only the central macular DC amplitude at 96% contrast was reduced in myopic children. The fact that paracentral IC amplitudes were reduced at middle contrast in myopic adults indicates that inner retinal function is weakened in

these subjects. This study demonstrates the difference in retinal electrophysiological activity between children and adult myopes in terms of regions and retinal components affected.

Chapter 8 - Experiment III - Myopia progression in children is linked with reduced foveal mfERG function

(Adapted from the manuscript published in Investigative Ophthalmology and Visual Science 2012, 53, 5320-5325)

Abstract

Previous studies have suggested that there is a difference in the retinal electrophysiology of myopic children and adults. This study aimed to investigate the changes in retinal electrophysiology in children during myopia progression over a 1-year period.

Twenty-six children aged from 9 to 13 years were recruited for the global flash mfERG measured at 49% and 96% contrasts, in two visits 1-year apart. The amplitudes and implicit times of both DC and IC responses measured at these two visits were analyzed and compared. Pearson's correlation was used to study the association between the changes of mfERG response and myopia progression over the test period.

Myopia increased by -0.48 ± 0.32 D ($p < 0.001$) over the year, with 24 of 26 children becoming more myopic (range = 0.00 ~ -1.38 D); axial length increased by 0.25 ± 0.11 mm ($p < 0.001$) (range = 0.05 ~ 0.47 mm) over the year. The increased myopia was highly correlated with increase in axial length ($r = -0.70$; $p < 0.001$). The central DC and IC amplitudes at 49% contrast were significantly reduced as myopia progressed and the paracentral responses of these two components were slightly reduced.

Our findings suggested that the inner retinal functions in the central retina, with

some involvement of the paracentral region, were significantly decreased as myopia progressed.

8.1. Introduction

In Experiment 2 (Chapter 7), myopia produced different effects on retinal function in adults and children in terms of the regions and the retinal components affected. Specifically, myopic children showed reduced retinal function in the central macular region, while myopic adults had weaker retinal function in the paracentral region. Moreover, the functional changes appeared to occur at the outer retinal level in myopic children but at the inner retinal level in myopic adults. These findings matched those of Luu and his co-workers (2006), who found that mfERG response was reduced and delayed in myopic adults but was only delayed in myopic children.

However, there are currently no longitudinal data available on changes of retinal physiology in children during myopia progression. Luu and his colleagues (2007) characterized the mfERG response prospectively in children with progressing myopia; they measured both the refraction and mfERG response at the first visit and only the refraction at the follow-up visit. They found that children who had weaker foveal mfERG response at the initial visit exhibited a

higher rate of myopia progression (Luu et al., 2007). Since retinal electrophysiology was not measured at the second visit, it is not known whether there was a change in retinal function in these children. The paracentral retina has been shown to be affected in adult myopes (Experiment 1; Chapter 6), and thus the present study aimed to investigate the regional changes of retinal function in children during myopia progression. The global flash mfERG with different contrasts stimulation was used to separate the inner and outer retinal contributions to the mfERG response.

8.2. Methods

8.2.1. Subjects

Twenty-six subjects aged from 9 to 13 years (mean = 10.6 ± 1.2 years; median = 11.0 years) were recruited. All subjects received eye examinations at the initial visit and again at a follow-up visit scheduled one year later. This eye examination included objective and subjective refraction (see below), axial length measurement and mfERG recording. In both visits, all subjects had best corrected visual acuity of logMAR 0.00 or better in both eyes, normal colour vision, and ocular health. Exclusion criteria were any ocular disease, clinically significant retinal degeneration, systemic disease and history of epilepsy.

All subjects were accompanied by their parent(s) or legal guardian(s) throughout the ophthalmic examination and experiment. Before the experiment began, the aim of the study was fully explained and written consent was obtained from the parents or legal guardians. All the experimental procedures followed the tenets of the Declaration of Helsinki. This study was reviewed and approved by the Human Ethics Committee of The Hong Kong Polytechnic University.

8.2.2. Refraction and axial length measurement

Before the ophthalmic examination, one drop of 0.4% Oxybuprocaine (Agepha Pharmaceuticals, Austria) was instilled, followed by 2 drops of 1% Tropicamide (Alcon Laboratories, Inc., Fort Worth, TX, USA) (5 minutes apart) to dilate the pupils of both eyes and paralyze accommodation temporarily. Cycloplegic refraction was measured objectively with an auto-refractor (Model: KR 8800, Itabashi-ku, Tokyo, Japan) at least 30 minutes after the instillation of eyedrops; this was followed by subjective refraction and measurement of visual acuity. The objective refraction was measured three times to obtain a mean value. The reading was regarded as valid if the range of the three readings, for either spherical or cylindrical component, was equal to or smaller than 0.25 D. Axial length was measured with a non-contact optical biometer (IOL Master, V.4.08,

Carl Zeiss Meditec, Inc., Dublin, CA, USA). The axial length was measured five times to obtain a mean value. The readings of axial length were valid if the range of the five readings was equal to or smaller than 0.10 mm and the signal score of each reading was equal to or greater than 2.0, as stated in the IOL Master User's Manual.

8.2.3. mfERG stimulation

The mfERG stimulus pattern was presented on a 22-inch liquid crystal display (Model: 2232GW+, SAMSUNG, Tianjin, China) controlled by VERIS (VERIS Science 6.0.09d19, Electro-Diagnostic Imaging, Redwood City, CA, USA). The stimulus consisted of a 61-hexagon array, scaled with eccentricity (Stretch factor = 12.18). The hexagonal array subtended 39° horizontally and 37° vertically at a working distance of 40 cm.

The video frame sequence of the global flash mfERG stimulation began with a multifocal flash frame, followed by a dark frame, a global flash and a second dark frame for each m-sequence stimulation, at a video frame rate of 75 Hz (Figure 8.1a) (Chu et al., 2006; Fortune et al., 2002; Shimada et al., 2001). For the multifocal flash frame, each hexagon was flickered between bright and dark stimulation, according to the chosen pseudorandom binary m-sequence.

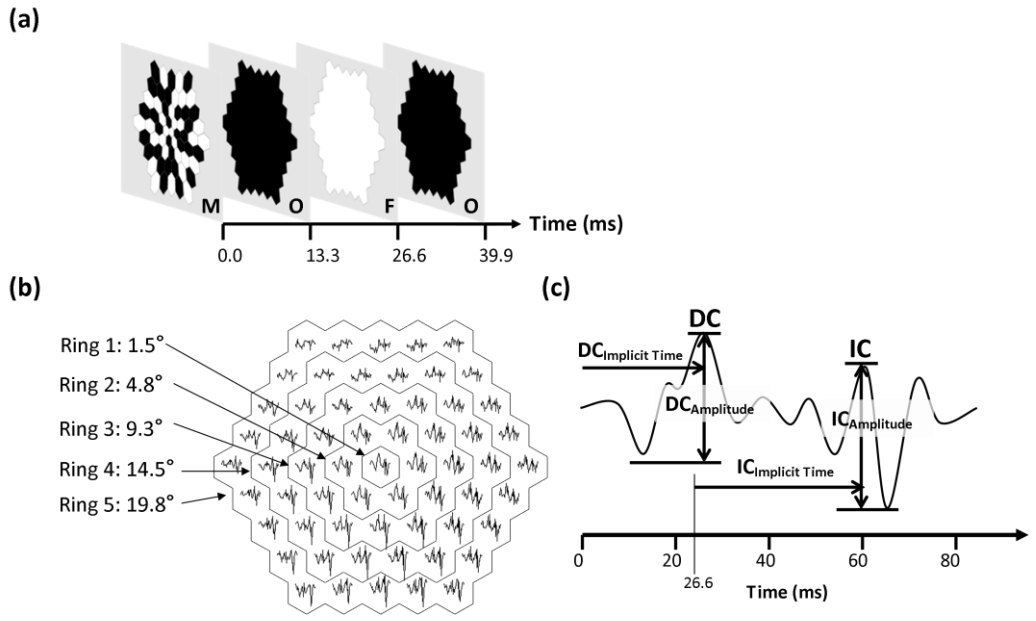

Figure 8.1. (a) A schematic diagram showing the video frames of the global flash mfERG in each m-sequence stimulation, which consisted of a multifocal flash frame ("M"), a dark frame ("O"), a global flash frame ("F"), and a second dark frame ("O"). (b) The 61 local responses were pooled into 5 concentric rings for analyses. The value indicated the eccentricity boundary (in visual angles) of each region. (c) The typical global flash mfERG response was shown (See text in details).

The global flash mfERG was measured at 49% and 96% contrasts. These contrasts were produced by the luminance differences of the bright and dark hexagons of the multifocal flash, set at 60 cd/m^2 and 96 cd/m^2, while the mean luminance of the multifocal flash was set at 50 cd/m^2. For each condition, the recording time was 3 minutes and 40 seconds with a 2^{12} binary m-sequence; the whole process was divided into 16 slightly overlapping segments for recording. The order of presentation of the two contrast conditions was randomized.

8.2.4. mfERG recording

For each subject, the eye with the lower magnitude of astigmatism was chosen for recording and the other eye was occluded during measurement. If the magnitude of astigmatism was equal between the two eyes, one eye was randomly chosen for recording.

The mfERG examination started after the pupil was dilated to at least 7 mm. A DTL thread electrode was placed in the inferior fornix of the tested eye to contact with the inferior cornea as the active electrode. Gold cup electrodes were placed 10 mm lateral to the outer canthus of the tested eye and at the central forehead, to serve as reference and ground electrodes respectively. The refractive error of the tested eye was corrected for the working distance of the mfERG stimulator (40 cm) with spectacle trial lens(es) of 35 mm diameter. The mfERG signal was amplified 100,000 times and the band pass was set at 10 to 300 Hz (Model: 15A54, Physiodata Amplifier system, Grass Technologies, Astro-Med, Inc., West Warwick, RI, U.S.A.). The signal was monitored by the examiner using the real-time response provided by the VERIS program; any segment contaminated by blinks or loss of fixation was immediately re-recorded.

8.2.5. Analysis

The 61 local mfERG responses were pooled into five concentric rings for analysis (Figure 8.1b). The amplitudes of DC and IC responses were analyzed by using peak-to-peak measurement (Figure 8.1c). The implicit times of DC and IC responses were measured from the onset of multifocal flash and global flash respectively to their response peaks. The changes in mfERG response (including both amplitude and implicit time domains) were obtained by subtracting the mfERG responses at the follow-up visit from those at the initial visit.

The averaged value of the three objective refraction findings provided by the auto-refractor was converted into spherical-equivalent value (SE) (= spherical component + 0.5 x cylindrical component). Myopia progression was calculated as the difference in cycloplegic objective refraction (in SE value) between two visits, i.e. subtracting the refractive error at the follow-up visit from the refractive error at the initial visit. Pearson's correlation was used to investigate any association between myopia progression and changes in mfERG response. Bonferroni adjustment was applied to correct for multiple comparisons of different retinal regions, i.e., the level of significance was set at 0.01. SPSS (Version 15.0, SPSS Inc., Chicago, IL, USA) was used to carry out the statistical analysis.

8.3. Results

Twenty-three of the 26 subjects were myopic at the initial visit. One more child became myopic at the follow-up visit. Twenty-four children showed a myopic shift during the study. Table 8.1 summarizes the refractive error and axial length findings, as well as the changes in these ocular parameters between the two visits. There was a statistically significant increment in myopic refractive error of 0.48 D (paired t-test, $t = 7.58$, $p < 0.001$) and an increase of axial length of 0.25 mm (paired t-test, $t = -11.57$, $p < 0.001$) during the study. The increase in myopia was significantly correlated with the increase in axial length (Pearson's correlation, $r = -0.70$, $p < 0.001$) (Figure 8.2). However, the refractive error in the first visit did not correlate with the myopia progression (Pearson's correlation, $r = 0.22$, $p = 0.28$) (Figure 8.3).

	Range		**Mean**	**SD**	**Median**
	Minimum	**Maximum**			
Refractive error (in SE, D)					
Initial	+0.50	-6.25	-2.14	1.62	-2.00
Follow-up	+0.25	-7.00	-2.62	1.72	-2.38
Changes in refractive error (= Follow up – initial)	0.00	-1.38	-0.48	0.32	-0.50
Axial length (mm)					
Initial	22.94	26.07	24.36	0.80	24.41
Follow-up	23.19	26.31	24.61	0.84	24.62
Changes in axial length (= Follow up – initial)	0.05	0.47	0.25	0.11	0.25

Table 8.1. Refractive error and axial length of the subjects at the initial and follow-up visits.

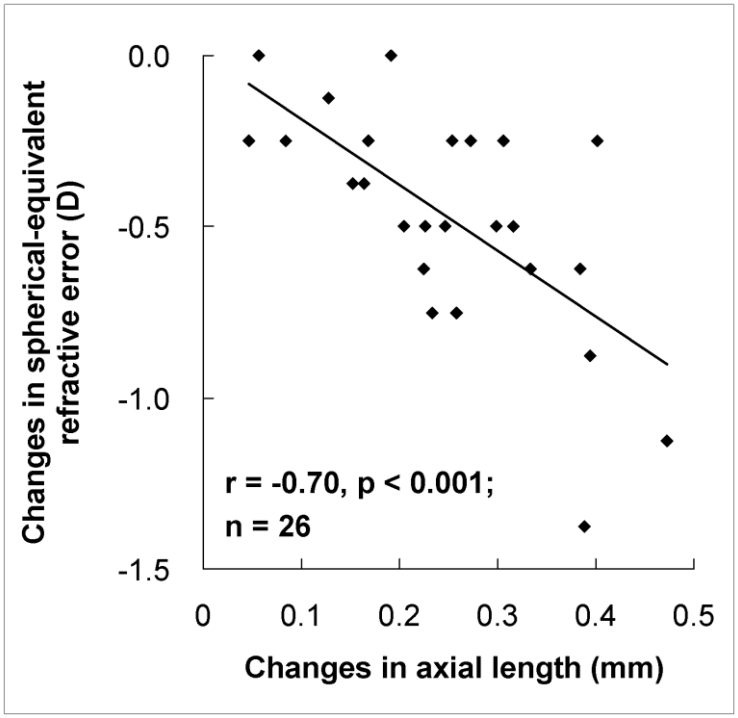

Figure 8.2. The correlation between changes in axial length and myopia progression.

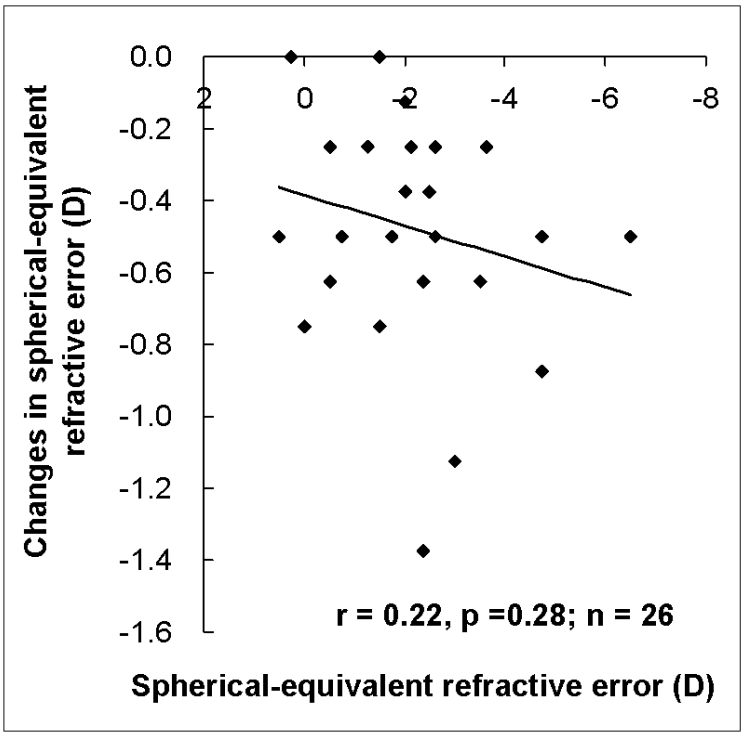

Figure 8.3. The correlation between the refractive error at the first visit and myopia progression over the 1-year period.

Figure 8.4 illustrates the typical global flash mfERG waveforms recorded at 49% and 96% contrasts for a subject at the initial visit. As shown, the waveforms consisted of both DC and IC responses for all regions examined. For both contrasts, both DC and IC responses had reduced amplitudes and mildly reduced implicit times with increasing eccentricity.

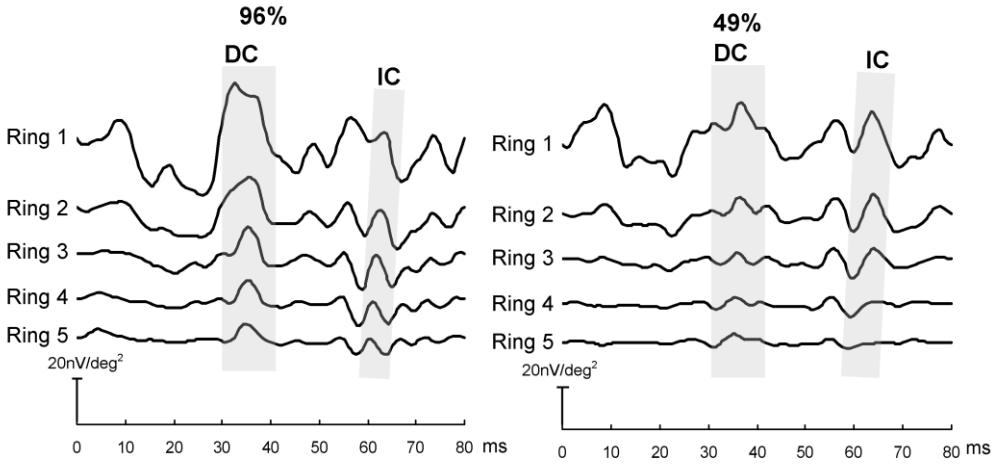

Figure 8.4. The global flash mfERG response recorded from a subject at 96% contrast (left) and 49% contrast (right) (refractive error: -3.75/-1.25x5).

Tables 8.2 and 8.3 show the changes of mfERG response at 49% and 96% contrasts for different regions during myopia progression over the 1-year period of this study. As myopia increased, the DC amplitudes at 96% contrast, and both the DC and IC amplitudes at 49% contrast, of all regions examined were reduced. The IC amplitudes at 96% contrast of central Rings 1 and 2 were reduced, but the amplitudes of Rings 3 and 4 were slightly increased (Table 8.2).

For the time domain (Table 8.3), the IC implicit times at both contrast levels tended to be reduced. In contrast, the DC implicit times at 49% contrast of Rings 1 and 2 were increased and that of paracentral region from Rings 3 to 5 were decreased. The DC implicit times at 96% contrast were slightly increased for all regions examined, except Ring 1.

Parameter	**Changes of amplitude (nV/deg^2) (mean ± SD)**			
Contrast	96%		49%	
Component / Region	DC	IC	DC	IC
Ring 1	-11.69±26.24	-12.27±25.63	-11.42±24.16	-5.32±19.81
Ring 2	-6.17±11.38	-0.59±14.76	-3.15±8.12	-1.46±6.30
Ring 3	-2.37±5.46	1.53±10.33	-0.63±4.08	-1.14±4.19
Ring 4	-2.22±3.54	0.52±7.07	-0.15±2.81	-0.70±2.37
Ring 5	-1.58±2.62	-0.49±4.14	-0.81±2.10	-0.20±1.69

Table 8.2. Changes of global flash mfERG response amplitude (= follow-up - initial) of the children at 96% and 49% contrasts over the 1-year period.

Parameter	**Changes of implicit time (ms) (mean ± SD)**			
Contrast	96%		49%	
Component / Region	DC	IC	DC	IC
Ring 1	-0.46±2.65	-0.23±2.67	0.15±4.02	0.44±2.58
Ring 2	0.25±2.36	-0.33±2.40	0.02±3.01	-0.48±2.15
Ring 3	0.19±1.29	-0.36±3.06	-0.21±3.53	-0.57±2.47
Ring 4	0.38±1.47	-0.64±2.36	-0.16±1.88	-0.02±2.73
Ring 5	0.30±1.65	-0.26±2.00	-0.41±2.68	0.30±3.07

Table 8.3. Changes of global flash mfERG implicit time (= follow-up - initial) of the children at 96% and 49% contrasts over the 1-year period.

Tables 8.4 and 8.5 summarize the Pearson's correlation (r) values between the changes in refraction and those in global flash mfERG response. Myopia progression mainly influenced the global flash mfERG response at 49% contrast but not at 96% contrast. For the amplitude domain (Table 8.4), at 49% contrast, the DC amplitudes for Rings 1 and 2 were significantly reduced as myopia progressed ($r = 0.45 \sim 0.50$, both $p < 0.05$), though only the correlation for Ring 1 was statistically significant after Bonferroni correction. The change in DC amplitudes from Rings 3 to 5 was not significantly correlated with the change in refraction. On the other hand, the IC amplitudes for Rings 1 and 3 were significantly reduced as myopia progressed ($r = 0.44 \sim 0.53$, $p < 0.05$) but only the correlation for Ring 1 reached the Bonferroni corrected significance level. The amplitudes for Rings 2, 4 and 5 were not significantly affected by myopia progression. For the time domain (Table 8.5), as myopia progressed, the DC implicit time for Ring 3 was significantly reduced ($r = 0.54$, $p < 0.01$) and the IC implicit time for Ring 4 was significantly increased ($r = -0.40$, $p < 0.05$). However, only the change in DC implicit time for Ring 3 reached the Bonferroni corrected significance level. The implicit times of both DC and IC responses for the remaining regions were not significantly changed. At the 96% contrast, neither the amplitudes nor implicit times of DC and IC responses were

significantly changed as myopia progressed.

Parameter	**Amplitude**							
Contrast	**96%**				**49%**			
Component / Region	DC		IC		DC		IC	
	r	p	r	p	r	p	r	p
Ring 1	0.34	0.09	-0.09	0.66	**0.50**	**<0.01***	**0.53**	**<0.01***
Ring 2	0.15	0.48	-0.08	0.69	**0.45**	**0.02**	0.26	0.21
Ring 3	0.17	0.41	0.02	0.91	-0.02	0.94	**0.44**	**0.02**
Ring 4	0.08	0.70	-0.02	0.92	0.08	0.71	0.04	0.86
Ring 5	0.15	0.46	-0.08	0.69	-0.05	0.81	0.17	0.41

Table 8.4. Pearson's correlation (r) between the change in refraction and the change in global flash mfERG response amplitude of both DC and IC responses for different regions and their corresponding significance levels (p). Values in bold-face are statistically significant (p < 0.05) and those marked with "*" reach the Bonferroni-corrected statistically significant level (p < 0.01).

Parameter	**Implicit time**							
Contrast	**96%**				**49%**			
Component / Region	DC		IC		DC		IC	
	r	p	r	p	r	p	r	p
Ring 1	-0.03	0.88	-0.20	0.33	-0.11	0.58	0.22	0.28
Ring 2	-0.18	0.37	-0.32	0.11	0.12	0.95	-0.19	0.37
Ring 3	-0.11	0.60	-0.24	0.25	**0.54**	**<0.01***	-0.26	0.19
Ring 4	-0.01	0.96	0.24	0.24	0.32	0.11	**-0.40**	**0.04**
Ring 5	-0.08	0.68	**0.49**	**0.01**	0.10	0.63	-0.29	0.15

Table 8.5. Pearson's correlation (r) between the change in refraction and the change in global flash mfERG response implicit time of both DC and IC responses for different regions and their corresponding significance levels (p). Values in bold-face are statistically significant (p < 0.05) and those marked with "*" reach the Bonferroni-corrected statistically significant level (p < 0.01).

8.4. Discussion

We found that myopia progression mainly affected retinal function from central to paracentral regions (i.e. Rings 1 to 3, within eccentricity values to 9.3°; Tables 8.4 and 8.5), independent of the initial refractive status (Figure 8.3). There is no longitudinal study in the literature investigating the change of retinal function in children during myopia progression. Luu and his colleagues (2007) examined the mfERG response in children with progressing myopia. However, they only measured the mfERG response at the initial visit but not at the follow-up visit. They showed that retinal function in the foveal region was substantially reduced before the subjects became more myopic. Our study demonstrated that attenuated retinal function was present mainly in the central region as myopia progressed, in agreement with the conclusion of Luu et al. (2007).

Chen and her co-workers (2006a; 2006b) characterized the mfERG response of adults with progressing myopia. They classified their subjects into either stable or progressing myopes by comparing the current refractive status with their previous clinical records. They showed that myopia progression predominantly affected paracentral to mid-peripheral regions with either a reduced response amplitude (Chen et al., 2006a) or a shortened implicit time of

mfERG response (Chen et al., 2006b), depending on the stimulation used (see Section 3.3). Similarly, our current study showed that the paracentral DC (Ring 2) and IC (Ring 3) amplitudes at 49% contrast were also considerably reduced in the eyes of children showing more myopic progression (Table 8.4). Our results suggest that the central region is the critical area adversely affected during myopia progression in children (i.e. Ring 1; within eccentricity 1.5°; Table 8.4), in agreement with the findings of Luu and colleagues (2007). The difference between our study and those of Chen et al. (2006a; 2006b) might be due to the different modes of mfERG stimulation employed and, most likely, the age of the subjects (children versus young adults).

The DC implicit time was reduced in children with progressing myopia (Table 8.5). Chen et al. (2006b) used the slow flash paradigm (i.e. a multifocal flash frame followed by three dark frames for each of the m-sequence stimulation) and extracted the oscillatory potentials by filtering, thereby restricting the signal to the high frequency range (100-300Hz). They reported that the implicit times of these oscillatory potentials were reduced in adults with progressing myopia. In contrast to their protocol, we used a global flash paradigm, it has been found that the contour of DC response in the global flash paradigm superimposed several "oscillatory potentials" in porcine eyes (Chu et al., 2008). The reduction of DC

implicit time in children with progressing myopia may also be related to the alteration of the activity of these “sheltered” oscillatory potentials. The reduction of the DC implicit time in the paracentral region is generally consistent with the findings of Chen et al. (2006b).

Myopia progression predominantly affected both central and paracentral mfERG responses at middle contrast (i.e. 49%) stimulation but not at high contrast (i.e. 96%) (Table 8.4). Specifically, the central DC response and the central to paracentral IC responses for middle contrast stimulation were significantly reduced as myopia progressed. In contrast, the mfERG response at high contrast was virtually unaffected during myopia progression. The IC response originates from retinal ganglion cells and amacrine cells of the inner retina (see Section 6.4, Paragraph 2). The reduced central IC response suggests that inner retinal function is reduced as myopia progresses. This idea is supported by the finding that eye disease involving inner retinal defects, e.g., glaucoma, also shows significant reduction in DC amplitude at middle contrast but only mild reduction in DC amplitude at high contrast (Chu et al., 2006; Fortune et al., 2002). Taken together, our results suggest that inner retinal function from central to paracentral regions is predominantly attenuated during myopia progression.

Our results of reduced inner retinal function in myopic children is consistent

with the results reported by Fujikado et al. (1996) in a chicken model of myopia development. In a longitudinal study of the electrophysiological change in chick eye during form-deprivation induced myopia, Fujikado et al. (1996) found that the oscillatory potentials of the full-field ERG response, which predominantly represents the activity from inner plexiform cells (Wachtmeister, 1998), were reduced gradually during myopia development and occurred prior to axial elongation. In contrast, the b-wave of the full-field ERG response, representing response of outer retinal cells such as bipolar cells and Müller cells (Sieving et al., 1994), was left unaffected throughout myopia development (Fujikado et al., 1996). These results support the hypothesis that inner retinal function is most affected during myopia progression.

The myopia progression is associated with the axial elongation (Figure 8.2). The increase in eyeball length is linked with the decline in photoreceptor cell density (Chui et al., 2008). Therefore, it is possible that the reduced mfERG response amplitude may reflect the decline in cell density, instead of the change in retinal function. However, the change in cell density should affect the mfERG response amplitude for both contrasts, rather than the response at 49% contrast only. The photoreceptor density decreased from 15300 cells/mm^2 in low myopes of axial length 24.72 mm to 13600 cells/mm^2 in emmetropic eye with axial

length of 23.24 mm at eccentricity of 1° (Chui et al., 2008). In other words, the cell density is reduced by 1149 cells/mm^2 per millimetre increase in axial elongation (~ 8% reduction per millimetre axial elongation). While the axial length of the children on average was increased by 0.25 mm over this one year period, the DC and IC amplitudes at 49% contrast were reduced by 11.42 nV/deg^2 (~ 27% reduction) and 5.32 nV/deg^2 (~23% reduction) respectively (Table 8.2). Therefore, small change in cell density cannot fully account for the mfERG response reduction.

In addition to the results of Experiment 1 (Chapter 6), adult myopes showed reduced retinal function from paracentral to peripheral regions (Chan and Mohidin, 2003; Chen et al., 2006a; Kawabata and Adachi-Usami, 1997) (see Section 3.2.1). Children with progressing myopia showed reduced retinal function from central to paracentral regions, especially in the central region. There is regional change in reduced retinal function from children to adults as myopia progressed. Both adults with myopia (Experiment 1; Chapter 6) and children with progressing myopia consistently show functional losses in the paracentral retina. We believe that the functional losses of the paracentral retina in children during myopia progression may be related to impaired retinal function of the paracentral retina in adults with myopia. On the other hand, we

did not expect to find, as we did, reduced function of the central region in children with progressing myopia but no such finding in adults with myopia. We speculate that this difference in central macular function between myopic children and adults may be related to age-dependent modulation of eye growth as well as myopia progression, which requires further investigations.

8.5. Conclusions

During myopia progression, the DC and IC responses for middle contrast stimulation were significantly reduced in the central region of the retina and these responses were also considerably weakened in the paracentral region. Our findings suggest that the inner retinal functions of the central and perhaps paracentral regions, deteriorate during myopia progression in children.

Chapter 9 - Experiment IV - Sign-dependent changes in retinal electrical activity with positive and negative defocus in the human eye

(Adapted from the manuscript published in Vision Research 2012, 52, 47-53)

Abstract

The purpose of this study was to investigate the effect of optical defocus on changes of electrical response as a function of retinal region.

Twenty-three subjects (aged from 19 to 25 years) with normal ocular health were recruited for global flash mfERG recordings under the control condition (in-focus, fully corrected), short-term positive defocus conditions (+2 D and +4 D) and short-term negative defocus conditions (-2 D and -4 D). The amplitudes and implicit times of DC and IC responses were pooled into six concentric rings for analyses.

The mfERG responses demonstrated more significant changes in amplitude in paracentral retinal regions than in the central regions under defocused conditions. The paracentral DC amplitudes showed a significant reduction under negative defocus conditions. In contrast, the paracentral IC amplitudes showed a significant increment under positive defocus conditions. Interestingly, the central IC responses showed significant reduction in amplitude only to negative defocus, while increasing their amplitude to positive defocus. However, the DC and IC implicit times were virtually unaffected under defocused conditions.

Our findings suggest that human retina is able to differentiate defocus signals and to identify positive and negative defocus, and that paracentral retina reacts more

vigorously to optical defocus than does central retina.

9.1. Introduction

The eye is found to compensate for optically imposed positive defocus and negative defocus in animal studies (Howlett and McFadden, 2009; Hung et al., 1995; Irving et al., 1992; Norton and Siegwart, 1995; Schaeffel et al., 1988; Smith and Hung, 1999). Therefore, eye growth has been thought to be a visually-guided process (see Section 4.2.3.1). In the case of regionally imposed defocus, the posterior contour of the eyeball shows compensatory eye growth in the region of defocus, indicating that eye growth is regulated by local visual signals (Diether and Schaeffel, 1997; Smith et al., 2010). It is still controversial regarding to the involvement of higher visual centres for interpretation of the signs of defocus; study in guinea pig supports for it (McFadden and Wildsoet, 2009), whereas, studies in chicks against for it (Choh et al., 2006; Schmid and Wildsoet, 1996; Wildsoet, 2003). The discrepancy of findings may be related to the difference in animal species. Therefore, it is very important to study such as issue directly in human eye, in order to understand the underlying mechanism in eye growth.

The retina receives the focus signals and then triggers a cascade within the

signaling pathway involving a range of biochemical messengers, for instance, dopamine (Guo et al., 1995), retinoic acid (Mertz et al., 1999) and glucagon (Buck et al., 2004) to initiate the eye growth process. Amacrine cells have been hypothesized to be one of the key retinal cells in detecting eye growth signals because of its sign-dependent changes of ZENK expression (Fischer et al., 1999). It is still unknown whether other retinal cells are involved in detecting optical defocus. In addition, Liu and Wildsoet (2011) have recently found that imposing peripheral defocus in chicks (while maintaining clear central vision in regions of varying size) had profound effects on the refractive error development of the whole globe. Their study implies that different parts of the retina react differently to optical defocus signals. However, the basis for the regional variations in discriminating the defocus signals is still unknown. The lack of appropriate tools to measure the regional retinal activity to defocus has been one of the barriers to this research.

The mfERG, however, can assess electrical activity of multiple retinal loci in response to light stimuli (Sutter and Tran, 1992). The global flash paradigm of the mfERG generates two separated components illustrating the activity from outer and inner retina (Chu et al., 2008). Thus, it can help to investigate the instantaneous change of electrical activity from different parts of the retina to the

defocus signals.

Zhu and co-workers (2005) had chicks wear +10 D or -7 D or -8.6 D lenses for 10 minutes, and there were increases or decreases in choroidal thickness in response to the positive or negative lenses respectively. The choroid in human eyes also showed thinning under negative defocus and thickening under positive defocus (Read et al., 2010). The aim of the present experiment was to investigate the short-term effects of optical defocus on retinal activity in humans, in different retinal regions, using the global flash mfERG.

9.2. Methods

9.2.1. Subjects

Twenty-three young adults aged from 19 to 25 years (mean = 22.5 ± 1.3 years; median = 22.0 years) were recruited. They received a comprehensive eye examination including cycloplegic subjective refraction and ocular health assessment. All had best corrected logMAR visual acuity of 0.00 or better, astigmatism of 1.00 D or less, normal colour vision and ocular health. Subjects with any ocular pathology, any known systemic disease, or history of epilepsy were excluded from this study. The refractive errors (in SE) of the subjects ranged from +1.50 to -5.25 D (mean = -1.92 ± 0.42 D; median = -2.13 D) and

astigmatism ranged from 0.00 to -1.00 D (mean = -0.47 ± 0.36 D; median = -0.50 D).

After detailed explanation of the experiment, all subjects gave informed consent. This experiment adhered to the tenets of the Declaration of Helsinki and was reviewed and approved by the Human Ethics Committee at The Hong Kong Polytechnic University.

9.2.2. mfERG stimulation

The stimulus array consisted of 103 non-scaled hexagons presented on a 22-inch colour liquid crystal display (Model: 2232GW plus, SAMSUNG, Tianjin, China). The stimulus pattern subtended 29° horizontally and 24° vertically at a working distance of 67 cm. The VERIS (VERIS Science 6.0.6d19; Electro-Diagnostic Imaging Inc., Redwood City, CA, USA) was used to present the global flash mfERG stimulation. The stimulation sequence consisted of a multifocal flash frame, a dark frame, a full screen global flash and a dark frame in each cycle (Chu et al., 2006; Fortune et al., 2002; Shimada et al., 2001) (Figure 9.1a). For the multifocal flash frame, the luminance of the bright and dark stimuli were 180 cd/m^2 and 1 cd/m^2 respectively. Each hexagonal stimulus was temporally modulated between bright and dark stimulus, according to a

pseudo-random binary m-sequence stimulation. The frame rate was 75 Hz. The luminance of the global flash frame was 180 cd/m^2 and that of the background was 90 cd/m^2.

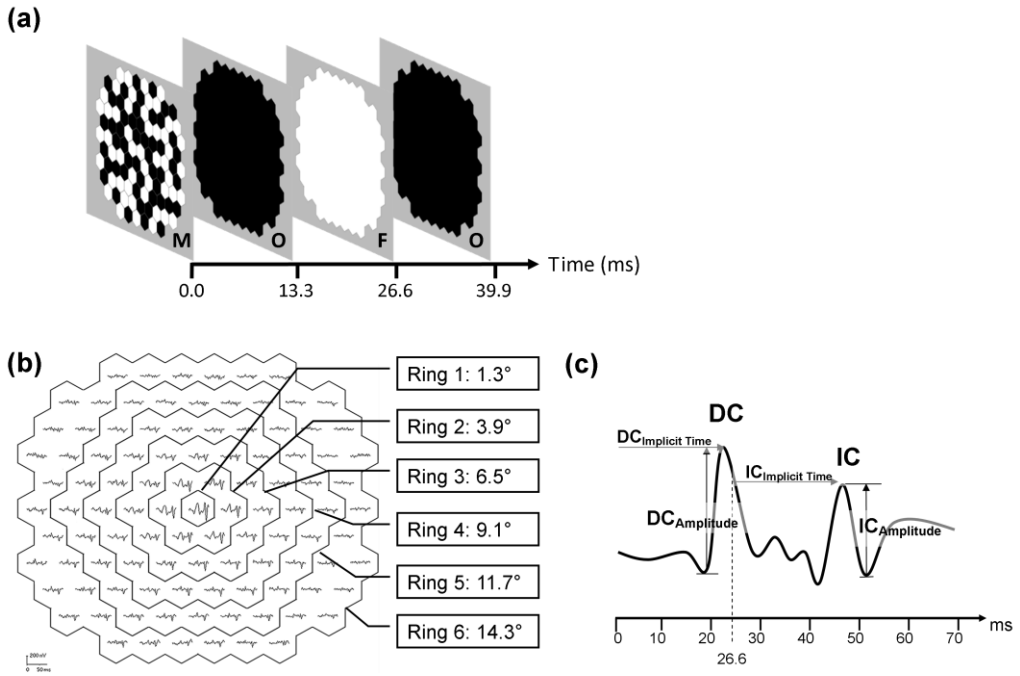

Figure 9.1. (a) The stimulus array of the global flash mfERG consisted of 103 non-scaled hexagons and each multifocal flash frame (M) was followed by a dark frame (O), a global flash frame (F) and a second dark frame (O). The video frame rate was 75 Hz and each frame interval was 13.3 ms. (b) The 103 local responses were grouped into 6 regions. The eccentricity boundary of each ring is indicated in the figure. (c) The typical first order kernel global flash mfERG waveform consisting of DC and IC responses is shown (See text in details).

9.2.3. mfERG recording

One eye from each subject was chosen at random for mfERG recording. Two drops of 1% Tropicamide (Alcon Laboratories Inc., Fort Worth, TX, USA)

were instilled with a 5-minute interval before measurements commenced. A DTL thread electrode was placed behind the lower eyelid to contact with the cornea as the active electrode. Gold-cup reference and ground electrodes were placed 10 mm lateral to the outer canthus of the tested eye and at the central forehead, respectively. The fellow eye was occluded during recording.

The mfERG signal was filtered between 10 and 300 Hz and was amplified 100,000 times (Model: 15A54, Physiodata Amplifier system, Grass Technologies, Astro-Med, Inc., West Warwick, RI, USA). The total recording time for each condition was 7 minutes and 17 seconds with the 2^{13} binary m-sequence used; the record was divided into 32 slightly overlapping segments. The signal was monitored by the examiner using the real-time response provided by the VERIS and any segments contaminated with blinks or other artifacts were re-recorded immediately. The room illuminance was about 240 lux.

The mfERG was measured after the pupil was dilated to at least 7 mm in diameter and the cycloplegic effect was steady (see below). Spherical trial lenses of 35 mm diameter were used to correct refractive errors as well as to impose different amounts of optical defocus including control (in-focus, fully corrected), positive defocus (+2 D and +4 D) and negative defocus (-2 D and -4 D) conditions. The order of defocused conditions was randomized. The mfERG

examination started immediately after the corrective lens was placed in front of the subjects. Most subjects took about 10 minutes to complete each set of mfERG recordings for a particular defocused condition.

9.2.4. Evaluation of cycloplegic effect

The cycloplegic effect was tested 20 minutes after the instillation of the eye drops and was also assessed before and after the mfERG examination under each defocused condition. This was done to ensure that the cycloplegic effect was constant throughout the experiment. The same examiner, who was masked to the defocused condition to be used, measured the residual accommodation of the tested eye of all subjects using the push-up method. Subjects were corrected according to the subjective refraction with the near addition power of +2 D which resulted from this test. The end point used was the subject's report of blur in the line of letters at their best visual acuity when the target was slowly moved from a working distance of 50 cm toward them. The residual accommodation was the amplitude of accommodation measured minus 2 D (i.e. the near addition power given). Five readings were obtained to give an average result. The mfERG examination began if the difference in residual accommodation for three consecutive measurements measured at 5-minute intervals was equal to or less

than 0.25 D. To impose a certain magnitude of negative defocus, the residual accommodation was compensated for to ensure constant levels of retinal defocus (e.g., if a subject was found to have 1 D of residual accommodation, -3 D was used to achieve -2 D of defocus). Most subjects were found to have 1 to 2 D of residual accommodation. The data set was omitted if the difference in residual accommodation measured before and after mfERG examination was greater than 0.25 D.

9.2.5. mfERG response analysis

The mfERG responses were pooled into six concentric rings for analyses (Figure 9.1b). The amplitudes and implicit times of the DC and IC responses in the first order kernel were analyzed (Figure 9.1c). The DC amplitude was measured from the first negative trough to the first positive peak while the IC amplitude was measured from the second positive peak to the second negative trough. The implicit time of the DC was measured from the presentation of the multifocal flash while that of IC was measured from the presentation of the global flash (i.e. at 26.6 ms).

9.2.6. Statistical analysis

Statistical analysis of the data was carried out using SPSS (Version 15.0, SPSS Inc., Chicago, IL, USA). To determine the effect of optical defocus on the regional mfERG response, the percentage change in mfERG response with respect to the control condition was calculated in each region and compared across different defocused conditions. For the time domain, the implicit time was regarded as being lengthened if the change in implicit time was greater than zero; it was considered as shortened if the change in implicit time was less than zero. One-sample t-tests were conducted to determine if the changes in mfERG response were significantly different from zero. Bonferroni adjustment was done to correct the level of significance due to multiple comparisons of different retinal regions. The level of significance was set at 0.008.

To investigate the magnitude of refractive error on the change of mfERG response with defocus, Pearson's correlation was applied to examine the association between refractive error and change of mfERG with defocus. Bonferroni correction was also conducted to compensate for the effect of multiple comparisons of different retinal regions at the same time.

9.3. Results

Figure 9.2 shows the typical global flash mfERG waveforms measured under control, -4 D defocus, and +4 D defocus conditions from one subject. Under fully corrected (in-focus) conditions, the waveforms consisted of two distinct peaks in all six regions, with the first and second peaks corresponding to the DC and IC responses, respectively. The DC amplitude was markedly reduced under negative defocus condition but only mildly reduced under positive defocus condition. In contrast, the IC amplitude was minimally changed under negative defocus condition but moderately increased under positive defocus condition. The two distinct peaks are still present under +2 D and -2 D defocus, and the amplitudes of DC and IC responses show similar changes for the same sign of defocus (data not shown).

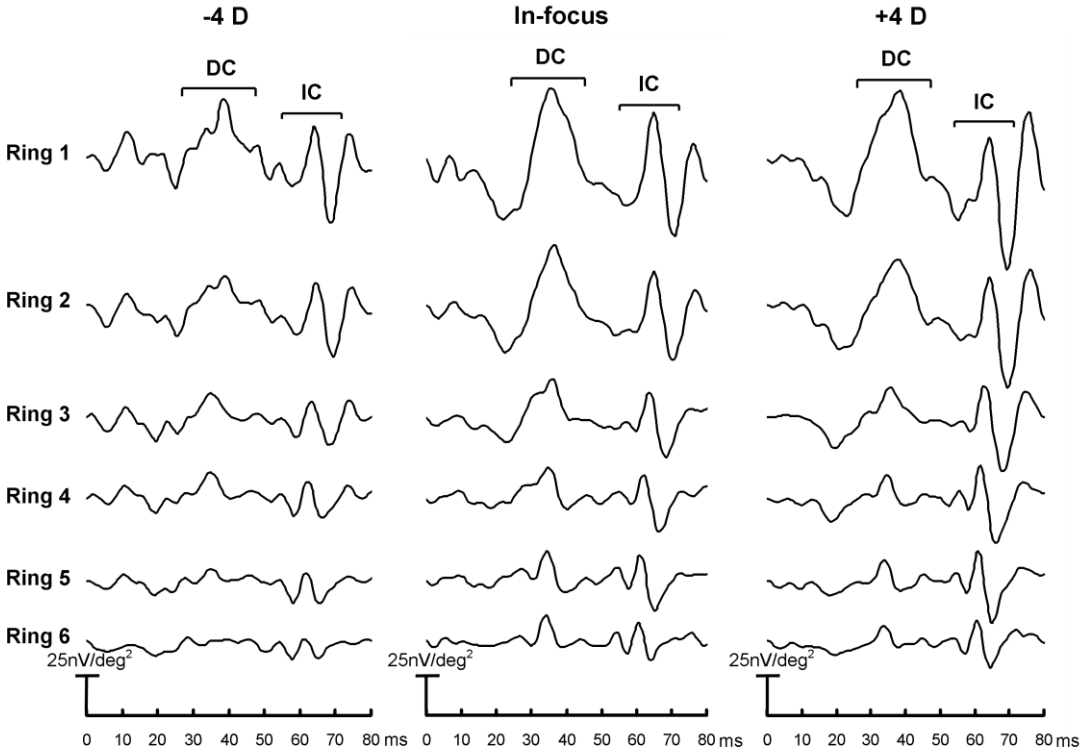

Figure 9.2. The typical global flash mfERG waveforms measured from one subject under in-focus (fully corrected; centre), -4 D defocus (left) and +4 D defocus (right) conditions for six different retinal regions.

Figure 9.3 illustrates the average percentage changes (mean ± SEM) in DC amplitudes (a) and IC amplitudes (b) with respect to control condition under different defocused conditions. The DC amplitude was reduced significantly by about 18% under -2 D defocus from Rings 5 and 6 (all $p < 0.002$), and the amplitude was reduced by 17 to 24% under -4 D defocus from Rings 1 to 2 and Rings 5 to 6 (all $p < 0.004$). However, the DC amplitude did not show any statistically significant change for either +2 D or +4 D of defocus for any of the six regions.

In contrast, the IC amplitude was generally reduced under negative defocus in the central retina, but only at Ring 2 under -2 D defocus was statistically significant reduced (all $p < 0.001$). However, the IC amplitude increased significantly from Ring 3 to 5 under both +2 D and +4 D defocus (all $p < 0.003$); there was about 40% increment of amplitude at Ring 4 under positive defocus, the highest value shown. On the other hand, the IC amplitude showed no significant change at Ring 6 under all defocused conditions.

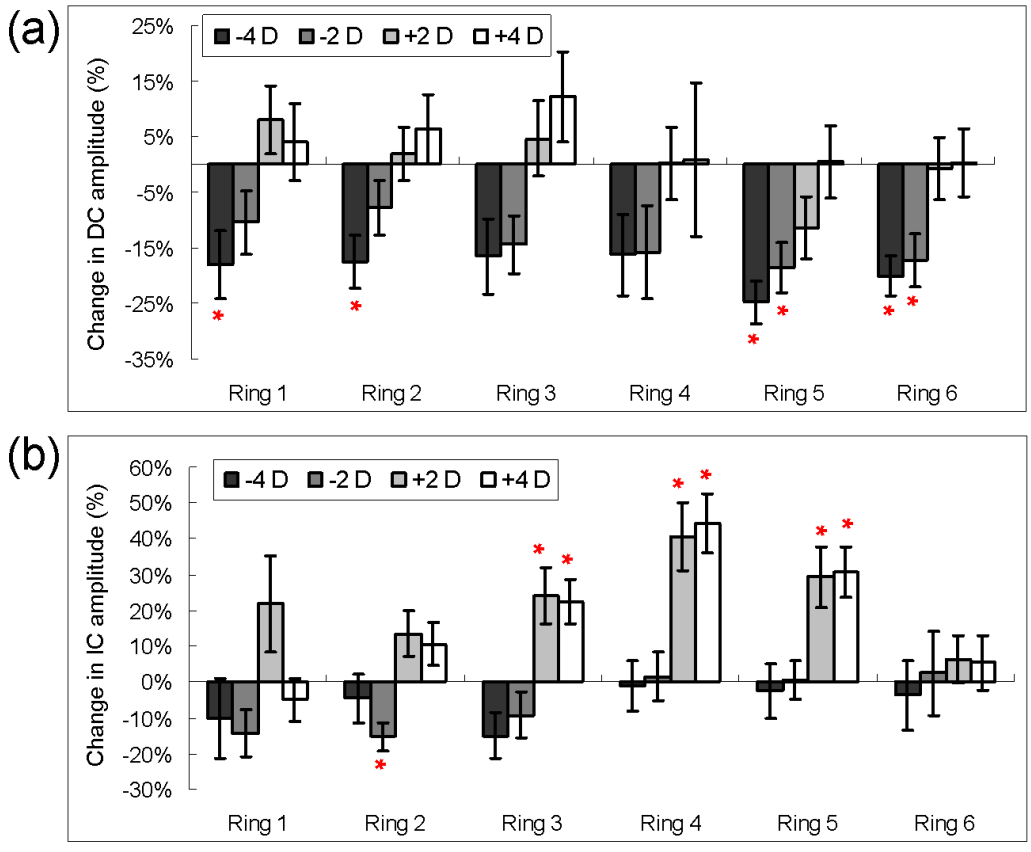

Figure 9.3. The percentage change (mean ± SEM) in (a) DC and (b) IC amplitudes with respect to control condition at different retinal regions for various defocused conditions. Those marked with an asterisk "*" are statistically different from the in-focus (0 D) condition. The error bars indicate the standard error of the mean (SEM).

Figure 9.4 shows the percentage changes in DC and IC implicit times with respect to control condition at various retinal regions for the four defocused conditions. In general, the DC showed a shorter implicit time under both positive and negative defocus conditions. Interestingly, the DC response at Ring 2 demonstrated progressively shortened implicit time from negative to positive defocus, although only the implicit time at Ring 2 under +4 D defocus was significantly reduced ($p = 0.001$). On the other hand, the IC response from Rings 2 to 6 also showed a systematic change in implicit time from negative to positive defocus, depending on the eccentricity. Specifically, the IC responses at Rings 2 and 3 showed gradually shortening of implicit time from -4 D to +4 D defocus, in which only the changes of implicit time at both Rings 2 and 3 under +4 D defocus were statistically significant (all $p < 0.002$). The IC implicit time at Rings 4 to 6 tended to lengthen under negative defocus and shorten under positive defocus. The IC implicit time at Ring 1 did not show an obvious and specific change but only it showed a significant shortening under +4 D defocus ($p < 0.05$).

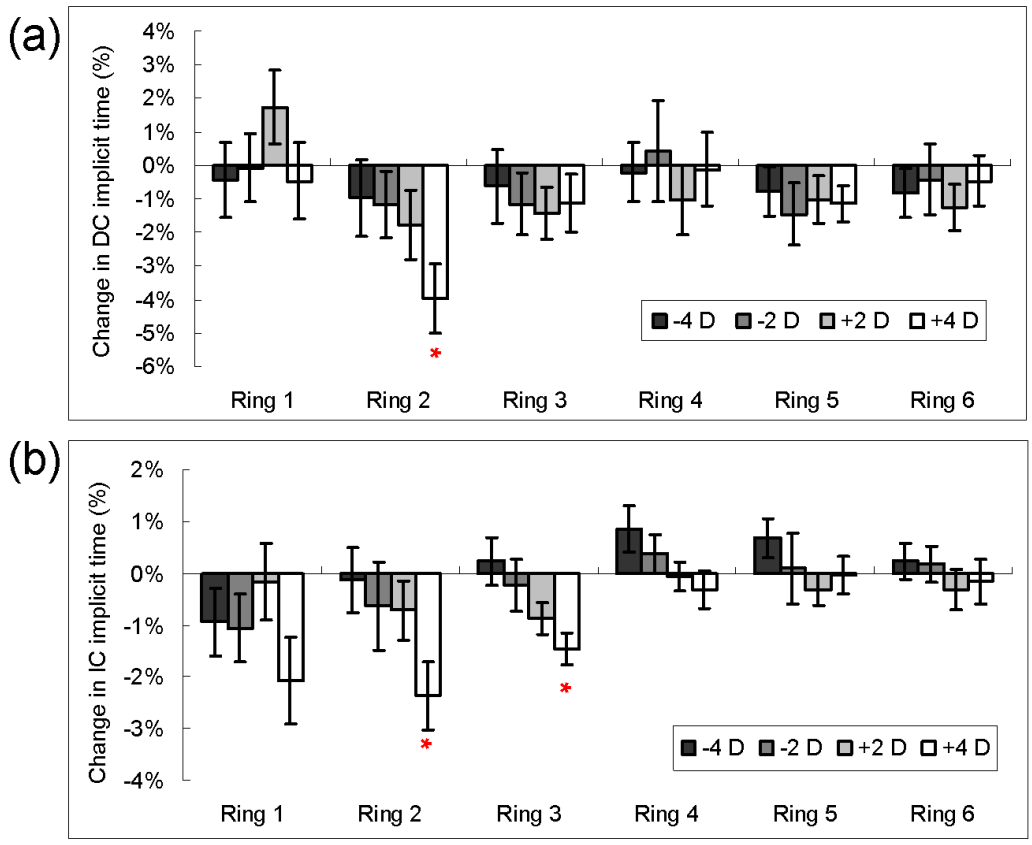

Figure 9.4. The percentage change (mean ± SEM) in (a) DC and (b) IC implicit times with respect to control condition at different retinal regions, for various defocused conditions. Those marked with an asterisk "*" are statistically different from the in-focus (0 D) condition. The error bars indicate the standard error of the mean (SEM).

Neither the change in amplitude nor implicit time of both the DC and IC responses with defocus was correlated with the refractive error of the subjects (Tables 9.1 to 9.4).

Defocus (D) / Region	-4		-2		+2		+4	
	r	p	r	p	r	p	r	p
Ring 1	0.16	0.46	0.01	0.97	-0.09	0.70	-0.05	0.81
Ring 2	0.10	0.65	0.25	0.25	-0.01	0.96	0.23	0.29
Ring 3	-0.13	0.57	0.25	0.26	<0.01	0.99	0.02	0.92
Ring 4	0.14	0.52	0.28	0.19	0.20	0.37	0.18	0.41
Ring 5	-0.09	0.69	-0.16	0.46	-0.39	0.06	-0.03	0.88
Ring 6	0.09	0.68	0.21	0.34	-0.21	0.35	0.06	0.80

Table 9.1. Pearson's correlation between magnitudes of refractive error and change in DC amplitude with different defocused conditions at various regions. Those p-values less than 0.008 are Bonferroni-corrected statistically significant.

Defocus (D) / Region	-4		-2		+2		+4	
	r	p	r	p	r	p	r	p
Ring 1	-0.01	0.95	0.04	0.86	-0.16	0.46	-0.36	0.09
Ring 2	-0.18	0.42	0.11	0.61	-0.50	0.02	-0.23	0.29
Ring 3	0.13	0.54	0.08	0.73	-0.13	0.57	-0.11	0.63
Ring 4	-0.14	0.54	-0.20	0.37	-0.28	0.20	-0.31	0.15
Ring 5	-0.02	0.93	-0.10	0.64	-0.45	0.03	-0.44	0.03
Ring 6	-0.02	0.93	-0.17	0.44	-0.27	0.21	-0.22	0.31

Table 9.2. Pearson's correlation between magnitudes of refractive error and change in IC amplitude with different defocused conditions at various regions. Those p-values less than 0.008 are Bonferroni-corrected statistically significant.

Defocus (D) / Region	-4		-2		+2		+4	
	r	p	r	p	r	p	r	p
Ring 1	-0.01	0.97	-0.08	0.72	0.33	0.12	-0.28	0.20
Ring 2	-0.06	0.79	-0.10	0.64	0.19	0.40	-0.18	0.43
Ring 3	0.15	0.51	0.21	0.35	0.52	0.01	0.41	0.05
Ring 4	-0.04	0.56	0.15	0.49	0.34	0.11	0.16	0.45
Ring 5	-0.11	0.63	0.23	0.29	0.41	0.05	0.18	0.41
Ring 6	0.14	0.54	0.15	0.48	0.48	0.02	0.30	0.16

Table 9.3. Pearson's correlation between magnitudes of refractive error and change in DC implicit time with different defocused conditions at various regions. Those p-values less than 0.008 are Bonferroni-corrected statistically significant.

Defocus (D) / Region	-4		-2		+2		+4	
	r	**p**	**r**	**p**	**r**	**p**	**r**	**p**
Ring 1	-0.29	0.18	0.05	0.81	-0.07	0.74	-0.09	0.68
Ring 2	-0.07	0.74	0.09	0.67	0.08	0.71	-0.13	0.56
Ring 3	-0.39	0.07	0.05	0.84	-0.28	0.19	0.03	0.90
Ring 4	0.09	0.69	-0.03	0.90	0.15	0.49	0.07	0.75
Ring 5	-0.18	0.40	-0.28	0.20	-0.16	0.47	-0.16	0.47
Ring 6	-0.17	0.45	0.16	0.48	0.19	0.39	0.02	0.94

Table 9.4. Pearson's correlation between magnitudes of refractive error and change in IC implicit time with different defocused conditions at various regions. Those p-values less than 0.008 are Bonferroni-corrected statistically significant.

9.4. Discussion

The key finding is that different signs of defocus can affect different components of the global flash mfERG response (Figure 9.3). The DC amplitudes from Rings 1 to 2 and Rings 5 to 6 were significantly reduced under negative defocus, especially in the paracentral regions (i.e. Ring 5, eccentricities from 9.1 to 11.7°); but the amplitudes were not significantly altered by positive defocus. In contrast, the IC response showed a remarkable increment in amplitude under positive defocus, especially in the paracentral region (Ring 4, eccentricities from 6.5 to 9.1°), but IC response changed only minimally, though significantly in certain regions, under conditions of negative defocus. Although the recruited subjects were with a range of refractive errors, the change in response with defocus was not affected by the magnitudes of refractive error

(Tables 9.1 to 9.4). The DC and IC responses mainly represent the activity from outer (e.g. photoreceptors and ON- and OFF-bipolar cells) and inner retina (e.g. amacrine cells and retinal ganglion cells) respectively (see Section 6.4, Paragraphs 1 and 2). Negative and positive defocuses predominantly affect DC and IC responses respectively, suggesting that the sign of defocus is probably decoded differentially in inner and outer retina.

In addition to the sign-preference of the mfERG response amplitude, the time domain of the mfERG response also demonstrated similar sign-dependence to the defocus but the change was less obvious than that in the amplitude domain (Figure 9.4). The DC implicit time was progressively shortened for Ring 2 with increasing magnitude of positive defocus, but this was not found in other regions. In addition, there was systematic change in IC implicit time from negative defocus to positive defocus, even though the trend was different at various eccentricities. Specifically, the IC implicit times were almost unchanged for Rings 2 and 3 under negative defocus but were progressively shortened under positive defocus in these regions, especially for +4 D defocus. The underlying alteration in biochemical activity within the retina is still unknown. However, peripheral defocus is well known to affect the refractive error development of the eye (Smith et al., 2009). According to our findings, optical defocus also affects

the time domain of the mfERG response. Additionally, changes in the time component of the mfERG response have been shown in progressing myopes by Chen and co-workers (2006b), although they used a different stimulation protocol. The underlying changes in the IC implicit times from Rings 2 to 3 under optical defocus may represent retinal signals involved in eye growth. Further investigation is needed to explore the signal cascade between defocus and eye growth to clarify this issue.

In the chick eye, the blockage of ON and OFF pathways has been shown to inhibit compensatory responses induced by negative and positive defocus respectively (Crewther and Crewther, 2003). This indicates that the detection of defocus signals is probably initiated at the retinal level and involves two different pathways. Moreover, in chicks, the level of ZENK expression in glucagon-containing amacrine cells (Fischer et al., 1999) and retinoic acid synthesis (Mertz et al., 1999) depends on the sign of defocus signals. In monkeys, on the other hand, the activities of ON-bipolar cells and GABAergic amacrine cells have been shown to be focus-sensitive. These cells have been shown to be more reactive for in-focus stimuli and those with positive defocus, compared to those with negative defocus, by using immunocytochemical markers (Zhong et al., 2004). This indicates that bipolar cells as well as amacrine cells are involved

in detecting defocus signals. Taken together, this evidence suggests that retinal activity changes differently when the retina is presented with defocus signals of opposite signs. The sign-dependent changes in retinal activity are consistent with the findings of global flash mfERG responses over the range of defocus obtained in this experiment.

Paracentral vision may have a profound effect on the growth process of the whole eyeball. The foveal region provides good spatial vision because of its high resolution. However, imposing peripheral negative defocus, leaving clear central vision, can cause myopia accompanied by axial elongation, in both chicks (Liu and Wildsoet, 2011) and monkeys (Smith et al., 2009). In addition, peripheral defocus has no effect on axial refraction development if the peripheral defocus is in the far retinal periphery (beyond ~ 50°, at least for the chick's eye) (Liu and Wildsoet, 2011; Schippert and Schaeffel, 2006). Liu and Wildsoet (2011) recently used two-zone concentric bifocal lenses and demonstrated that peripheral defocus is more important than central defocus in refractive error development in the chick. It seems clear that the retinal region sensitive to defocus is not limited to the central visual area. Our study showed that the paracentral retina reacts more vigorously to optical defocus than does the central retina, probably indicated that paracentral retina may involve in the refractive error development

in human.

Our experiment focused on the central retina to about 15° eccentricity but did not include the region beyond 15°. It should be noted that previous studies in human subjects have shown the magnitudes of peripheral refraction (in SE) and astigmatism were insignificant up to an eccentricity of 20° (Millodot, 1981). While single-power spherical ophthalmic lenses were used to induce optical defocus in present experiment (Experiment 4), the effect of peripheral refraction should be considered in the investigation of the retinal response to optical defocus in the peripheral retina (i.e. beyond an eccentricity of 20°). Peripheral refractive error is dominated by oblique astigmatism when the central refractive error is corrected (Jaeken and Artal, 2012). The changes of mfERG response at peripheral retina may ultimately depend on the location of the two principal meridians of astigmatism. In case of mixed astigmatism, one of the focal planes is in front of the retina and the other is behind the retina. It becomes more difficult to predict the changes of mfERG response because it has been reported that the strength of positive and negative defocus (with equal magnitude) on the eye growth was not the same (Tse and To, 2011).

Optical defocus does alter the image size and brightness of the stimulus compared to an in-focus image projected onto the retina. However, it is unlikely

that the discrepancy in the optical factors was a key element to account for the changes in mfERG response under different optical defocus conditions. First, the characteristics of defocus-response functions were different at various eccentricities particularly the IC responses (Figure 9.3). We would expect that the change in mfERG response would be approximately the same among all six regions examined. Second, the relative change in mfERG response amplitude (both DC and IC responses) was particular higher at paracentral region (Rings 4 and 5) than at central region (Rings 2 and 3), i.e. about 40% increment in IC amplitude at Ring 4 under positive defocus and about 25% decrement in DC amplitude at Ring 5 under negative defocus (see Section 9.3). Since we chose the non-scaled (equal size) hexagonal array as stimulus, alternation of these optical parameters at central region, due to the huge amount of retinal cells, should produce greater change in response than at paracentral region. However, the result is opposite in our findings. Third, the defocus-response curves between DC and IC responses for each region were different. The global flash mfERG generated two response components, illustrating the outer and inner retinal activities (Chu et al., 2008). The outer retinal activity is assumed to transmit the signals to inner retina. If the changes in mfERG response under various defocused conditions are related to the optical factors, an alternation of the outer

retinal activity (DC response) should trigger corresponding change in inner retinal activity (IC response). Moreover, even the focal and global flash intensity increased from 50 to 400 cd/m^2, both the DC and IC amplitudes were only mildly increased (see Figures A.1 and A.2 in Appendix A). So, it is unlikely that optical factor would be a key factor to account for the unique retinal response under particular sign of defocus.

Usually, scaled hexagonal array was chosen as the stimulus in human studies. This design of the stimulus is to follow the retinal magnification (change in cone cell density) and make sure the signal-to-noise ratio among all regions tested being approximately the same (Sutter and Tran, 1992). However, non-scaled (equal size) hexagon was chosen as the stimulus in the study because the spatial frequency of the stimulus can affect the eye growth process (Schmid and Wildsoet, 1997). The use of the non-scaled hexagon allows for fair comparison of the change of retinal responses under defocused conditions against control condition at different eccentricities, without being confounded by the variation of the stimulus size (spatial frequency) across the retina.

9.5. Conclusions

Paracentral retina showed greater change than central retina in DC and IC

amplitudes under defocused conditions. Moreover, different components of the global flash mfERG response are differentially affected by negative and positive defocus. These results suggest that the paracentral retina gives reduced DC responses to negative defocus and increased IC responses to positive defocus. This provides evidence that the human retina not only identifies optical defocus, but also differentiates the sign of optical defocus.

Chapter 10 - Outcomes, Discussion, Conclusions and Future Studies

10.1. Outcomes

Experiment 1

- Myopic adults showed reduced retinal function in the paracentral region.
- Inner retinal function was reduced more than outer retinal function in the myopic eye.
- Retinal function, including both outer and inner retinal layers, in the central region appears normal in myopic adults.

Experiment 2

- The effect of myopia on retinal function was different between children and adults with myopia.
- Myopic adults had impaired inner retinal function from paracentral to mid-peripheral regions.
- Myopic children showed reduced function of the outer retina in the central region.

Experiment 3

- Children with progressing myopia showed reduced inner retinal function from central to paracentral regions but the outer retinal function was virtually unaffected.

Experiment 4

- The human eye responded to different optical defocus at the retinal level.
- The retina differentiated the sign of defocus signals.
- The paracentral retina responded more vigorously to optical defocus than did the central retina.

10.2. Discussion

Effect on uncorrected peripheral refractive error on the mfERG response in myopes

Single vision corrective lens was used to correct the refractive errors of the subjects (Experiment 1 to 3) and to impose different magnitudes of defocus (Experiment 4). However, myope is associated with relative hyperopic refraction at the peripheral retina in both children (Mutti et al., 2000; Schmid, 2003) and adults (Millodot, 1981) with myopia. The peripheral refractive error has not been corrected with the single vision lens. In Experiment 2, both the refractive error and axial length of the subjects in children and adults groups were not different from each others. We assumed that it does not have significant difference in peripheral refractive error between two groups. If the uncorrected peripheral refractive error in myopic eye affects the paracentral mfERG response, the same

mfERG response component would be expected to be altered. However, the paracentral IC response was reduced in adult myopes but was unchanged in children myopes. It indicates that the peripheral refractive error is not a dominant factor to account for the difference in mfERG response between children and adults with myopia in this study.

Regional changes in retinal functional loss from children to adults with myopia

The regional variations of functional deterioration in the retina during myopia development appear to indicate different underlying causes for myopia at different developmental stages. The retinal functions at both outer and inner retinal layers were generally unaffected by the severity of myopia in children. Myopia progression was associated with functional changes in the inner retina from central to paracentral regions. However, the relationship between reduced central function and myopia increment is still not clear. Previous studies indicated that impairing retinal function by pharmacological intervention during the developmental period could cause myopia formation in animals (Fischer et al., 1997; Fischer et al., 1998b; Wildsoet and Pettigrew, 1988). In addition, children with reduced foveal function have been reported to be more likely to have a

higher myopia progression rate later in life than those children with normal foveal function (Luu et al., 2007). Smith and his co-workers (2009) carried out a study on monkeys regarding the role of the fovea in the emmetropization process. Those monkeys with foveas photo-ablated with an argon laser had no obvious difference in refractive errors as compared to the control eye, but with more fluctuated in terms of the range of refractive errors. These suggest that the fovea is not essential in the eye growth. However, we hypothesized that the eye needs to have a site in the retina for the determination of the end-point of eye growth. Most likely the fovea is the best site because of the highest visual resolution. If the fovea is damaged, it cannot detect any signals and properly the other retinal areas next to damaged fovea will become the detector to determine the end-point of eye growth. This may be why the refractive errors in the foveal-ablated monkeys were more fluctuated. In Experiment 3, foveal function reduced as myopia increased in children. We speculated that the foveal function should have some linkage to the eye growth process. We further hypothesize that reduced foveal function in children may facilitate the development of myopia or exacerbate the myopia progression rate, which requires further investigation.

The reduced retinal function in the paracentral region is probably a consequence of the compensatory eye growth to peripheral defocus

The impaired retinal function from paracentral to mid-peripheral regions may be related to the effect of peripheral defocus on eye growth. It has been suggested that relative peripheral hyperopic refraction is associated with myopia (Hoogerheide et al., 1971; Mutti et al., 2000). We found that peripheral retina responds more vigorously to optical defocus than does central retina in adults. In addition, peripheral defocus was shown to affect the axial refraction of the eye in animal studies (Liu and Wildsoet, 2011; Smith et al., 2009). We speculate that the off-axis refraction may drive the development or progression of myopia in humans. In turns, the eye compensates for the off-axis refraction and leads to an alternation of the retinal structure and function.

10.3. Conclusions

The effect of myopia on retinal function varies with age and mainly affects inner retinal layers. In addition, there is a progressive change of location in terms of reduced retinal function from central to paracentral/mid-peripheral regions between myopic children and myopic adults. Specifically, retinal function, including that of both outer and inner retina, in myopic children is generally

unaffected by the magnitudes of myopia, except the outer retinal function in the foveal region. As children become more myopic, the inner retinal function deteriorates more, and the central to paracentral regions are mainly affected. Compared to myopic children, the retinal region and retinal components affected in myopic adults are quite different. Inner retinal function, from paracentral to mid-peripheral regions, is predominantly affected in myopic adults but the outer retinal function of these regions is only mildly reduced. We speculate that the reduced retinal function from paracentral to mid-peripheral regions is probably related to the effect of peripheral defocus which is driving the eye growth. While peripheral defocus is shown to have stronger influence on eye growth than central defocus in animal studies, our study has also demonstrated that paracentral retina reacts more strongly to defocus signals than does central retina in humans. Moreover, outer and inner retina reacted differently to defocus signals of opposite sign.

10.4. Future studies

We have reported that the there is a progressive change of location in terms of reduced retinal function from central to paracentral/mid-peripheral regions between myopic children and myopic adults; it is still unknown whether this

particular retinal dysfunction is a cause or an effect of myopia development. First, this study only investigated the correlation between mfERG response and magnitudes of refractive error. The causal relationship between these two factors is uncertain. Second, all the subjects recruited had already developed myopia in this study. It is not known whether any preceding functional change had occurred at the retinal level before myopia developed. However, it has been reported that the foveal function is substantially reduced in children with progressing myopia before any increase in their myopia (Luu et al., 2007). In addition, in studies on animals, impaired retinal function during the early postnatal period leads to myopia (Fischer et al., 1997; Fischer et al., 1998b; Wildsoet and Pettigrew, 1988). Taken together, the functional integrity of the retina would likely affect refractive error development later in life. Therefore, the further understanding of the underlying cause of myopia development can be enhanced by characterization of the functional integrity of the retina. Moreover, our current study, together with the findings of Luu et al. (2007) have shown that reduced foveal function is associated with myopia progression in children. So, we should not ignore the role of foveal function on eye growth, in addition to the effect of peripheral refraction (Mutti et al., 2007).

Optical defocus has also been found to affect retinal electrical activity;

opposite signs of defocus can influence the activity of various retinal components differently. However, we could not identify any gradual or incremental change in terms of amplitude or implicit time with increasing magnitudes of defocus within the range of defocus power being studied. This may be related to the subtle change in retinal response over the range of defocus power. It is, however, of particular importance to examine how the retina interprets the magnitude of defocus which affects the end-point of eye growth in myopia progression. In addition, our study only focused on the changes of retinal electrical activity over a very short period of optical defocus (~ 10 minutes). Previous studies in chicks have shown that the exposure time required for defocus to influence ocular structure (Zhu et al., 2005), eye growth (Schmid and Wildsoet, 1996) or the release of eye-growth messengers (Bitzer et al., 2000; Fischer et al., 1999) is different for positive and negative defocus. Hence, it is important to study the effect of exposure time to optical defocus on retinal activity, in order to have a better understanding of the temporal effects of optical defocus on eye growth.

Although myopia can be corrected by optical aids, it is still an “irreversible” refractive disorder. High myopia is associated with higher risks of developing ocular complications such as glaucoma (Mitchell et al., 1999; Saw et al., 2005; Wu et al., 1999), cataract (Chang et al., 2005; Wong et al., 2003; Wu et al., 1999)

and retinal detachment (Saw et al., 2005). Early intervention to slow myopia progression could definitely reduce the chance of developing these ocular complications. Although various treatments, for example, orthokeratology (Cho et al., 2005), specially-designed spectacle lenses (Sankaridurg et al., 2010) or contact lenses (Sankaridurg et al., 2011), dual-power contact lenses (Anstice and Phillips, 2011), can effectively retard myopia progression, there is no clinical assessment or tool available to identify those children whose myopia will progress rapidly or those who will develop myopia. Thus, future studies on the interaction between myopia progression and retinal function, especially for foveal vision, will provide a new direction to help us understand the mechanism of the progression of myopia and assist in the design of better treatments for myopia control.

APPENDICES

Appendix A - Effect of luminance change on global flash mfERG response

Purpose

To investigate the effect of luminance change of focal and global flash on the global flash mfERG response.

Methods

The results from Lung and Chan (2010)'s study was adapted and re-analyzed. The global flash mfERG responses measured under both local and global flash intensity at 50, 100, 200 and 400 cd/m^2 were studied. The amplitude and implicit time of DC and IC responses were plotted against the luminance of the focal and global flash intensities.

Results

Figure A.1 showed the results of the amplitude domain. The central IC responses was almost the same over the range of intensity tested, whereas the central and peripheral DC amplitudes and peripheral IC amplitude were found to have mildly increment in amplitude with increasing intensity level. For the time domain (Figure A.2), both central and peripheral DC and IC implicit times showed weakly increase in implicit time with increasing intensity level.

Conclusions

The global flash mfERG response was weakly increased in amplitude and implicit time over the range of focal and global flash intensity from 50 to 400 cd/m^2.

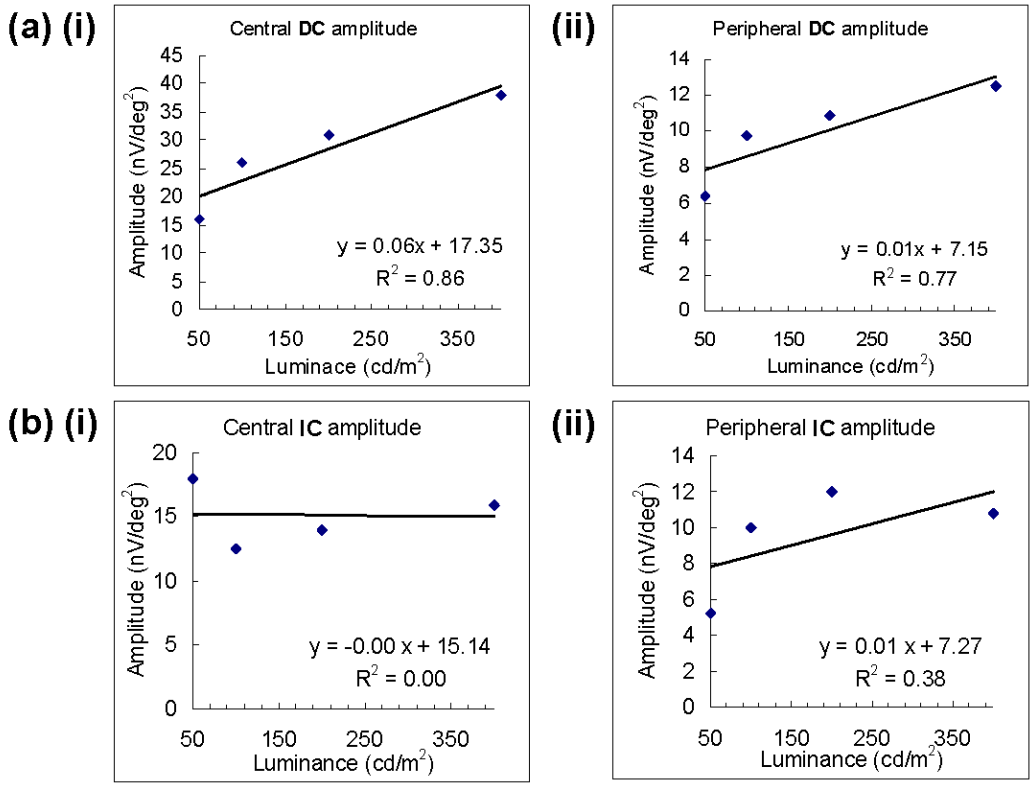

Figure A.1. The relationship between the global flash mfERG response amplitude [(a) DC and (b) IC amplitude] and the intensity of the stimulus at (i) central and (ii) peripheral regions.

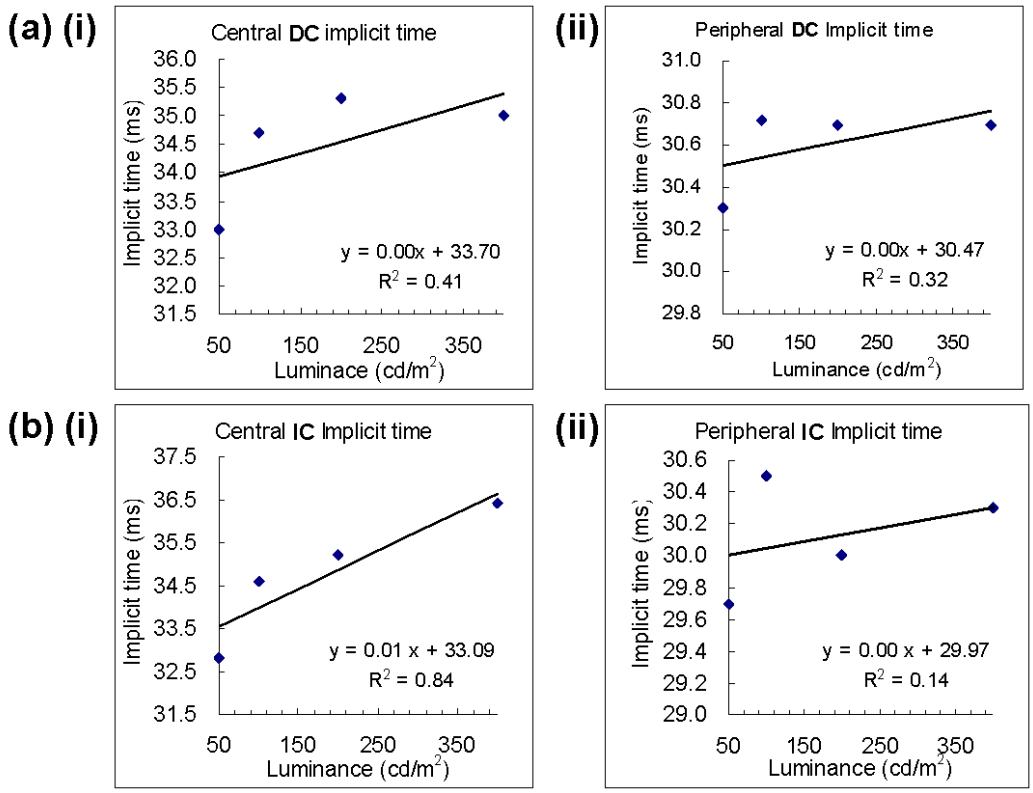

Figure A.2. The relationship between the global flash mfERG response implicit time [(a) DC and (b) IC implicit time] and the intensity of the stimulus at (i) central and (ii) peripheral regions.

Appendix B - Regional variation of the retinal response to the defocus signals

Purpose

Previous study in guinea pig showed regional variation of form deprivation on eye growth (Zeng and McFadden, 2010). This study is to investigate the effect of defocus on the global flash mfERG response at each quadrant.

Method

Twenty-three subjects (aged from 19 to 25 years) received the global flash mfERG recordings under control, positive defocus (+2 D and +4 D) and negative defocus (-2 D and -4 D) conditions. The local retinal responses were pooled into four quadrants for analysis: superior temporal, inferior temporal, inferior temporal and inferior nasal retina as shown in Figure B.1. Both the DC and IC responses were analyzed. The change of global flash mfERG response under defocused conditions against the control condition was calculated. One-sample t-tests were used to study the effect of defocus on the mfERG response at different quadrants.

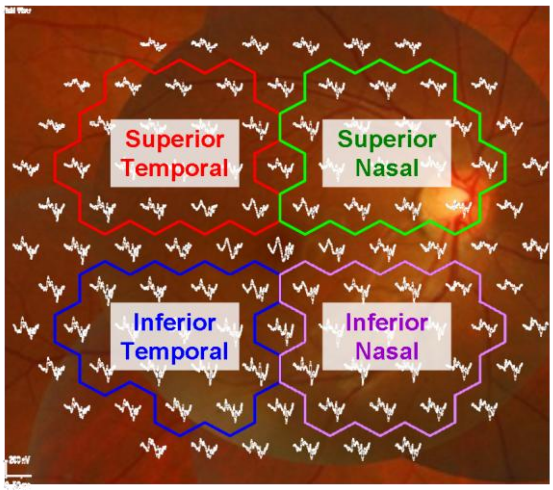

Figure B.1. The local response responses were pooled into 4 quadrants for analysis: superior temporal, superior nasal, inferior temporal and inferior nasal retina.

Results

Compared to control condition, the DC amplitudes at superior temporal retina were significantly reduced under both -2 D and -4 D defocus ($p < 0.01$), whereas, the amplitude at remaining quadrants showed general reduction in response. The DC amplitudes at all four quadrants were not significantly changed under positive defocus. In contrast, the IC amplitudes at superior temporal and inferior temporal retina were significantly increased under both +2 D and +4 D defocus ($p < 0.01$) and also the superior nasal retina under +4 D defocus ($p < 0.01$) and inferior nasal retina under +2 D defocus ($p = 0.001$). However, the IC amplitudes under negative defocus were not significantly changed. Only the DC implicit time at superior temporal retina was significantly reduced under +2 D defocus ($p = 0.004$) and only the IC implicit times at inferior temporal retina

under both -2 D and -4 D defocus were significantly increased ($p < 0.01$).

Conclusions

Human retina responds differently to different defocus signals. Unlike animal study, we could not find a retinal quadrant where gives particularly stronger response to defocus signals.

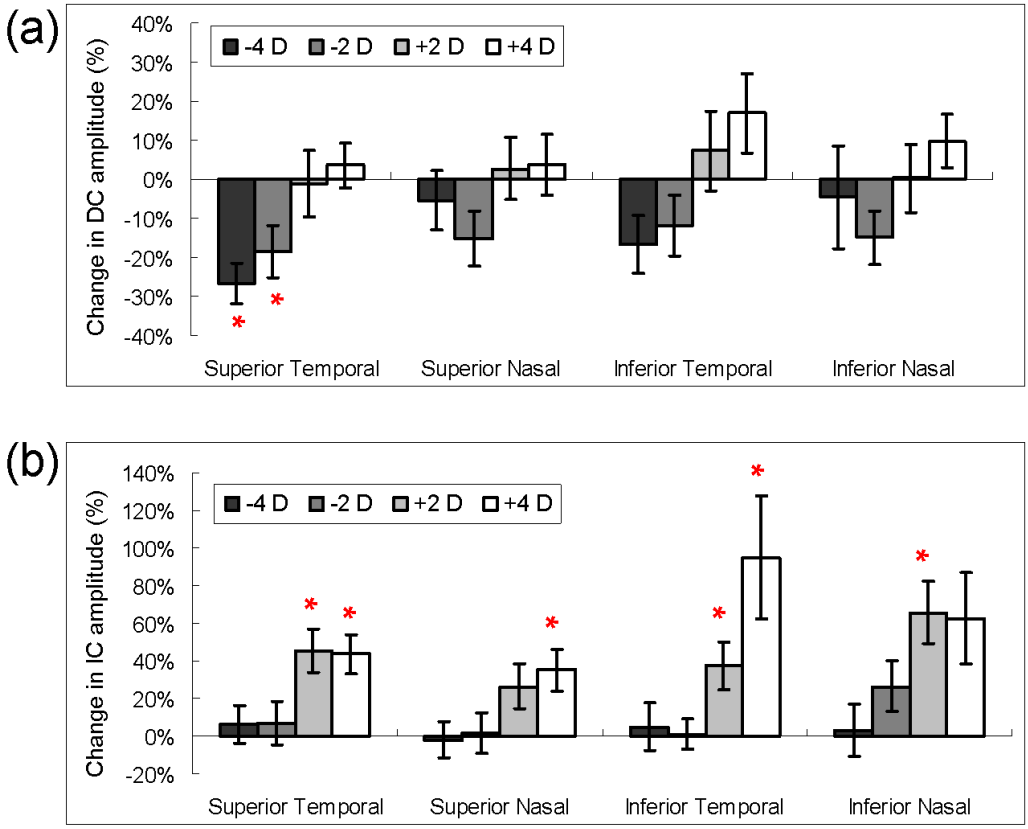

Figure B.2. The percentage change (mean ± SEM) in (a) DC and (b) IC amplitudes with respect to control condition at different retinal quadrants, for various defocused conditions. Those marked with an asterisk "*" are statistically different from the in-focus (0 D) condition. The error bars indicate the standard error of the mean (SEM).

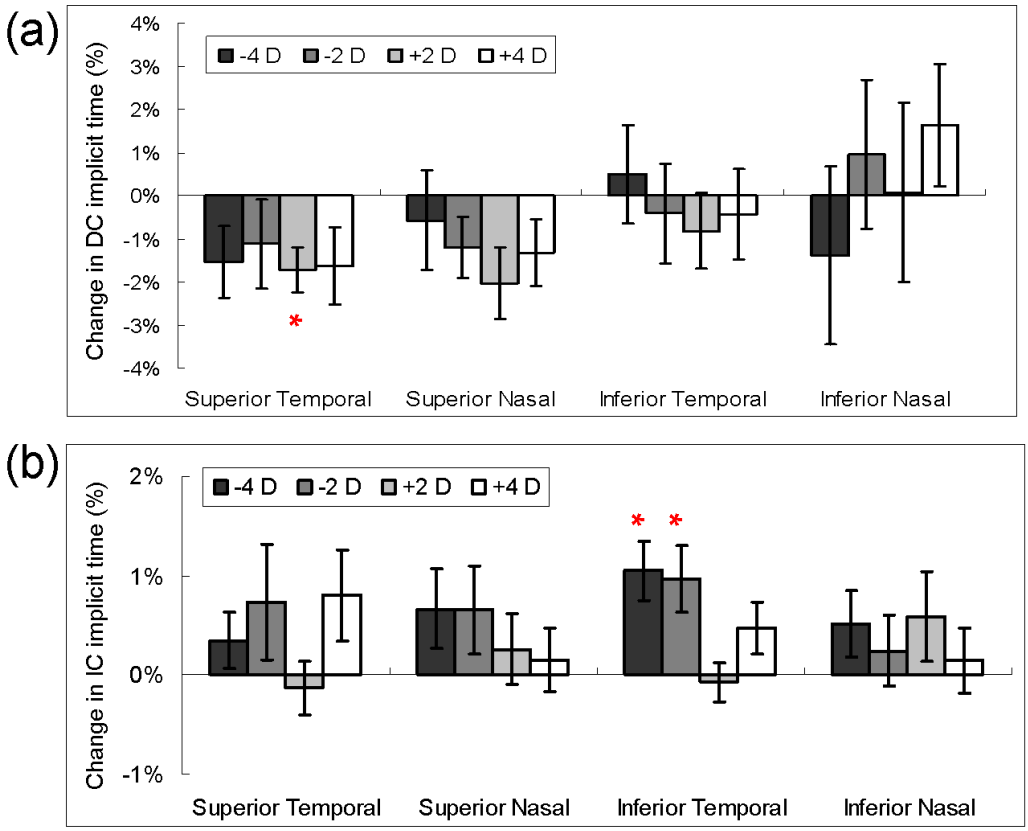

Figure B.3. The percentage change (mean ± SEM) in (a) DC and (b) IC implicit times with respect to control condition at different retinal quadrants, for various defocused conditions. Those marked with an asterisk "*" are statistically different from the in-focus (0 D) condition. The error bars indicate the standard error of the mean (SEM).

Appendix C - Raw data of Experiment I

Subject No.	Refractive error (D)	Axial length (mm)
2	-6.13	26.22
3	-2.75	24.38
4	-3.00	24.81
5	0.00	22.52
6	-2.75	25.48
7	-1.38	24.27
8	-6.25	26.37
11	-8.00	28.00
12	-1.75	23.88
14	-7.75	27.73
16	-6.88	27.34
18	-7.00	26.40
19	-2.00	24.10
21	-2.75	24.85
22	-7.75	26.20
23	-2.63	24.03
24	-2.50	26.33
25	-6.50	26.45
26	-6.13	26.17
27	-1.00	24.72
28	-3.88	25.34
29	-3.75	25.61
30	-4.25	23.42
34	-3.50	24.37
35	-5.25	26.69
36	-3.38	25.21
37	-5.25	25.76

Subject No.	Refractive error (D)	Axial length (mm)
39	-4.00	25.82
40	-2.38	25.29
41	-6.13	25.13
42	-1.50	24.67
44	-8.13	27.01
46	-3.63	24.57
47	-1.75	24.42
49	-2.25	25.54
50	-6.63	26.30
51	-4.13	26.73
52	-3.50	25.25
53	-2.00	23.87
54	-0.13	23.74
55	-2.50	24.99
57	-1.75	24.92
59	-2.38	24.82
60	-3.75	25.46
62	-5.00	25.66
63	-4.00	26.11
64	-6.50	25.55
65	-7.25	26.68
68	-3.25	25.67
70	-4.13	24.95
71	-0.25	23.57
72	-4.75	24.93
74	-4.50	26.38
75	-5.75	25.44

DC Implicit time (ms) from Rings 1 to 3

Ring	Ring 1				Ring 2				Ring 3			
Contrast (%)	29	49	65	96	29	49	65	96	29	49	65	96
Subject No.												
2	27.7	29.5	29.2	31.0	27.7	29.5	30.2	30.3	27.0	27.7	28.5	31.0
3	21.9	31.9	31.9	33.6	21.9	31.4	31.9	32.8	27.0	27.7	28.5	30.2
4	30.3	29.5	32.8	33.6	30.3	29.5	31.4	33.2	29.5	29.5	29.9	31.0
5	27.7	31.4	28.1	31.0	27.0	31.7	29.2	30.3	27.4	29.2	27.0	28.8
6	27.0	29.4	28.1	28.8	24.1	26.3	29.5	31.4	24.8	26.3	27.0	31.4
7	26.3	27.0	30.6	29.9	28.4	29.2	29.5	30.3	28.4	28.4	28.8	29.5
8	27.0	30.6	28.5	31.0	25.2	32.8	30.2	31.9	29.4	28.5	31.0	32.7
11	26.6	30.6	27.7	27.4	25.2	29.9	29.4	32.7	28.1	28.5	28.5	31.0
12	28.1	29.9	28.1	31.7	27.7	30.3	28.5	32.7	26.0	27.7	27.7	30.3
14	26.8	27.7	26.6	29.5	26.3	27.4	28.1	28.1	24.8	25.9	25.9	27.0
16	30.3	29.5	31.7	33.9	30.3	31.4	29.9	32.8	32.5	32.8	31.0	31.0
18	21.0	28.5	24.4	29.4	26.3	27.7	23.5	28.5	26.8	26.6	27.4	27.7
19	30.6	31.7	33.2	29.2	30.3	29.5	31.4	29.2	29.2	29.4	30.2	30.2
21	27.7	29.5	29.2	30.6	28.4	29.2	28.5	30.3	29.9	28.8	28.5	30.3
22	30.2	29.4	31.7	28.4	30.6	29.2	29.5	29.2	27.7	27.7	27.0	28.4
23	24.8	25.9	31.0	31.0	27.7	26.6	27.0	29.2	26.8	26.6	26.6	28.4
24	27.4	30.3	29.2	31.0	28.1	31.0	27.7	27.4	25.5	26.6	27.0	28.1
25	29.4	34.3	30.3	29.2	29.9	35.0	31.7	32.1	30.6	31.0	30.6	31.9
26	31.0	27.7	29.9	27.7	27.4	28.5	30.2	28.4	26.8	27.7	27.7	29.9
27	27.7	31.0	31.7	32.7	28.4	29.4	31.0	28.1	28.4	28.5	28.4	29.2
28	28.8	27.4	32.1	28.1	28.4	29.2	28.8	28.1	27.4	27.0	27.4	28.1
29	30.3	29.5	31.0	30.6	31.0	29.9	32.1	31.4	28.5	29.2	28.5	33.6
30	24.4	31.9	31.4	30.2	24.4	32.1	30.6	32.7	27.0	29.4	30.2	32.7
34	29.5	31.0	30.6	31.4	31.0	31.0	30.3	32.1	28.1	29.4	28.5	29.2
35	28.1	31.7	30.2	28.8	29.2	32.1	29.5	32.1	36.1	31.4	31.4	28.1
36	30.3	26.6	28.8	30.6	28.1	23.5	28.8	29.9	28.5	27.7	28.5	29.4
37	29.9	30.6	32.5	31.4	31.0	31.7	32.8	31.7	31.7	29.4	32.5	33.6
39	25.5	31.0	32.5	33.9	30.6	30.2	33.6	32.7	31.0	29.4	32.7	31.0
40	29.9	31.0	32.5	33.6	28.4	29.2	29.2	29.4	28.1	28.5	28.1	28.4
41	27.7	27.7	32.1	31.4	27.0	27.7	31.4	31.4	27.4	27.7	27.7	28.8
42	21.8	28.1	30.3	30.6	28.5	27.7	31.0	29.9	27.7	26.8	27.0	27.7
44	29.2	31.4	29.9	31.4	29.2	30.6	29.9	31.4	28.5	28.5	28.5	31.9

46	28.4	29.5	31.0	33.2	30.3	29.5	31.0	33.6	25.9	27.7	27.7	30.2
47	27.7	28.8	30.2	30.2	27.7	27.7	28.8	30.2	27.7	26.8	28.1	29.2
49	30.6	30.3	31.7	32.1	31.0	29.4	27.4	32.5	31.0	27.7	28.5	31.9
50	28.4	31.4	33.9	34.3	29.9	31.0	33.6	35.2	30.2	29.5	33.6	35.2
51	30.3	27.7	32.5	30.2	31.4	31.7	33.6	32.1	31.0	31.0	30.2	31.9
52	29.4	31.0	31.0	29.9	29.2	30.6	31.4	33.9	30.2	30.3	31.4	33.6
53	29.2	31.7	28.4	28.5	30.2	31.7	32.8	31.0	30.2	31.0	31.0	31.9
54	32.1	28.1	26.6	30.3	29.9	27.7	26.6	30.6	28.1	27.7	28.1	29.2
55	32.1	31.4	33.2	29.2	32.1	31.9	31.0	29.9	25.9	29.2	30.2	29.9
57	31.0	30.3	28.8	29.9	29.4	29.9	28.5	31.0	29.4	29.4	28.5	30.3
59	31.0	27.4	31.4	32.8	27.7	26.3	31.7	33.6	30.2	29.9	30.2	32.7
60	31.4	28.4	30.3	30.6	27.7	28.1	29.2	29.2	27.7	27.7	27.4	28.1
62	27.7	26.3	30.3	31.0	29.2	28.4	31.0	31.9	28.1	28.1	28.5	31.9
63	29.5	30.3	28.1	28.4	28.1	26.6	27.7	27.7	26.8	26.0	25.5	26.8
64	28.1	32.1	30.6	32.5	32.8	31.7	31.4	31.7	31.9	31.0	30.3	30.6
65	31.7	32.5	30.3	29.4	32.1	30.3	27.4	28.5	30.6	35.7	28.1	28.4
68	27.7	31.0	31.9	31.0	27.7	29.2	31.0	30.6	27.7	29.4	30.2	31.7
70	32.7	31.0	32.5	32.1	31.0	30.6	31.4	31.9	31.0	31.0	30.3	31.0
71	26.7	29.2	27.5	28.3	26.7	29.2	27.5	28.3	27.5	28.3	27.5	28.3
72	26.7	30.0	30.0	35.8	28.3	30.0	29.2	35.0	28.3	29.2	28.3	30.0
74	35.0	33.3	32.5	30.0	31.7	29.2	29.2	29.2	28.3	28.3	28.3	29.2
75	31.7	28.3	30.0	29.2	30.0	28.3	29.2	27.5	27.5	28.3	27.5	27.5

DC implicit time (ms) from Rings 4 to 6

Ring	Ring 4				Ring 5				Ring 6			
Contrast (%)	29	49	65	96	29	49	65	96	29	49	65	96
Subject No.												
2	27.7	27.7	28.5	29.4	28.5	28.5	28.5	29.4	29.4	28.8	28.5	29.4
3	27.7	27.7	27.7	29.4	30.2	29.4	29.4	30.2	30.3	30.3	30.3	30.6
4	29.2	29.5	29.9	30.3	29.5	29.5	29.5	29.9	30.2	30.2	30.2	30.2
5	26.6	27.4	26.6	28.5	26.3	27.0	26.8	28.5	26.3	27.7	26.8	29.4
6	25.2	25.9	25.9	28.8	24.8	25.9	25.9	28.1	25.5	25.9	25.9	28.4
7	28.1	28.1	28.4	28.4	28.1	28.4	28.5	28.5	28.5	28.5	28.8	28.8
8	27.7	27.7	28.5	28.5	27.7	26.8	27.7	27.7	27.7	26.8	27.7	27.7
11	27.7	28.1	27.7	29.4	29.4	29.4	28.5	29.4	30.2	30.2	29.4	30.2
12	25.2	27.7	26.8	28.5	26.0	27.7	27.7	28.1	27.7	28.5	27.7	27.7
14	25.2	26.0	25.5	26.6	26.0	26.8	26.3	28.1	26.8	27.7	26.8	28.8
16	31.9	31.9	31.0	31.9	31.0	31.9	31.4	31.9	31.0	31.0	31.0	31.9
18	26.8	26.3	26.3	27.7	26.0	26.0	26.3	27.7	26.0	26.8	26.8	26.8
19	29.4	30.2	30.2	31.0	32.7	32.8	31.9	31.9	32.8	32.8	32.7	32.7
21	29.9	29.9	28.5	29.9	29.5	29.9	29.4	30.2	29.4	29.9	29.4	29.4
22	26.8	26.8	27.0	27.7	27.7	27.0	27.7	27.7	28.1	27.7	28.1	28.1
23	26.0	26.8	26.8	27.7	26.8	27.7	26.8	28.5	28.1	28.5	27.7	28.5
24	26.0	25.9	26.3	27.4	26.0	26.3	27.0	27.7	26.8	26.8	27.7	28.4
25	30.2	30.3	30.2	30.2	30.2	30.2	30.2	30.2	30.3	31.0	30.3	30.2
26	25.9	27.0	27.0	28.1	26.6	28.4	27.7	28.1	28.5	29.4	28.5	29.4
27	27.7	27.7	27.7	28.1	27.7	27.4	27.7	28.1	27.4	27.7	27.4	28.5
28	25.9	26.6	26.6	27.4	26.8	27.0	27.4	27.7	27.7	27.7	27.7	28.1
29	27.7	28.5	28.1	30.2	27.7	28.5	28.5	29.4	29.5	29.4	28.8	29.4
30	27.7	29.4	30.2	29.4	31.9	30.2	30.2	29.4	30.2	30.2	30.2	30.2
34	28.5	28.5	28.1	29.4	30.2	30.6	28.5	30.2	31.0	31.0	29.4	30.2
35	31.0	31.0	31.4	31.0	31.0	31.0	31.0	31.0	31.0	31.0	31.0	31.0
36	28.5	27.7	27.7	27.7	28.5	27.7	27.7	27.4	29.4	28.5	28.5	27.7
37	29.4	29.4	28.8	31.0	29.4	30.2	28.5	31.0	30.2	30.2	29.4	31.0
39	27.7	26.6	28.5	28.5	27.7	27.7	28.5	28.5	28.5	27.7	29.4	28.5
40	27.7	27.7	27.7	28.1	27.7	27.7	27.7	28.5	28.5	27.7	27.7	28.5
41	26.8	26.8	27.0	27.7	26.8	27.7	27.7	28.1	26.6	27.7	28.5	28.5
42	26.8	26.8	27.0	27.7	26.8	27.7	27.7	28.5	27.7	27.7	27.7	29.2
44	27.7	28.5	28.5	29.4	28.5	28.5	28.8	29.4	29.5	29.4	29.4	29.4

46	26.3	27.7	29.4	29.4	29.4	28.5	29.4	28.5	30.2	29.4	29.4	29.4
47	27.7	26.8	27.7	28.4	27.7	26.8	28.1	28.8	28.1	27.7	28.5	28.5
49	29.4	27.7	28.1	29.4	29.4	34.3	28.5	29.4	30.3	29.4	29.4	30.2
50	29.4	29.4	29.4	31.4	30.2	29.4	29.4	31.0	30.2	29.4	29.4	30.6
51	30.3	31.0	29.4	31.0	30.6	31.0	30.2	30.3	31.4	31.9	30.2	30.6
52	30.6	31.0	30.6	31.0	31.0	30.3	31.0	31.0	31.0	31.0	31.0	31.0
53	30.3	30.2	30.3	30.2	30.6	30.3	30.2	30.2	31.0	30.2	30.2	30.2
54	27.4	27.0	27.7	27.7	27.4	27.7	28.1	27.7	28.1	28.5	28.5	28.5
55	30.2	28.5	29.4	29.2	30.2	28.5	29.4	29.2	30.6	29.4	30.2	30.2
57	29.4	28.8	28.5	29.4	30.2	29.4	29.4	29.4	30.3	30.2	30.2	30.2
59	28.8	29.4	29.4	30.2	28.5	29.4	29.4	29.4	29.2	29.4	29.4	29.4
60	28.1	27.7	27.7	27.7	29.4	28.5	27.7	28.5	30.2	29.4	28.5	29.4
62	27.7	27.7	27.7	29.2	28.5	27.7	27.7	28.4	28.5	28.5	28.1	28.8
63	26.0	26.0	26.0	26.8	25.5	25.5	25.5	26.8	26.0	26.0	25.5	26.3
64	30.6	30.2	29.5	29.2	30.2	30.2	29.5	29.2	30.2	30.2	29.5	29.4
65	31.0	30.2	29.4	30.2	31.0	30.2	29.4	29.4	31.0	30.2	29.4	29.5
68	27.7	28.5	29.4	30.6	28.5	28.5	29.4	30.2	29.4	29.4	29.4	30.2
70	31.0	31.0	30.3	31.0	32.7	31.9	31.0	31.0	31.9	31.9	31.4	31.9
71	27.5	28.3	28.3	28.3	28.3	28.3	28.3	29.2	29.2	29.2	29.2	29.2
72	28.3	29.2	28.3	29.2	28.3	29.2	28.3	29.2	28.3	29.2	28.3	29.2
74	28.3	28.3	28.3	28.3	28.3	28.3	28.3	29.2	29.2	29.2	29.2	29.2
75	27.5	27.5	27.5	26.7	27.5	27.5	27.5	26.7	27.5	27.5	27.5	26.7

IC Implicit time (ms) from Rings 1 to 3

Ring	Ring 1				Ring 2				Ring 3			
Contrast (%)	29	49	65	96	29	49	65	96	29	49	65	96
Subject No.												
2	30.3	31.4	31.8	33.2	29.6	29.9	30.3	32.1	28.8	28.1	28.5	29.6
3	32.8	32.8	32.5	36.5	27.7	30.3	28.1	36.9	27.0	27.4	27.7	29.2
4	32.5	33.2	33.2	34.3	31.4	31.8	31.4	32.8	30.4	30.4	30.4	31.0
5	31.0	32.5	30.7	32.1	30.3	30.3	30.3	31.8	28.5	29.6	28.8	29.9
6	33.9	33.6	34.3	37.2	27.4	28.1	28.1	32.8	27.0	27.9	27.9	30.3
7	32.1	31.8	32.5	32.1	31.3	29.9	31.0	31.4	29.6	29.6	29.6	29.2
8	33.0	33.0	33.2	33.6	33.6	33.2	32.8	33.9	27.0	27.0	28.1	29.2
11	31.3	31.0	31.8	31.4	30.7	29.6	30.7	31.0	28.1	28.1	28.1	28.8
12	31.8	31.4	32.8	34.3	27.7	29.6	32.5	30.3	26.3	27.0	26.6	28.5
14	30.3	28.1	28.1	31.8	27.7	28.1	28.1	27.7	27.1	27.1	27.1	27.4
16	31.8	34.7	34.3	36.1	32.1	35.4	29.9	36.1	25.2	28.8	28.5	31.0
18	30.7	31.4	33.0	30.3	28.8	29.9	29.2	29.9	28.5	28.8	28.1	28.5
19	32.1	32.5	32.8	32.5	30.7	30.7	31.0	31.8	29.2	29.6	29.6	30.3
21	28.1	29.6	28.8	30.7	28.8	29.2	28.5	29.6	28.8	29.2	28.5	29.2
22	31.0	30.3	30.7	31.8	30.7	29.6	29.6	30.4	28.5	28.1	28.8	29.2
23	32.5	33.6	29.6	30.3	26.3	27.4	27.7	28.8	26.3	27.1	27.4	28.1
24	28.8	32.1	31.4	32.1	28.8	28.8	29.2	30.3	27.4	27.9	27.9	28.5
25	32.8	28.5	33.6	34.3	32.1	34.3	28.1	33.6	28.1	23.7	29.2	30.3
26	31.8	31.8	32.8	32.5	28.1	31.4	28.8	32.1	27.0	27.4	27.4	27.4
27	33.6	32.1	33.2	33.2	29.2	29.9	29.2	31.0	28.8	28.8	28.8	29.6
28	31.0	31.4	31.3	32.1	29.6	30.4	29.9	30.3	28.5	28.8	28.8	28.5
29	32.8	32.5	33.2	34.7	32.1	31.8	30.3	38.7	27.7	28.8	27.7	29.9
30	31.0	31.4	32.1	32.8	30.7	31.4	31.0	32.5	28.1	29.2	29.2	29.9
34	33.2	32.8	32.5	32.5	32.5	32.5	32.1	31.4	28.1	28.8	28.1	29.6
35	35.5	26.6	36.5	36.3	37.1	27.4	29.6	35.8	27.0	29.9	30.3	33.9
36	31.8	32.5	37.1	38.0	33.2	27.0	36.5	37.6	33.2	26.6	26.6	27.4
37	32.5	33.6	34.3	37.6	33.6	33.9	34.3	42.0	27.4	28.1	28.1	30.7
39	31.8	32.8	33.0	32.5	31.4	31.4	33.6	32.1	28.1	27.7	35.4	29.6
40	30.7	30.7	31.0	31.0	31.3	30.4	30.7	29.9	28.1	28.8	28.5	29.2
41	31.4	31.8	32.1	32.1	31.0	30.7	30.7	31.8	27.7	28.1	27.7	27.7
42	33.6	27.0	32.1	32.1	27.7	28.1	28.1	29.2	27.4	27.7	27.7	28.5
44	31.8	32.8	33.6	33.9	31.8	31.8	34.3	36.5	27.4	27.7	28.8	28.8

46	30.3	31.0	31.8	32.8	28.5	30.7	31.4	26.6	25.9	26.3	26.3	27.4
47	31.3	33.9	31.8	32.8	30.3	29.2	30.4	30.3	29.2	27.7	29.2	29.6
49	31.0	31.8	33.2	33.6	27.7	30.3	31.0	35.8	28.1	26.6	28.1	29.6
50	31.8	33.0	33.6	34.6	31.4	32.1	33.6	35.0	29.2	29.6	29.2	31.0
51	31.8	33.2	33.0	35.0	31.8	32.5	31.4	33.9	30.7	31.0	29.6	31.4
52	30.7	35.0	34.7	36.5	30.7	30.3	29.6	33.2	29.6	27.4	28.8	31.0
53	28.5	34.3	34.7	35.8	29.2	41.3	39.8	35.4	28.8	29.2	29.6	31.0
54	27.0	33.9	30.7	34.3	26.6	30.3	30.7	31.4	27.7	28.8	29.2	29.6
55	33.0	33.8	33.8	33.9	31.8	32.5	33.0	30.7	30.3	29.6	29.9	29.6
57	31.4	31.8	32.1	34.3	31.0	30.7	30.7	30.3	28.8	28.1	28.5	29.6
59	31.4	32.5	32.5	35.4	31.8	38.3	38.7	33.9	27.4	27.7	34.7	30.7
60	31.3	31.3	31.4	31.4	31.3	29.9	29.9	30.3	28.8	28.8	27.9	28.8
62	31.4	31.4	31.8	32.5	31.0	30.7	31.4	31.8	27.7	28.8	29.2	30.7
63	31.8	32.1	31.4	33.8	28.5	31.0	30.3	29.6	27.7	27.4	27.1	27.0
64	32.8	32.1	32.1	32.8	32.5	32.1	31.4	32.1	29.9	30.3	30.3	30.4
65	32.8	38.7	32.8	34.3	32.1	24.5	32.5	35.0	28.8	26.6	27.4	29.9
68	32.5	32.8	33.2	33.2	32.1	29.6	34.3	27.4	26.3	28.8	28.1	29.9
70	31.8	32.1	32.5	32.1	32.1	31.4	31.8	31.4	30.7	30.7	30.7	30.7
71	29.2	30.0	30.0	30.0	28.4	30.0	29.2	29.2	0.9	28.4	28.4	28.4
72	30.9	30.9	30.9	32.5	29.2	29.2	30.0	31.7	27.5	27.5	27.5	29.2
74	31.7	31.7	31.7	31.7	30.9	30.9	30.9	30.9	30.0	30.0	30.0	30.0
75	31.7	30.9	31.7	32.5	30.0	30.0	30.0	31.7	28.4	28.4	28.4	26.7

IC implicit time (ms) from Rings 4 to 6

Ring	Ring 4				Ring 5				Ring 6			
Contrast (%)	29	49	65	96	29	49	65	96	29	49	65	96
Subject No.												
2	27.0	27.4	27.4	28.5	27.0	27.0	27.0	28.5	27.0	27.0	27.0	28.5
3	26.6	27.0	27.4	28.8	26.3	26.6	27.0	28.8	26.3	26.3	27.0	29.2
4	29.9	29.9	29.6	30.4	29.6	29.6	29.6	29.9	29.9	29.9	29.9	29.9
5	27.4	28.8	27.9	28.5	27.0	27.9	27.4	28.5	27.0	27.4	26.6	28.8
6	27.1	27.1	27.1	27.0	26.2	27.1	26.3	26.6	25.9	26.6	26.3	27.0
7	28.8	28.8	28.8	28.5	28.5	28.8	28.8	28.1	28.5	28.5	28.5	28.5
8	27.4	27.0	27.4	27.7	27.0	26.6	27.4	27.0	27.0	26.6	27.0	27.0
11	27.0	27.4	27.4	28.5	25.9	27.0	27.0	28.5	26.3	26.6	23.7	28.5
12	25.6	26.6	26.3	27.4	25.6	26.6	26.3	27.0	25.2	26.6	25.9	27.0
14	26.6	26.3	26.6	26.6	26.6	26.6	26.6	27.0	26.6	27.0	26.6	27.4
16	24.5	28.8	28.5	30.7	24.1	28.5	28.1	30.7	23.7	28.5	28.5	30.7
18	27.7	27.9	27.4	27.4	27.0	27.0	27.1	27.0	26.6	26.6	27.0	26.6
19	28.8	29.2	29.2	29.9	28.5	28.8	28.8	30.3	28.5	28.1	27.7	30.3
21	29.2	29.2	28.1	29.2	29.6	29.2	28.5	28.8	28.8	29.2	28.1	28.8
22	27.0	27.0	27.1	27.4	26.6	26.6	27.0	27.1	27.4	27.0	27.4	27.9
23	25.9	26.3	26.6	27.4	25.9	26.3	26.6	27.0	24.8	21.9	26.3	27.4
24	26.6	27.1	27.0	27.4	26.6	27.1	27.1	27.4	27.0	27.0	27.4	27.9
25	28.5	29.6	28.8	29.6	28.8	29.6	29.2	29.6	28.8	29.6	28.1	29.6
26	26.6	26.6	27.1	27.0	26.6	27.0	27.0	27.4	26.6	27.0	27.0	27.7
27	27.7	27.9	27.9	28.5	27.0	27.4	27.4	27.7	26.6	27.0	27.0	27.4
28	27.7	27.9	27.9	27.9	27.4	27.9	27.9	27.9	27.7	27.9	27.7	27.9
29	27.0	28.1	27.4	28.8	27.0	28.1	27.4	28.8	27.4	28.1	31.4	28.5
30	28.1	28.1	28.5	28.8	27.7	28.8	29.2	28.8	28.5	29.6	29.6	29.2
34	27.4	28.5	27.7	28.8	29.2	28.1	27.7	28.8	28.8	27.7	27.4	29.2
35	29.2	29.9	29.9	30.7	29.9	30.3	30.7	30.7	29.2	30.3	30.7	30.3
36	26.3	26.6	26.6	27.1	27.0	27.0	27.0	27.1	27.0	27.0	27.0	27.0
37	27.4	27.7	27.7	29.9	28.8	28.5	28.1	29.9	28.5	29.2	28.5	29.9
39	27.4	27.1	28.1	28.5	27.4	27.0	28.1	28.1	27.7	27.4	28.5	28.1
40	27.4	27.7	27.7	28.8	27.0	27.4	27.4	28.1	27.0	27.4	27.4	27.7
41	27.0	27.4	27.1	27.4	27.0	27.4	27.4	27.7	27.4	27.7	27.7	27.7
42	27.0	27.0	27.1	27.4	26.6	27.0	27.0	27.7	26.6	27.4	27.0	28.1
44	27.4	27.7	28.1	28.5	27.7	28.1	28.5	28.5	28.5	28.8	28.8	28.8

46	25.6	25.9	25.9	27.4	24.5	26.3	25.6	27.7	24.8	25.9	24.8	27.7
47	28.1	27.4	28.5	28.8	28.1	27.4	28.5	28.8	28.1	27.4	28.1	28.5
49	28.1	27.0	27.7	28.5	27.7	27.4	27.7	28.5	27.4	28.1	28.1	28.5
50	27.4	28.8	28.8	30.3	27.0	23.7	28.1	29.6	27.0	27.0	27.7	29.2
51	29.6	30.3	29.2	30.3	29.2	30.3	29.2	29.9	29.2	29.9	28.8	29.9
52	28.8	27.7	28.8	29.9	28.8	29.6	29.6	29.9	29.2	29.6	29.9	29.9
53	28.8	29.2	29.6	29.6	28.8	29.6	29.6	29.2	29.2	29.6	29.6	29.6
54	27.0	27.7	28.1	28.1	27.0	27.7	28.1	28.1	27.4	27.7	28.1	28.1
55	29.2	28.8	29.2	29.2	29.2	28.8	29.2	28.8	29.2	29.2	29.2	29.2
57	28.1	28.1	28.5	28.8	29.6	28.5	28.5	28.8	32.1	29.6	29.2	28.8
59	27.4	27.7	28.1	29.2	27.0	28.1	28.1	28.5	27.4	28.1	28.1	28.5
60	27.7	28.1	27.0	27.9	28.1	28.1	27.4	28.1	28.5	28.1	27.7	28.1
62	27.7	27.7	28.1	28.1	27.7	28.1	27.9	28.1	27.4	27.7	27.7	28.1
63	26.6	26.6	26.3	26.6	26.3	26.3	26.2	26.3	26.3	25.9	26.2	26.3
64	28.8	29.6	29.6	29.6	28.8	29.2	29.2	28.8	28.8	28.8	28.8	28.5
65	32.5	28.8	28.1	29.2	33.6	28.5	27.7	29.2	29.2	28.8	27.7	28.5
68	26.6	27.7	27.7	29.2	27.4	28.1	28.5	29.2	28.8	28.5	28.5	28.8
70	30.3	30.3	30.3	30.3	30.3	30.3	30.3	30.7	25.2	30.3	31.4	30.7
71	27.5	28.4	27.5	28.4	27.5	28.4	27.5	28.4	27.5	28.4	28.4	28.4
72	26.7	27.5	27.5	28.4	26.7	27.5	27.5	28.4	26.7	27.5	26.7	27.5
74	29.2	29.2	29.2	29.2	28.4	28.4	28.4	29.2	28.4	28.4	28.4	29.2
75	27.5	27.5	27.5	26.7	26.7	26.7	27.5	25.9	26.7	26.7	26.7	25.9

Appendix D - Raw data of Experiment II

Children

Subject no	Refractive error (D)	Axial length (mm)
1	-1.00	24.37
2	-3.00	24.97
3	-3.50	25.11
6	-3.00	25.30
8	-0.25	23.42
9	-2.00	24.70
11	-0.88	23.19
13	-2.38	24.53
14	-1.13	24.86
17	-2.25	24.27
18	-0.63	23.18
19	-3.00	24.02
20	-2.00	23.39
23	-1.38	25.11
26	-2.63	24.27
28	-0.38	22.94
29	-0.13	24.37
31	-1.00	24.27
32	-2.38	23.80
33	-1.75	24.15
34	-5.13	26.01
35	-3.25	23.70
37	-3.75	25.83
38	-1.75	24.54
39	-2.25	24.75
43	-1.88	24.45

Subject no	Refractive error (D)	Axial length (mm)
46	-3.13	24.76
47	-1.13	24.07
49	-1.00	23.07
50	-4.75	24.98
51	-4.75	25.66
52	-0.75	24.01
53	-5.50	25.07
55	-4.50	25.03
57	-0.88	24.01
58	-4.38	25.00
59	-4.63	24.38
60	-3.50	24.47
61	-3.88	24.80
62	-1.63	24.34
63	-0.50	23.51
64	-4.50	24.86
67	-1.00	24.75
68	-2.25	23.27
69	-3.25	24.91
70	-5.00	25.65
71	-2.25	24.01
72	-2.13	24.42
74	-0.63	22.91
75	-3.50	24.39
76	-2.88	24.13
77	-1.25	23.40

DC implicit time (ms) from Rings 1 to 5 in children

Ring	Ring 1		Ring 2		Ring 3		Ring 4		Ring 5	
Contrast (%)	**49**	**96**	**49**	**96**	**49**	**96**	**49**	**96**	**49**	**96**
Subject no.										
1	37.5	37.2	37.8	38.6	37.5	37.5	37.5	37.5	37.2	36.7
2	32.8	35.0	38.3	35.0	38.3	34.2	38.1	33.3	37.5	32.5
3	31.4	38.3	38.1	37.5	36.4	35.8	35.8	35.0	35.0	35.0
6	40.0	36.9	40.3	38.3	39.2	37.5	37.8	37.5	38.3	37.2
8	36.7	34.2	35.8	35.0	35.0	34.2	33.1	33.3	32.5	33.3
9	38.3	34.2	36.7	35.0	35.6	34.2	33.6	34.2	33.3	34.2
11	35.8	35.0	35.6	35.0	35.6	35.0	34.2	35.0	34.4	34.2
13	31.7	38.9	32.5	38.3	32.8	37.2	37.5	36.9	37.5	36.7
14	37.8	36.7	37.5	37.5	36.4	36.7	34.7	35.0	34.2	34.7
17	36.9	36.4	37.2	36.7	37.5	36.1	36.7	35.3	35.0	35.0
18	38.3	33.3	36.7	33.3	35.8	35.0	35.8	35.0	33.6	34.2
19	33.9	37.5	35.0	37.5	29.2	34.2	33.9	35.6	33.9	34.2
20	30.0	39.4	34.4	34.7	34.2	34.4	34.2	34.2	33.3	34.2
23	36.7	36.7	37.5	35.8	41.7	34.2	42.5	34.2	42.5	34.2
26	33.6	33.3	33.9	38.1	38.9	33.6	36.7	36.4	36.7	35.8
28	33.9	36.7	32.5	35.0	35.0	35.0	35.3	35.6	35.0	35.0
29	34.7	35.8	37.5	35.0	38.9	35.0	38.3	33.3	32.5	32.5
31	35.8	39.2	36.7	38.3	37.2	36.7	35.6	35.8	35.0	35.8
32	37.5	35.0	38.1	35.8	36.1	35.8	35.6	35.0	35.0	35.0
33	38.3	35.8	34.2	35.0	35.0	35.3	35.8	35.0	34.4	35.0
34	34.2	36.7	36.9	35.8	36.4	35.8	35.8	35.0	35.6	34.2
35	36.7	37.5	37.5	38.3	37.5	36.7	33.1	35.8	33.1	36.4
37	36.9	39.2	36.7	36.7	36.7	35.8	36.4	35.8	36.7	35.8
38	37.5	38.6	38.3	33.3	34.4	33.3	34.4	33.3	32.8	33.9
39	33.3	38.1	32.5	37.5	31.1	37.5	30.6	36.9	30.0	36.7
43	39.4	35.0	40.0	34.2	34.4	34.2	35.0	34.2	34.2	33.3
46	35.8	39.2	35.0	37.5	36.7	35.8	36.1	35.8	35.8	35.8
47	34.2	36.7	36.1	36.1	36.4	35.3	35.8	35.3	35.0	35.0
49	31.7	36.7	38.3	37.5	37.5	36.7	36.7	35.8	35.8	35.8
50	35.0	37.5	35.8	35.8	35.8	35.0	40.0	35.0	39.2	34.2
51	34.7	38.1	34.2	36.7	31.4	37.2	32.8	36.1	39.2	34.2
52	35.6	34.4	35.8	35.0	35.8	35.3	35.8	35.0	35.3	35.0

53	34.2	35.3	35.0	35.8	35.0	35.0	35.0	34.2	40.8	34.2
55	37.5	40.0	38.1	37.5	38.1	37.5	37.5	36.7	35.8	35.8
57	36.4	38.9	37.2	38.3	35.8	36.7	35.8	35.8	35.8	35.0
58	37.5	37.5	36.7	35.8	35.8	35.8	35.3	35.3	35.0	35.0
59	35.3	39.2	31.7	37.2	36.7	36.7	36.7	35.8	35.8	35.6
60	31.7	38.3	34.7	35.8	35.8	35.3	35.8	35.6	35.8	35.3
61	38.3	37.5	38.6	36.7	36.4	35.8	35.8	35.8	35.8	35.8
62	33.1	35.8	35.8	35.8	36.1	35.0	35.0	34.4	34.2	34.2
63	34.7	35.0	35.0	35.8	35.0	35.0	34.2	34.2	34.2	33.3
64	33.3	37.5	34.7	36.1	35.3	35.0	34.2	34.4	33.9	34.2
67	38.1	40.0	35.8	36.7	35.8	35.0	35.8	35.0	35.8	36.7
68	35.6	39.2	35.6	41.4	36.7	36.7	35.8	36.7	35.8	35.8
69	33.6	32.8	33.6	33.3	30.6	35.0	35.8	35.8	35.0	35.8
70	36.7	35.8	36.1	35.0	35.0	34.4	33.3	34.2	32.5	33.9
71	35.6	35.8	35.8	35.8	35.8	35.6	35.0	35.0	34.2	34.7
72	39.4	34.2	39.2	33.3	36.1	36.7	35.8	35.8	35.0	35.0
74	31.9	38.6	34.2	36.4	35.3	35.6	34.4	34.4	32.8	33.9
75	33.3	38.3	34.2	36.4	34.7	34.7	34.2	34.4	34.2	34.4
76	36.4	35.0	37.8	35.3	30.6	35.3	34.4	34.7	34.2	34.2
77	35.6	35.8	35.0	35.0	34.2	35.0	33.9	34.2	33.3	33.6

IC implicit time (ms) from Rings 1 to 5 in children

Ring	Ring 1		Ring 2		Ring 3		Ring 4		Ring 5	
Contrast (%)	**49**	**96**	**49**	**96**	**49**	**96**	**49**	**96**	**49**	**96**
Subject no.										
1	36.2	38.4	38.4	37.6	38.4	37.0	38.1	36.5	38.4	35.6
2	37.0	35.9	30.6	35.3	29.5	33.4	31.5	32.6	26.5	32.0
3	37.8	39.0	37.0	37.3	36.2	36.2	35.3	35.1	34.5	34.2
6	39.0	38.1	37.6	37.0	36.7	36.5	36.2	36.2	35.3	35.6
8	36.5	36.5	35.9	35.9	34.2	34.2	33.4	32.8	32.6	32.3
9	37.6	38.4	37.3	36.2	40.9	34.8	42.6	33.7	42.3	33.4
11	37.6	38.7	35.9	36.7	35.3	35.1	34.2	34.2	36.2	32.8
13	38.1	38.7	37.6	37.3	36.7	36.7	36.2	36.2	35.6	35.6
14	33.1	39.2	37.0	37.3	37.6	35.6	40.9	34.5	39.8	34.0
17	37.6	36.7	37.0	35.9	36.2	35.3	35.6	34.8	35.1	34.5
18	37.8	34.2	36.5	34.0	35.9	34.5	35.6	34.8	35.6	34.2
19	35.1	37.8	36.2	36.7	37.3	34.8	35.9	34.8	38.1	33.4
20	37.3	36.2	39.8	34.5	39.5	33.1	37.3	32.6	37.0	32.3
23	43.4	38.4	42.3	38.4	37.0	37.6	37.8	33.7	39.0	32.3
26	39.8	37.6	35.6	31.2	36.5	27.6	36.5	27.0	36.2	27.8
28	41.5	35.1	41.7	35.1	40.6	36.5	38.1	35.1	37.8	34.0
29	40.9	37.6	38.4	38.1	38.1	37.6	37.3	37.6	37.0	37.6
31	38.7	38.4	39.0	30.1	40.3	29.2	39.5	28.4	39.8	28.4
32	37.3	37.6	36.5	36.2	35.3	34.8	34.8	34.2	34.0	34.2
33	36.7	34.0	44.0	29.5	38.7	29.2	37.3	28.1	37.0	27.0
34	38.1	36.2	42.6	35.9	34.8	35.1	34.8	34.2	39.5	33.4
35	39.2	38.4	37.6	36.7	37.6	35.3	36.7	35.1	40.6	34.8
37	39.8	38.4	38.1	36.7	37.0	35.6	36.5	35.1	35.9	34.8
38	41.2	40.3	40.9	35.3	37.6	34.5	37.3	33.1	42.8	32.6
39	38.7	38.4	38.1	37.6	36.7	36.5	36.7	36.2	37.0	35.9
43	34.5	37.0	35.1	35.9	35.1	34.2	38.7	33.4	38.4	32.8
46	38.1	38.4	37.8	36.7	36.7	35.6	36.5	34.8	35.3	34.0
47	37.3	34.8	37.0	35.1	35.6	34.5	35.3	34.0	32.8	33.1
49	40.6	38.7	37.0	37.6	36.5	36.5	35.9	35.6	36.5	34.8
50	41.5	37.8	36.2	35.9	35.6	34.5	34.8	34.2	34.0	33.7
51	39.2	36.5	36.5	36.7	37.8	35.6	38.4	34.2	35.9	34.0
52	37.8	36.7	36.2	36.2	35.3	35.3	35.1	34.8	34.5	34.2

53	38.4	36.7	37.3	35.9	37.0	34.5	37.8	33.4	37.0	32.8
55	38.4	38.7	38.1	37.6	36.5	37.0	36.2	36.2	35.9	35.3
57	37.3	38.7	36.7	36.7	37.0	35.3	36.5	34.5	40.9	33.7
58	36.2	37.6	37.6	36.5	37.8	35.3	38.7	34.8	35.3	34.0
59	35.1	39.0	36.7	36.7	36.2	35.6	36.2	34.8	39.0	34.2
60	37.0	36.5	36.5	35.9	35.9	35.3	35.6	34.8	35.6	34.8
61	36.7	37.8	37.0	36.7	35.9	35.9	35.1	34.8	34.5	34.5
62	39.2	31.7	40.1	29.5	39.8	34.8	38.7	34.2	38.4	34.0
63	39.8	37.6	39.5	35.1	39.8	34.0	40.1	33.1	34.0	32.6
64	36.7	37.0	36.7	35.6	35.6	34.2	34.2	32.8	31.5	32.6
67	38.4	35.1	38.7	35.1	39.5	34.8	39.8	34.2	39.2	34.2
68	39.2	39.0	40.9	37.3	37.6	36.2	37.3	35.6	38.4	34.5
69	38.4	37.3	38.4	36.2	39.5	35.9	39.8	35.3	40.1	34.5
70	37.0	37.0	35.3	35.1	40.1	33.7	40.6	32.6	42.3	32.0
71	39.5	37.3	37.6	36.5	36.7	35.3	35.6	34.2	33.7	33.7
72	36.7	37.3	36.7	36.7	35.6	35.6	34.8	34.8	33.4	34.5
74	37.3	37.6	37.0	36.7	34.0	34.8	33.4	34.0	33.1	33.1
75	36.7	37.3	35.9	35.9	34.8	34.8	34.0	34.0	33.7	33.4
76	38.1	34.5	37.6	36.2	35.9	35.3	39.2	34.5	39.2	33.7
77	35.3	35.1	35.3	34.5	34.5	34.0	34.0	33.1	37.3	32.6

Adults

Subject no.	Refractive error (D)	Axial length (mm)
A21	-3.25	25.55
A23	-3.75	24.70
A24	-5.00	25.02
A25	-2.63	23.64
A26	-0.88	25.38
A27	-0.13	24.49
A28	-0.25	23.29
A29	-5.38	23.91
A30	-1.63	23.47
A31	-0.13	22.83
A33	-2.25	23.36
A32	-0.13	22.89
A35	-1.50	23.64
A36	-2.38	25.33
A37	-3.00	25.38
A38	-2.00	23.87
A39	-2.25	23.48
A40	-5.50	26.21
A41	-4.13	26.66

DC implicit time (ms) from Rings 1 to 5 in adults

Ring	Ring 1		Ring 2		Ring 3		Ring 4		Ring 5	
Contrast (%)	**49**	**96**	**49**	**96**	**49**	**96**	**49**	**96**	**49**	**96**
Subject no.										
A21	38.6	38.3	37.8	37.8	36.7	36.7	35.8	35.6	35.0	35.0
A23	38.3	36.7	36.9	35.8	36.7	35.8	36.1	35.8	36.4	36.4
A24	35.0	35.8	36.4	34.2	35.0	34.2	34.2	33.9	33.9	34.2
A25	39.2	37.2	39.7	39.2	38.9	37.5	40.8	36.7	36.4	36.4
A26	36.9	36.7	36.7	36.7	35.8	35.0	34.4	34.2	34.2	35.0
A27	33.3	38.3	32.5	37.2	31.4	36.1	35.8	35.6	35.8	35.3
A28	34.7	36.9	34.4	35.8	34.2	35.0	34.2	35.0	34.2	35.0
A29	35.0	35.0	36.7	35.0	36.1	35.8	35.8	35.8	35.8	35.0
A30	36.4	36.9	28.1	36.7	34.4	35.6	34.2	35.0	34.2	34.2
A31	34.2	35.8	35.0	35.8	35.8	35.8	35.8	35.6	35.6	35.0
A33	37.5	35.0	36.1	35.3	36.1	35.8	35.8	35.8	35.8	35.8
A32	35.0	35.0	35.0	34.2	34.4	34.2	34.7	34.2	34.2	34.2
A35	35.6	39.2	36.7	37.5	35.8	35.0	35.0	35.0	35.0	35.3
A36	36.9	35.8	34.2	36.7	36.7	36.7	36.7	36.7	35.8	36.7
A37	35.8	35.8	35.8	35.8	36.1	35.0	34.2	34.4	34.2	34.2
A38	38.3	35.8	36.7	35.8	35.6	35.8	35.3	35.0	35.0	35.0
A39	32.5	34.2	33.6	34.2	34.2	35.0	34.2	35.0	34.2	35.0
A40	33.9	36.9	35.3	36.4	36.4	37.5	36.9	36.9	36.7	36.4
A41	35.6	38.9	38.1	38.3	38.1	38.1	37.5	37.5	37.5	37.5

IC implicit time (ms) from Rings 1 to 5 in adults

Ring	Ring 1		Ring 2		Ring 3		Ring 4		Ring 5	
Contrast (%)	**49**	**96**	**49**	**96**	**49**	**96**	**49**	**96**	**49**	**96**
Subject no.										
A21	39.0	39.2	38.4	38.4	37.8	36.7	35.3	35.3	34.8	34.5
A23	37.6	37.8	36.7	36.5	36.2	35.9	36.2	35.9	36.7	35.6
A24	37.8	39.2	34.5	35.3	33.7	34.2	33.4	33.7	34.2	33.4
A25	35.1	42.6	34.5	36.7	30.1	36.2	29.2	35.1	31.5	34.5
A26	37.8	36.7	39.0	35.9	38.1	35.1	40.6	34.2	42.6	34.2
A27	37.8	37.6	37.0	37.0	35.9	36.2	35.3	35.3	34.8	34.8
A28	37.6	38.1	36.2	37.3	35.1	35.6	34.2	34.8	33.7	34.2
A29	33.1	38.7	32.6	37.6	38.1	36.2	39.8	35.3	34.8	34.8
A30	32.6	40.3	33.4	40.3	35.9	40.9	37.8	40.6	38.1	40.6
A31	38.7	39.2	37.3	37.8	35.9	36.5	35.1	35.9	34.2	35.3
A33	30.6	38.7	37.0	36.7	36.2	35.9	35.3	35.6	35.1	35.3
A32	37.0	39.0	34.5	33.7	33.7	34.0	33.4	34.0	33.1	33.4
A35	37.8	39.2	36.7	34.8	35.3	34.8	34.8	34.2	34.0	34.0
A36	39.8	39.5	38.4	37.3	36.7	36.7	36.2	36.5	33.1	36.2
A37	39.5	35.6	35.1	35.6	34.5	34.2	39.0	34.0	40.1	33.4
A38	37.6	37.6	37.0	36.2	35.3	35.1	34.8	34.5	34.0	34.2
A39	37.3	37.0	36.2	36.5	34.8	35.3	34.0	34.5	33.4	34.0
A40	35.1	39.8	37.3	39.5	37.6	37.0	35.9	36.5	35.3	35.9
A41	37.8	40.1	37.8	37.8	37.6	37.3	37.3	37.0	39.5	36.5

Appendix E - Raw data of Experiment III

	1st visit		2nd visit	
Subject no.	**Refractive error (D)**	**Axial length (mm)**	**Refractive error (D)**	**Axial length (mm)**
1	-1.25	24.37	-1.50	24.54
3	-3.63	25.11	-3.88	25.42
6	-3.00	25.30	-4.13	25.77
7	0.50	23.21	0.00	23.43
8	-1.25	23.42	-1.50	23.82
9	-2.38	24.70	-3.00	25.04
13	-2.63	24.53	-2.88	24.61
14	-1.75	24.86	-2.25	25.17
16	0.25	23.89	0.25	24.08
17	-2.63	24.27	-3.13	24.57
18	-0.50	23.18	-1.13	23.41
20	-2.00	23.39	-2.13	23.52
23	-1.50	25.11	-2.25	25.34
26	-2.38	24.27	-3.75	24.66
28	-0.50	22.94	-0.75	23.19
29	0.00	24.37	-0.75	24.63
32	-2.13	23.80	-2.38	23.85
39	-2.63	24.75	-2.88	25.02
41	-6.50	26.07	-7.00	26.31
43	-2.00	24.45	-2.38	24.60
51	-4.75	25.66	-5.25	25.87
58	-4.75	24.60	-5.63	25.00
67	-0.75	24.75	-1.25	25.06
69	-3.50	24.91	-4.13	25.30
71	-2.50	24.01	-2.88	24.17
77	-1.50	23.40	-1.50	23.46

DC implicit time (ms) in the first visit

Ring	Ring 1		Ring 2		Ring 3		Ring 4		Ring 5	
Contrast (%)	**49**	**96**	**49**	**96**	**49**	**96**	**49**	**96**	**49**	**96**
Subject no.										
1	37.5	36.9	37.8	38.3	37.5	37.5	37.5	37.5	37.2	36.7
3	31.4	38.3	38.1	37.5	36.4	35.8	35.8	35.0	35.0	35.0
6	40.0	41.4	40.3	38.1	39.2	37.5	37.8	37.5	38.3	36.7
7	36.7	35.8	36.7	35.8	35.6	35.6	35.6	35.0	35.3	35.0
8	36.7	35.0	35.8	35.0	35.0	34.2	33.1	33.3	32.5	33.3
9	38.3	35.3	36.7	35.0	35.6	34.2	33.6	34.2	33.3	34.4
13	31.7	38.3	32.5	38.3	32.8	37.2	37.5	36.9	37.5	36.7
14	37.8	36.7	37.5	37.2	36.4	36.7	34.7	35.0	34.2	34.7
16	34.2	36.9	33.9	33.9	33.3	35.0	33.9	34.2	36.1	34.2
17	36.9	36.1	37.2	36.7	37.5	36.1	36.7	35.3	35.0	35.0
18	38.3	32.8	36.7	33.6	35.8	34.7	35.8	35.0	33.6	34.2
20	30.0	39.2	34.4	34.7	34.2	34.7	34.2	34.2	33.3	34.2
23	36.7	36.9	37.5	35.8	41.7	33.3	42.5	34.2	42.5	34.2
26	33.6	33.6	33.9	33.6	38.9	37.5	36.7	36.7	36.7	35.8
28	33.9	36.7	32.5	35.0	35.0	35.0	35.3	35.6	35.0	35.0
29	34.7	35.8	37.5	35.0	38.9	34.2	38.3	33.3	32.5	32.5
32	37.5	35.0	38.1	35.8	36.1	35.8	35.6	35.0	35.0	35.0
39	33.3	38.1	32.5	37.5	31.1	37.5	30.6	36.9	30.0	36.7
41	33.6	38.9	33.1	38.3	31.9	35.6	31.9	36.7	32.2	33.3
43	39.4	35.0	40.0	34.2	34.4	34.2	35.0	34.2	34.2	33.9
51	34.7	38.1	34.2	36.7	31.4	37.2	32.8	36.1	39.2	34.2
58	37.5	32.5	36.7	35.8	35.8	35.8	35.3	35.0	35.0	35.0
67	38.1	36.4	35.8	36.7	35.8	35.8	35.8	35.0	35.8	35.8
69	33.6	38.3	33.6	37.5	30.6	36.9	35.8	35.8	35.0	35.0
71	35.6	35.8	35.8	35.8	35.8	35.6	35.0	35.0	34.2	34.7
77	35.6	35.8	35.0	35.0	34.2	35.0	33.9	34.2	33.3	34.2

IC implicit time (ms) in the first visit

Ring	Ring 1		Ring 2		Ring 3		Ring 4		Ring 5	
Contrast (%)	**49**	**96**	**49**	**96**	**49**	**96**	**49**	**96**	**49**	**96**
Subject no.										
1	36.2	38.4	38.4	37.8	38.4	37.0	38.1	36.5	38.4	35.6
3	37.8	39.0	37.0	37.3	36.2	35.9	35.3	34.8	34.5	34.2
6	39.0	37.3	37.6	36.7	36.7	36.7	36.2	36.2	35.3	35.6
7	38.1	37.6	37.0	35.6	34.8	34.5	34.2	34.0	34.5	33.7
8	36.5	36.5	35.9	35.9	34.2	34.2	33.4	33.1	32.6	32.3
9	37.6	37.6	37.3	36.7	40.9	34.8	42.6	33.7	42.3	33.4
13	38.1	38.4	37.6	37.3	36.7	36.7	36.2	36.2	35.6	35.6
14	33.1	39.5	37.0	37.0	37.6	35.6	40.9	34.5	39.8	34.0
16	34.5	37.6	36.2	38.7	37.6	37.0	37.6	34.8	37.8	34.0
17	37.6	36.7	37.0	35.9	36.2	35.3	35.6	34.8	35.1	34.5
18	37.8	34.0	36.5	35.1	35.9	34.2	35.6	34.5	35.6	34.2
20	37.3	36.2	39.8	34.2	39.5	33.1	37.3	32.6	37.0	32.3
23	43.4	38.4	42.3	38.4	37.0	37.8	37.8	38.4	39.0	32.6
26	35.4	36.7	35.6	30.9	36.5	27.0	36.5	36.5	36.2	37.6
28	41.5	35.1	41.7	35.1	40.6	36.5	38.1	35.1	37.8	34.0
29	40.9	37.8	38.4	37.6	38.1	37.6	37.3	37.6	37.0	37.6
32	37.3	37.6	36.5	36.2	35.3	34.8	34.8	34.2	34.0	34.0
39	38.7	38.7	38.1	37.6	36.7	36.5	36.7	36.2	37.0	35.9
41	35.1	35.9	36.7	35.9	36.5	34.2	37.0	32.6	35.6	32.6
43	34.5	37.0	35.1	35.9	35.1	34.2	38.7	33.4	38.4	32.8
51	39.2	36.5	36.5	36.7	37.8	35.6	38.4	34.2	35.9	34.0
58	36.2	37.8	37.6	36.5	37.8	35.3	38.7	34.8	35.3	34.0
67	38.4	35.1	38.7	35.1	39.5	34.8	39.8	34.5	39.2	34.0
69	38.4	33.4	38.4	36.2	39.5	35.9	39.8	35.1	40.1	34.2
71	39.5	37.3	37.6	36.5	36.7	35.3	35.6	34.2	33.7	33.7
77	35.3	35.1	35.3	34.5	34.5	34.0	34.0	33.1	37.3	32.6

DC amplitude (nV/deg^2) in the first visit

Ring	Ring 1		Ring 2		Ring 3		Ring 4		Ring 5	
Contrast (%)	**49**	**96**	**49**	**96**	**49**	**96**	**49**	**96**	**49**	**96**
Subject no.										
1	21.3	60.7	16.8	22.5	13.0	13.1	8.3	9.6	3.0	8.4
3	42.7	56.5	15.1	28.3	9.3	15.3	6.8	14.3	6.7	10.6
6	85.8	30.6	23.2	18.1	7.2	10.8	5.7	8.4	3.1	6.6
7	35.1	62.6	13.6	40.5	12.0	20.4	9.1	15.7	7.7	10.6
8	50.4	65.5	25.1	31.3	11.3	17.4	5.1	11.0	4.7	9.0
9	64.5	64.0	18.6	24.7	8.3	15.5	5.5	13.6	6.0	10.6
13	46.9	67.2	20.7	30.4	8.5	16.5	10.1	13.2	7.7	7.9
14	30.6	67.5	14.5	36.5	4.6	12.1	2.5	9.7	4.0	6.5
16	29.7	23.7	9.7	19.9	4.8	10.8	2.1	5.5	2.9	5.6
17	39.8	48.5	21.6	31.8	14.8	20.3	7.2	15.8	6.1	10.9
18	58.8	85.4	21.9	31.6	8.8	9.0	9.2	10.0	1.2	11.0
20	68.0	52.5	12.2	30.1	16.9	22.9	11.1	19.6	9.1	11.7
23	55.0	49.7	21.2	21.1	9.3	13.7	7.4	10.1	4.0	5.6
26	80.5	68.3	30.3	23.8	10.5	23.6	6.5	15.2	6.9	13.3
28	29.7	58.5	13.0	23.4	5.8	13.9	4.9	13.4	4.9	10.0
29	33.1	57.5	14.1	30.0	7.2	15.4	3.1	10.7	5.0	8.3
32	32.4	63.8	11.1	32.4	8.1	16.8	9.3	14.3	7.5	10.8
39	45.3	69.1	8.1	33.1	5.5	17.3	3.8	12.0	4.2	9.1
41	25.3	25.0	10.4	10.9	6.1	4.5	3.1	4.6	2.5	5.9
43	25.1	45.7	10.7	24.3	6.2	14.6	3.9	9.1	3.6	6.4
51	40.1	38.3	13.4	15.7	6.6	13.2	5.1	5.5	3.9	4.6
58	35.2	54.9	18.8	24.1	7.5	21.3	5.6	13.5	5.9	8.6
67	37.9	42.6	13.9	32.3	9.1	15.1	6.6	8.9	3.9	6.2
69	24.7	89.6	11.3	42.2	4.9	16.0	4.7	9.5	4.1	6.5
71	44.6	64.4	29.9	32.9	13.5	19.9	7.4	17.3	7.1	11.7
77	19.9	37.4	18.3	25.0	12.2	19.1	6.8	11.4	6.2	8.1

IC amplitude (nV/deg^2) in the first visit

Ring	Ring 1		Ring 2		Ring 3		Ring 4		Ring 5	
Contrast (%)	**49**	**96**	**49**	**96**	**49**	**96**	**49**	**96**	**49**	**96**
Subject no.										
1	12.3	30.9	8.7	25.8	3.4	14.8	3.2	6.7	3.0	3.1
3	20.4	53.3	18.8	38.8	10.6	28.0	5.3	19.8	6.7	13.4
6	51.6	25.6	10.4	18.6	7.2	17.2	1.3	14.2	3.1	8.7
7	33.4	50.3	13.5	21.6	7.8	15.0	4.9	13.8	7.7	7.3
8	20.0	75.3	10.9	35.9	4.6	18.0	2.6	14.0	4.7	8.9
9	16.2	109.7	4.9	43.2	6.4	15.7	2.5	10.3	6.0	6.9
13	38.8	54.3	17.1	26.6	6.0	22.8	3.2	13.7	7.7	7.3
14	15.2	46.6	1.7	11.3	3.7	10.3	1.6	8.1	4.0	5.9
16	34.5	24.6	10.2	10.0	5.4	1.6	3.0	2.2	2.9	3.1
17	28.3	51.3	13.3	43.9	6.8	26.6	2.4	15.2	6.1	9.2
18	11.3	81.7	9.0	13.1	8.8	8.8	2.9	7.7	1.2	4.8
20	16.7	83.7	8.9	25.8	3.5	19.3	1.7	13.1	9.1	6.4
23	34.4	16.1	7.7	5.2	6.8	6.3	2.9	4.7	4.0	2.2
26	56.2	45.1	11.5	9.9	14.7	12.5	6.0	4.1	6.9	3.2
28	20.8	7.7	5.8	6.0	3.4	4.3	2.1	1.6	4.9	2.1
29	9.5	17.5	11.3	3.5	9.0	7.1	6.2	4.3	5.0	1.1
32	20.5	34.0	12.5	29.9	6.6	20.9	2.6	16.7	7.5	10.0
39	24.8	73.0	5.3	31.5	9.6	25.3	5.8	14.8	4.2	8.3
41	12.6	13.9	12.7	6.4	2.8	2.7	3.5	5.3	2.5	5.1
43	12.7	40.7	11.4	13.9	3.0	12.4	3.1	11.9	3.6	8.4
51	14.8	45.0	7.5	19.4	6.3	8.5	2.5	6.5	3.9	2.4
58	18.5	17.2	16.6	19.2	9.5	15.8	1.5	9.4	5.9	6.4
67	7.5	45.6	4.9	27.7	3.2	14.1	0.9	9.2	3.9	5.3
69	48.2	26.6	14.6	25.5	4.0	16.3	2.9	6.6	4.1	4.2
71	6.1	57.8	0.8	30.2	2.8	24.3	0.6	15.0	7.1	10.0
77	26.3	54.0	14.4	37.5	9.3	23.3	5.0	11.2	6.2	6.8

DC implicit time (ms) in the second visit

Ring	Ring 1		Ring 2		Ring 3		Ring 4		Ring 5	
Contrast (%)	49	96	49	96	49	96	49	96	49	96
Subject no.										
1	37.2	33.9	37.2	34.2	36.9	35.6	36.1	36.7	35.8	37.8
3	38.3	37.5	38.3	36.7	35.8	35.8	35.0	35.3	35.0	34.7
6	38.6	33.1	38.3	36.7	39.4	37.5	36.4	36.7	36.1	37.2
7	35.3	36.9	35.8	36.7	35.8	35.8	35.8	35.3	35.6	35.0
8	38.3	35.8	36.7	35.8	35.0	34.2	34.2	33.9	33.3	33.3
9	34.7	35.8	33.6	35.8	33.3	35.0	33.3	35.0	33.6	35.0
13	36.7	32.5	37.2	32.8	37.8	37.2	37.2	36.7	36.4	35.8
14	35.0	39.2	35.8	37.5	37.2	36.7	35.6	35.8	36.1	35.8
16	35.8	37.8	36.1	38.6	36.1	33.9	35.8	33.9	30.0	35.0
17	38.1	38.3	38.3	37.5	37.5	36.4	36.4	35.8	35.8	35.0
18	39.7	34.4	35.6	35.3	36.4	35.6	36.1	35.0	36.1	35.0
20	36.7	36.1	37.2	35.3	35.8	35.0	34.7	35.0	34.7	35.0
23	36.9	37.5	36.7	36.7	36.4	35.8	35.6	35.8	33.3	34.2
26	39.7	35.0	39.4	37.2	26.7	36.7	37.5	36.7	36.7	36.1
28	34.2	35.0	34.7	35.0	35.0	35.0	35.0	34.2	34.7	33.9
29	38.1	35.0	34.4	35.0	34.2	34.2	33.9	33.3	33.1	32.2
32	34.2	33.3	33.9	33.3	34.7	34.7	35.0	35.6	34.7	35.6
39	28.3	35.8	27.2	36.7	27.2	36.7	32.5	36.7	33.3	36.7
41	40.0	35.8	39.2	35.8	34.2	35.0	33.1	34.4	32.8	34.7
43	36.1	35.8	35.8	35.8	35.6	35.3	35.0	34.7	34.4	34.2
51	34.4	42.2	32.8	42.2	33.9	42.2	34.2	42.5	34.2	34.2
58	34.2	33.3	34.2	36.7	36.1	35.8	35.6	35.8	35.0	35.8
67	31.7	36.7	36.7	35.8	35.8	35.6	35.8	35.0	35.6	35.0
69	37.5	39.4	37.2	38.6	36.7	36.4	36.1	36.1	35.0	35.8
71	31.7	35.8	35.3	35.8	35.8	35.8	35.0	35.8	35.0	35.8
77	29.7	35.8	36.7	35.8	36.1	35.6	35.6	35.0	35.0	34.4

IC implicit time (ms) in the second visit

Ring	Ring 1		Ring 2		Ring 3		Ring 4		Ring 5	
Contrast (%)	49	96	49	96	49	96	49	96	49	96
Subject no.										
1	39.0	36.2	35.9	35.3	35.9	35.3	36.2	34.8	36.2	35.1
3	37.8	37.6	36.7	36.7	35.9	35.9	35.3	35.1	35.9	34.0
6	39.0	33.4	38.7	32.0	40.3	30.1	41.2	29.8	39.5	29.2
7	37.3	35.9	35.9	35.9	35.1	35.1	34.8	34.5	35.3	34.0
8	38.7	36.5	37.3	35.3	35.3	34.0	33.1	33.4	32.3	32.6
9	37.8	38.7	36.7	37.0	35.9	35.1	40.6	34.0	39.5	33.7
13	38.4	37.8	37.6	37.0	37.0	36.7	36.7	35.9	36.5	35.1
14	36.2	39.5	37.0	37.8	36.7	36.5	36.5	35.6	40.1	35.1
16	40.6	34.0	35.6	30.9	38.1	29.8	39.0	28.4	38.7	33.7
17	37.8	38.4	37.0	36.2	37.0	35.6	39.5	35.1	38.7	34.8
18	37.0	37.3	36.5	35.9	36.2	35.1	36.2	34.8	38.1	34.2
20	39.2	36.2	36.2	34.8	33.7	34.2	33.4	33.7	32.8	33.7
23	38.7	38.1	37.6	36.7	36.2	35.3	40.6	34.2	41.5	33.7
26	37.4	42.3	37.6	37.3	37.6	36.5	38.7	35.9	40.3	35.6
28	35.6	33.4	35.1	34.8	35.1	34.2	34.5	33.7	39.2	32.8
29	39.2	30.3	37.3	35.6	39.5	32.0	40.1	31.7	32.8	30.9
32	38.4	38.1	39.0	36.5	39.5	35.9	38.7	35.1	38.7	34.8
39	42.8	37.8	37.6	36.7	36.7	35.9	36.7	35.6	35.9	35.9
41	35.9	37.8	36.7	37.6	36.5	34.2	37.3	34.0	34.5	32.6
43	37.3	36.5	35.6	35.6	34.8	34.5	34.5	34.0	34.8	33.7
51	36.7	34.5	36.5	35.9	37.0	35.9	37.3	35.3	38.1	35.1
58	38.4	37.3	38.1	36.5	38.7	35.6	40.9	35.3	40.3	34.5
67	37.0	36.7	35.9	36.2	34.8	35.1	34.5	34.5	32.0	34.5
69	36.7	38.1	38.4	36.7	37.8	35.9	40.1	35.3	38.7	34.8
71	40.3	36.7	40.9	36.2	35.3	35.9	35.1	35.1	33.4	34.5
77	35.6	36.2	35.9	35.6	34.8	34.8	34.2	34.2	39.0	33.7

DC amplitude (nV/deg^2) in the second visit

Ring	Ring 1		Ring 2		Ring 3		Ring 4		Ring 5	
Contrast (%)	**49**	**96**	**49**	**96**	**49**	**96**	**49**	**96**	**49**	**96**
Subject no.										
1	18.3	30.2	9.0	9.4	4.5	4.6	4.2	3.2	4.5	3.3
3	38.8	55.3	11.8	24.1	8.3	14.7	7.3	9.3	3.8	6.7
6	21.8	15.7	9.2	8.0	3.6	4.6	3.4	5.7	2.1	5.6
7	12.9	30.1	10.9	26.8	8.1	20.6	6.3	12.6	4.9	10.2
8	32.1	35.5	13.9	17.4	8.0	12.9	6.3	10.0	3.2	7.1
9	24.2	42.3	11.1	27.1	5.6	12.7	4.0	9.6	4.5	7.1
13	68.6	75.7	24.3	33.4	12.0	15.1	9.2	10.9	6.8	9.3
14	30.0	38.8	14.8	19.8	7.6	14.0	4.2	9.7	3.5	6.8
16	20.1	20.2	6.5	8.4	2.3	5.7	1.8	4.0	0.5	3.2
17	21.7	54.4	17.5	22.3	11.8	15.7	7.9	14.0	7.1	10.8
18	46.0	30.1	6.1	11.6	5.4	10.6	5.5	10.1	4.8	6.6
20	12.8	38.2	7.6	13.6	5.5	8.3	6.8	10.4	3.9	7.7
23	18.8	36.2	14.7	18.9	8.8	10.6	4.5	6.4	3.0	6.1
26	20.6	12.4	6.7	11.6	8.0	14.2	6.4	10.3	5.1	7.1
28	30.2	52.4	21.9	20.4	11.1	12.8	7.2	9.8	5.0	6.9
29	16.7	41.6	11.6	21.4	7.7	13.2	7.3	9.6	5.2	6.9
32	13.2	16.1	5.3	11.5	5.0	7.5	2.9	5.7	2.7	4.5
39	39.9	75.8	11.7	25.3	6.9	12.5	5.1	11.1	4.8	10.0
41	41.2	37.2	14.9	13.7	6.7	8.2	4.7	5.8	3.3	5.2
43	33.7	38.0	20.5	22.4	9.8	13.6	6.8	11.1	4.5	7.1
51	19.3	43.7	5.9	18.1	5.8	12.6	5.9	5.7	3.3	3.8
58	42.8	52.7	14.3	24.0	9.4	15.3	6.2	9.5	3.6	8.3
67	42.2	101.9	23.1	52.0	11.8	22.8	6.0	11.3	4.9	6.4
69	39.8	44.3	21.4	16.3	11.5	15.7	6.4	9.5	4.1	6.3
71	56.6	55.1	26.6	30.5	14.7	16.9	7.6	10.6	3.3	7.5
77	43.1	71.6	14.3	48.5	15.8	31.4	13.0	18.3	8.5	13.0

IC amplitude (nV/deg^2) in the second visit

Ring	Ring 1		Ring 2		Ring 3		Ring 4		Ring 5	
Contrast (%)	**49**	**96**	**49**	**96**	**49**	**96**	**49**	**96**	**49**	**96**
Subject no.										
1	8.0	20.9	3.2	9.4	3.4	4.6	1.9	3.2	1.2	3.3
3	24.6	26.9	9.7	24.1	5.2	14.7	2.4	9.3	0.2	6.7
6	13.3	12.4	4.3	8.0	1.9	4.6	0.5	5.7	0.5	5.6
7	3.4	24.1	4.6	26.8	7.0	20.6	4.3	12.6	2.0	10.2
8	15.4	23.2	4.2	17.4	1.7	12.9	2.0	10.0	2.4	7.1
9	29.6	74.9	11.6	27.1	1.8	12.7	0.6	9.6	1.5	7.1
13	15.6	38.8	16.3	33.4	10.7	15.1	1.9	10.9	1.0	9.3
14	4.5	12.7	6.8	19.8	4.1	14.0	0.1	9.7	0.3	6.8
16	18.4	15.8	2.5	8.4	1.1	5.7	1.1	4.0	1.1	3.2
17	23.2	34.9	15.1	22.3	7.2	15.7	4.4	14.0	1.9	10.8
18	21.8	48.4	17.7	11.6	11.6	10.6	2.6	10.1	1.9	6.6
20	13.2	33.9	2.4	13.6	7.8	8.3	6.5	10.4	3.9	7.7
23	10.1	15.8	4.8	18.9	2.5	10.6	1.5	6.4	0.8	6.1
26	6.2	20.7	0.7	11.6	5.2	14.2	4.4	10.3	1.8	7.1
28	14.5	7.7	11.1	20.4	5.2	12.8	2.4	9.8	0.5	6.9
29	13.5	30.0	6.0	21.4	0.4	13.2	0.1	9.6	0.5	6.9
32	12.5	6.0	7.2	11.5	1.9	7.5	0.4	5.7	0.7	4.5
39	26.4	16.0	8.7	25.3	4.5	12.5	1.2	11.1	1.3	10.0
41	19.4	12.0	6.6	13.7	4.4	8.2	0.2	5.8	0.6	5.2
43	47.1	40.5	13.1	22.4	5.3	13.6	4.2	11.1	0.2	7.1
51	14.5	37.1	7.3	18.1	6.8	12.6	4.3	5.7	2.2	3.8
58	0.6	18.1	7.2	24.0	4.2	15.3	2.5	9.5	0.3	8.3
67	16.6	69.1	11.4	52.0	6.8	22.8	4.1	11.3	3.8	6.4
69	19.3	80.9	13.5	16.3	8.4	15.7	4.3	9.5	2.2	6.3
71	31.2	54.8	6.0	30.5	6.6	16.9	1.5	10.6	3.7	7.5
77	50.3	86.8	24.4	48.5	9.8	31.4	2.6	18.3	1.9	13.0

REFERENCES

Abbott, C.J., Grunert, U., Pianta, M.J., and McBrien, N.A. (2011). Retinal thinning in tree shrews with induced high myopia: optical coherence tomography and histological assessment. *Vision Research, 51*, 376-385.

Akiba, J. (1993). Prevalence of posterior vitreous detachment in high myopia. *Ophthalmology, 100*, 1384-1388.

Anstice, N.S., and Phillips, J.R. (2011). Effect of dual-focus soft contact lens wear on axial myopia progression in children. *Ophthalmology, 118*, 1152-1161.

Aung, T., Foster, P.J., Seah, S.K., Chan, S.P., Lim, W.K., Wu, H.M., Lim, A.T., Lee, L.L., and Chew, S.J. (2001). Automated static perimetry: the influence of myopia and its method of correction. *Ophthalmology, 108*, 290-295.

Baker, B.J., and Pruett, R. (2004). Degenerative myopia, in: Yanoff, M., Duker, J.S., and Augsburger, J.J. (Eds.), *Ophthalmology*. Mosby, St. Louis, MO, pp. 934-937.

Bearse, M.A., Jr., Shimada, Y., and Sutter, E.E. (2000). Distribution of oscillatory components in the central retina. *Documenta Ophthalmologica, 100*, 185-205.

Bearse, M.A., and Sutter, E.E. (1998). Contrast dependence of multifocal ERG components, in: *Vision Science and its Applications: 1998 OSA Technical Digest Series*, 1. Optical Society of America Washington, D.C., pp. 24-27.

Bearse, M.A., Sutter, E.E., Smith, D.N., and Rose, S.J. (1995). Early detection of macular dysfunction in the topography of the electroretinogram, in: *Vision Science and its Applications: summaries of the papers presented at the topical meeting, February 3-7, 1995, Santa Fe, New Mexico*. Optical Society of America, Washington, D.C., pp. 318-321.

Beresford, J.A., Crewther, S.G., and Crewther, D.P. (1998). Anatomical correlates of experimentally induced myopia. *Australian and New Zealand Journal of Ophthalmology, 26 Suppl 1*, S84-87.

Bitzer, M., Feldkaemper, M., and Schaeffel, F. (2000). Visually induced changes in components of the retinoic acid system in fundal layers of the chick. *Experimental Eye Research, 70*, 97-106.

Bitzer, M., and Schaeffel, F. (2002). Defocus-induced changes in ZENK expression in the chicken retina. *Investigative Ophthalmology and Visual Science, 43*, 246-252.

Blach, R.K., Jay, B., and Kolb, H. (1966). Electrical activity of the eye in high myopia. *The British Journal of Ophthalmology, 50*, 629-641.

Bradley, D.V., Fernandes, A., Lynn, M., Tigges, M., and Boothe, R.G. (1999). Emmetropization in the rhesus monkey (Macaca mulatta): birth to young adulthood. *Investigative Ophthalmology and Visual Science, 40*, 214-229.

Brown, B., and Yap, M.K. (1996). Contrast and luminance as parameters defining the output of the VERIS topographical ERG. *Ophthalmic and Physiological Optics, 16*, 42-48.

Buck, C., Schaeffel, F., Simon, P., and Feldkaemper, M. (2004). Effects of positive and negative lens treatment on retinal and choroidal glucagon and glucagon receptor mRNA levels in the chicken. *Investigative Ophthalmology and Visual Science, 45*, 402-409.

Buehren, T., Iskander, D.R., Collins, M.J., and Davis, B. (2007). Potential higher-order aberration cues for sphero-cylindrical refractive error development. *Optometry and Vision Science, 84*, 163-174.

Bui, B.V., and Fortune, B. (2004). Ganglion cell contributions to the rat full-field electroretinogram. *The Journal of Physiology, 555*, 153-173.

Campbell, M.C., Kisilak, M., Hunter, J.J., Bueno, J.M., King, D., and Irving, E.L. (2002). Optical aberrations of the eye and eye growth: Why aberrations may be important to understanding refractive error development. *Journal of Vision, 2*, 111.

Carkeet, A., Luo, H.D., Tong, L., Saw, S.M., and Tan, D.T. (2002). Refractive error and monochromatic aberrations in Singaporean children. *Vision Research, 42*, 1809-1824.

Chan, H.H. (2005). Detection of glaucomatous damage using multifocal ERG. *Clinical and Experimental Optometry, 88*, 410-414.

Chan, H.L., and Brown, B. (1998). Investigation of retinitis pigmentosa using the multifocal electroretinogram. *Ophthalmic and Physiological Optics, 18*, 335-350.

Chan, H.L., and Mohidin, N. (2003). Variation of multifocal electroretinogram with axial length. *Ophthalmic and Physiological Optics, 23*, 133-140.

Chan, H.L., and Siu, A.W. (2003). Effect of optical defocus on multifocal ERG responses. *Clinical and Experimental Optometry, 86*, 317-322.

Chang, M.A., Congdon, N.G., Bykhovskaya, I., Munoz, B., and West, S.K. (2005). The association between myopia and various subtypes of lens opacity: SEE (Salisbury Eye Evaluation) project. *Ophthalmology, 112*, 1395-1401.

Chen, J.C., Brown, B., and Schmid, K.L. (2006a). Delayed mfERG responses in myopia. *Vision Research, 46*, 1221-1229.

Chen, J.C., Brown, B., and Schmid, K.L. (2006b). Evaluation of inner retinal

function in myopia using oscillatory potentials of the multifocal electroretinogram. *Vision Research, 46*, 4096-4103.

Chen, J.F., Elsner, A.E., Burns, S.A., Hansen, R.M., Lou, P.L., Kwong, K.K., and Fulton, A.B. (1992). The effect of eye shape on retinal responses. *Clinical Vision Sciences, 7*, 521-530.

Chen, P.C., Woung, L.C., and Yang, C.F. (2000). Modulation transfer function and critical flicker frequency in high-myopia patients. *Journal of the Formosan Medical Association, 99*, 45-48.

Cheng, S.C., Lam, C.S., and Yap, M.K. (2010). Retinal thickness in myopic and non-myopic eyes. *Ophthalmic and Physiological Optics, 30*, 776-784.

Cheng, X., Bradley, A., Hong, X., and Thibos, L.N. (2003). Relationship between refractive error and monochromatic aberrations of the eye. *Optometry and Vision Science, 80*, 43-49.

Chew, S.J., and Ritch, R. (1994). Parental history and myopia: taking the long view. *The Journal of the American Medical Association, 272*, 1255; author reply 1256.

Chihara, E., and Sawada, A. (1990). Atypical nerve fiber layer defects in high myopes with high-tension glaucoma. *Archives of Ophthalmology, 108*, 228-232.

Cho, P., Cheung, S.W., and Edwards, M. (2005). The longitudinal orthokeratology research in children (LORIC) in Hong Kong: a pilot study on refractive changes and myopic control. *Current Eye Research, 30*, 71-80.

Choh, V., Lew, M.Y., Nadel, M.W., and Wildsoet, C.F. (2006). Effects of interchanging hyperopic defocus and form deprivation stimuli in normal and optic nerve-sectioned chicks. *Vision Research, 46*, 1070-1079.

Chu, P.H., Chan, H.H., and Brown, B. (2006). Glaucoma detection is facilitated by luminance modulation of the global flash multifocal electroretinogram. *Investigative Ophthalmology and Visual Science, 47*, 929-937.

Chu, P.H., Chan, H.H., Ng, Y.F., Brown, B., Siu, A.W., Beale, B.A., Gilger, B.C., and Wong, F. (2008). Porcine global flash multifocal electroretinogram: possible mechanisms for the glaucomatous changes in contrast response function. *Vision Research, 48*, 1726-1734.

Chui, T.Y., Song, H., and Burns, S.A. (2008). Individual variations in human cone photoreceptor packing density: variations with refractive error. *Investigative Ophthalmology and Visual Science, 49*, 4679-4687.

Chui, T.Y., Yap, M.K., Chan, H.H., and Thibos, L.N. (2005). Retinal stretching limits peripheral visual acuity in myopia. *Vision Research, 45*, 593-605.

Coletta, N.J., and Watson, T. (2006). Effect of myopia on visual acuity measured with laser interference fringes. *Vision Research, 46*, 636-651.

Collins, M.J., Wildsoet, C.F., and Atchison, D.A. (1995). Monochromatic aberrations and myopia. *Vision Research, 35*, 1157-1163.

Crewther, S.G., and Crewther, D.P. (2003). Inhibition of retinal ON/OFF systems differentially affects refractive compensation to defocus. *Neuroreport, 14*, 1233-1237.

Curcio, C.A., and Allen, K.A. (1990). Topography of ganglion cells in human retina. *The Journal of Comparative Neurology, 300*, 5-25.

Deller, J.F., O'Connor, A.D., and Sorsby, A. (1947). X-ray measurement of the diameters of the living eye. *Proceedings of the Royal Society of Medicine, 134*, 456-467.

Diether, S., and Schaeffel, F. (1997). Local changes in eye growth induced by imposed local refractive error despite active accommodation. *Vision Research, 37*, 659-668.

Edwards, M.H. (1999). The development of myopia in Hong Kong children between the ages of 7 and 12 years: a five-year longitudinal study. *Ophthalmic and Physiological Optics, 19*, 286-294.

Edwards, M.H., and Lam, C.S. (2004). The epidemiology of myopia in Hong Kong. *Annals of the Academy of Medicine, Singapore, 33*, 34-38.

Feldkaemper, M.P., Wang, H.Y., and Schaeffel, F. (2000). Changes in retinal and choroidal gene expression during development of refractive errors in chicks. *Investigative Ophthalmology and Visual Science, 41*, 1623-1628.

Fischer, A.J., McGuire, J.J., Schaeffel, F., and Stell, W.K. (1999). Light- and focus-dependent expression of the transcription factor ZENK in the chick retina. *Nature Neuroscience, 2*, 706-712.

Fischer, A.J., Seltner, R.L., Poon, J., and Stell, W.K. (1998a). Immunocytochemical characterization of quisqualic acid- and N-methyl-D-aspartate-induced excitotoxicity in the retina of chicks. *The Journal of Comparative Neurology, 393*, 1-15.

Fischer, A.J., Seltner, R.L., and Stell, W.K. (1997). N-methyl-D-aspartate-induced excitotoxicity causes myopia in hatched chicks. *Canadian Journal of Ophthalmology, 32*, 373-377.

Fischer, A.J., Seltner, R.L., and Stell, W.K. (1998b). Opiate and N-methyl-D-aspartate receptors in form-deprivation myopia. *Visual Neuroscience, 15*, 1089-1096.

Fortune, B., Bearse, M.A., Jr., Cioffi, G.A., and Johnson, C.A. (2002). Selective loss of an oscillatory component from temporal retinal multifocal ERG

responses in glaucoma. *Investigative Ophthalmology and Visual Science, 43*, 2638-2647.

Fujikado, T., Hosohata, J., and Omoto, T. (1996). ERG of form deprivation myopia and drug induced ametropia in chicks. *Current Eye Research, 15*, 79-86.

Fujikado, T., Kawasaki, Y., Suzuki, A., Ohmi, G., and Tano, Y. (1997). Retinal function with lens-induced myopia compared with form-deprivation myopia in chicks. *Graefe's Aarchive for Clinical and Experimental Ophthalmology, 235*, 320-324.

Gee, S.S., and Tabbara, K.F. (1988). Increase in ocular axial length in patients with corneal opacification. *Ophthalmology, 95*, 1276-1278.

Gottlieb, M.D., Fugate-Wentzek, L.A., and Wallman, J. (1987). Different visual deprivations produce different ametropias and different eye shapes. *Investigative Ophthalmology and Visual Science, 28*, 1225-1235.

Graham, B., and Judge, S.J. (1999). The effects of spectacle wear in infancy on eye growth and refractive error in the marmoset (Callithrix jacchus). *Vision Research, 39*, 189-206.

Guo, S.S., Sivak, J.G., Callender, M.G., and Diehl-Jones, B. (1995). Retinal dopamine and lens-induced refractive errors in chicks. *Current Eye Research, 14*, 385-389.

Gurevich, L., and Slaughter, M.M. (1993). Comparison of the waveforms of the ON bipolar neuron and the b-wave of the electroretinogram. *Vision Research, 33*, 2431-2435.

He, J.C., Sun, P., Held, R., Thorn, F., Sun, X., and Gwiazda, J.E. (2002). Wavefront aberrations in eyes of emmetropic and moderately myopic school children and young adults. *Vision Research, 42*, 1063-1070.

He, M., Zeng, J., Liu, Y., Xu, J., Pokharel, G.P., and Ellwein, L.B. (2004). Refractive error and visual impairment in urban children in southern china. *Investigative Ophthalmology and Visual Science, 45*, 793-799.

Henson, D.B., and Hobley, A.J. (1986). Frequency distribution of early glaucomatous visual field defects. *American Journal of Optometry and Physiological Optics, 63*, 455-461.

Hidajat, R., McLay, J., Burley, C., Elder, M., Morton, J., and Goode, D. (2003). Influence of axial length of normal eyes on PERG. *Documenta Ophthalmologica, 107*, 195-200.

Hodos, W., and Kuenzel, W.J. (1984). Retinal-image degradation produces ocular enlargement in chicks. *Investigative Ophthalmology and Visual Science, 25*, 652-659.

Hood, D.C. (2000). Assessing retinal function with the multifocal technique. *Progress in Retinal and Eye Research, 19*, 607-646.

Hood, D.C., and Birch, D.G. (1993). Human cone receptor activity: the leading edge of the a-wave and models of receptor activity. *Visual Neuroscience, 10*, 857-871.

Hood, D.C., and Birch, D.G. (1995). Phototransduction in human cones measured using the alpha-wave of the ERG. *Vision Research, 35*, 2801-2810.

Hood, D.C., Frishman, L.J., Saszik, S., and Viswanathan, S. (2002). Retinal origins of the primate multifocal ERG: implications for the human response. *Investigative Ophthalmology and Visual Science, 43*, 1673-1685.

Hood, D.C., Greenstein, V., Frishman, L., Holopigian, K., Viswanathan, S., Seiple, W., Ahmed, J., and Robson, J.G. (1999). Identifying inner retinal contributions to the human multifocal ERG. *Vision Research, 39*, 2285-2291.

Hood, D.C., Holopigian, K., Greenstein, V., Seiple, W., Li, J., Sutter, E.E., and Carr, R.E. (1998). Assessment of local retinal function in patients with retinitis pigmentosa using the multi-focal ERG technique. *Vision Research, 38*, 163-179.

Hood, D.C., Seiple, W., Holopigian, K., and Greenstein, V. (1997). A comparison of the components of the multifocal and full-field ERGs. *Visual Neuroscience, 14*, 533-544.

Hoogerheide, J., Rempt, F., and Hoogenboom, W.P. (1971). Acquired myopia in young pilots. *Ophthalmologica, 163*, 209-215.

Howlett, M.H., and McFadden, S.A. (2006). Form-deprivation myopia in the guinea pig (Cavia porcellus). *Vision Research, 46*, 267-283.

Howlett, M.H., and McFadden, S.A. (2007). Emmetropization and schematic eye models in developing pigmented guinea pigs. *Vision Research, 47*, 1178-1190.

Howlett, M.H., and McFadden, S.A. (2009). Spectacle lens compensation in the pigmented guinea pig. *Vision Research, 49*, 219-227.

Hoyt, C.S., Stone, R.D., Fromer, C., and Billson, F.A. (1981). Monocular axial myopia associated with neonatal eyelid closure in human infants. *American Journal of Ophthalmology, 91*, 197-200.

Hung, L.F., Crawford, M.L., and Smith, E.L. (1995). Spectacle lenses alter eye growth and the refractive status of young monkeys. *Nature Medicine, 1*, 761-765.

Ip, J.M., Huynh, S.C., Robaei, D., Kifley, A., Rose, K.A., Morgan, I.G., Wang, J.J., and Mitchell, P. (2008). Ethnic differences in refraction and ocular

biometry in a population-based sample of 11-15-year-old Australian children. *Eye (London, England), 22*, 649-656.

Irving, E.L., Sivak, J.G., and Callender, M.G. (1992). Refractive plasticity of the developing chick eye. *Ophthalmic and Physiological Optics, 12*, 448-456.

Jaeken, B., and Artal, P. (2012). Optical quality of emmetropic and myopic eyes in the periphery measured with high-angular resolution. *Investigative Ophthalmology and Visual Science, 53*, 3405-3413.

Jaworski, A., Gentle, A., Zele, A.J., Vingrys, A.J., and McBrien, N.A. (2006). Altered visual sensitivity in axial high myopia: a local postreceptoral phenomenon? *Investigative Ophthalmology and Visual Science, 47*, 3695-3702.

Jobke, S., Kasten, E., and Vorwerk, C. (2008). The prevalence rates of refractive errors among children, adolescents, and adults in Germany. *Clinical Ophthalmology (Auckland, N.Z), 2*, 601-607.

Kawabata, H., and Adachi-Usami, E. (1997). Multifocal electroretinogram in myopia. *Investigative Ophthalmology and Visual Science, 38*, 2844-2851.

Kirby, A.W., Sutton, L., and Weiss, H. (1982). Elongation of cat eyes following neonatal lid suture. *Investigative Ophthalmology and Visual Science, 22*, 274-277.

Kolb, H., and Dekorver, L. (1991). Midget ganglion cells of the parafovea of the human retina: a study by electron microscopy and serial section reconstructions. *The Journal of Comparative Neurology, 303*, 617-636.

Kolb, H., Linberg, K.A., and Fisher, S.K. (1992). Neurons of the human retina: a Golgi study. *The Journal of Comparative Neurology, 318*, 147-187.

Kolb, H., and Marshak, D. (2003). The midget pathways of the primate retina. *Documenta Ophthalmologica, 106*, 67-81.

Kondo, M., and Sieving, P.A. (2002). Post-photoreceptoral activity dominates primate photopic 32-Hz ERG for sine-, square-, and pulsed stimuli. *Investigative Ophthalmology and Visual Science, 43*, 2500-2507.

Kretschmann, U., Ruther, K., Usui, T., and Zrenner, E. (1996). ERG campimetry using a multi-input stimulation technique for mapping of retinal function in the central visual field. *Ophthalmic Research, 28*, 303-311.

Kwan, W.C., Yip, S.P., and Yap, M.K. (2009). Monochromatic aberrations of the human eye and myopia. *Clinical and Experimental Optometry, 92*, 304-312.

Lam, B.L. (2005). Electrophysiology of vision: clinical testing and applications, Taylor & Francis, Boca Raton, Fla. pp 1-64.

Lam, C.S., Edwards, M., Millodot, M., and Goh, W.S. (1999). A 2-year

longitudinal study of myopia progression and optical component changes among Hong Kong schoolchildren. *Optometry and Vision Science, 76*, 370-380.

Lam, C.S., Goh, W.S., Tang, Y.K., Tsui, K.K., Wong, W.C., and Man, T.C. (1994). Changes in refractive trends and optical components of Hong Kong Chinese aged over 40 years. *Ophthalmic and Physiological Optics, 14*, 383-388.

Lam, C.S., Lam, C.H., Cheng, S.C., and Chan, L.Y. (2012). Prevalence of myopia among Hong Kong Chinese schoolchildren: changes over two decades. *Ophthalmic and Physiological Optics, 32*, 17-24.

Lam, D.S., Leung, K.S., Mohamed, S., Chan, W.M., Palanivelu, M.S., Cheung, C.Y., Li, E.Y., Lai, R.Y., and Leung, C.K. (2007). Regional variations in the relationship between macular thickness measurements and myopia. *Investigative Ophthalmology and Visual Science, 48*, 376-382.

Liang, C.L., Yen, E., Su, J.Y., Liu, C., Chang, T.Y., Park, N., Wu, M.J., Lee, S., Flynn, J.T., and Juo, S.H. (2004). Impact of family history of high myopia on level and onset of myopia. *Investigative Ophthalmology and Visual Science, 45*, 3446-3452.

Lim, M.C., Hoh, S.T., Foster, P.J., Lim, T.H., Chew, S.J., Seah, S.K., and Aung, T. (2005). Use of optical coherence tomography to assess variations in macular retinal thickness in myopia. *Investigative Ophthalmology and Visual Science, 46*, 974-978.

Lin, L.L., Shih, Y.F., Lee, Y.C., Hung, P.T., and Hou, P.K. (1996). Changes in ocular refraction and its components among medical students--a 5-year longitudinal study. *Optometry and Vision Science, 73*, 495-498.

Lin, Z., Martinez, A., Chen, X., Li, L., Sankaridurg, P., Holden, B.A., and Ge, J. (2010). Peripheral defocus with single-vision spectacle lenses in myopic children. *Optometry and Vision Science, 87*, 4-9.

Liou, S.W., and Chiu, C.J. (2001). Myopia and contrast sensitivity function. *Current Eye Research, 22*, 81-84.

Liu, Y., and Wildsoet, C. (2011). The effect of two-zone concentric bifocal spectacle lenses on refractive error development and eye growth in young chicks. *Investigative Ophthalmology and Visual Science, 52*, 1078-1086.

Llorente, L., Barbero, S., Cano, D., Dorronsoro, C., and Marcos, S. (2004). Myopic versus hyperopic eyes: axial length, corneal shape and optical aberrations. *Journal of Vision, 4*, 288-298.

Lung, J.C., and Chan, H.H. (2010). Effects of luminance combinations on the characteristics of the global flash multifocal electroretinogram (mfERG).

Graefe's Aarchive for Clinical and Experimental Ophthalmology, 248, 1117-1125.

Luo, H.D., Gazzard, G., Fong, A., Aung, T., Hoh, S.T., Loon, S.C., Healey, P., Tan, D.T., Wong, T.Y., and Saw, S.M. (2006). Myopia, axial length, and OCT characteristics of the macula in Singaporean children. *Investigative Ophthalmology and Visual Science, 47*, 2773-2781.

Luu, C.D., Foulds, W.S., and Tan, D.T. (2007). Features of the multifocal electroretinogram may predict the rate of myopia progression in children. *Ophthalmology, 114*, 1433-1438.

Luu, C.D., Lau, A.M., and Lee, S.Y. (2006). Multifocal electroretinogram in adults and children with myopia. *Archives of Ophthalmology, 124*, 328-334.

Maguire, P., and Vine, A.K. (1986). Geographic atrophy of the retinal pigment epithelium. *American Journal of Ophthalmology, 102*, 621-625.

Mantyjarvi, M., and Tuppurainen, K. (1995). Colour vision and dark adaptation in high myopia without central retinal degeneration. *The British Journal of Ophthalmology, 79*, 105-108.

Marmor, M.F., Fulton, A.B., Holder, G.E., Miyake, Y., Brigell, M., and Bach, M. (2009). ISCEV Standard for full-field clinical electroretinography (2008 update). *Documenta Ophthalmologica, 118*, 69-77.

Marsh-Tootle, W.L., and Norton, T.T. (1989). Refractive and structural measures of lid-suture myopia in tree shrew. *Investigative Ophthalmology and Visual Science, 30*, 2245-2257.

Mayer, D.L., Hansen, R.M., Moore, B.D., Kim, S., and Fulton, A.B. (2001). Cycloplegic refractions in healthy children aged 1 through 48 months. *Archives of Ophthalmology, 119*, 1625-1628.

McFadden, S.A. (2002). Partial Occlusion Produces Local Form Deprivation Myopia in the Guinea Pig Eye. *Investigative Ophthalmology and Visual Science, 43*, ARVO E-Abstract 189.

McFadden, S.A., and Wildsoet, C. (2009). Mammalian Eyes Need an Intact Optic Nerve to Detect the Sign of Defocus During Emmetropisation. *Investigative Ophthalmology and Visual Science, 50*, ARVO E-Abstract 1620.

McLellan, J.S., Marcos, S., and Burns, S.A. (2001). Age-related changes in monochromatic wave aberrations of the human eye. *Investigative Ophthalmology and Visual Science, 42*, 1390-1395.

Mertz, J.R., Howlett, M.H., McFadden, S., and Wallman, J. (1999). Retinoic acid from both the retina and choroid influences eye growth. *Investigative Ophthalmology and Visual Science, 40 (suppl.)*, ARVO Abstract 4473.

Meyer, C., Mueller, M.F., Duncker, G.I., and Meyer, H.J. (1999). Experimental animal myopia models are applicable to human juvenile-onset myopia. *Survey of ophthalmology, 44 Suppl 1*, S93-102.

Miller, R.F., and Dowling, J.E. (1970). Intracellular responses of the Muller (glial) cells of mudpuppy retina: their relation to b-wave of the electroretinogram. *Journal of Neurophysiology, 33*, 323-341.

Millodot, M. (1981). Effect of ametropia on peripheral refraction. *American Journal of Optometry and Physiological Optics, 58*, 691-695.

Mitchell, P., Hourihan, F., Sandbach, J., and Wang, J.J. (1999). The relationship between glaucoma and myopia: the Blue Mountains Eye Study. *Ophthalmology, 106*, 2010-2015.

Mojumder, D.K., Sherry, D.M., and Frishman, L.J. (2008). Contribution of voltage-gated sodium channels to the b-wave of the mammalian flash electroretinogram. *The Journal of Physiology, 586*, 2551-2580.

Morita, H., Funata, M., and Tokoro, T. (1995). A clinical study of the development of posterior vitreous detachment in high myopia. *Retina (Philadelphia, Pa), 15*, 117-124.

Mutti, D.O., Hayes, J.R., Mitchell, G.L., Jones, L.A., Moeschberger, M.L., Cotter, S.A., Kleinstein, R.N., Manny, R.E., Twelker, J.D., and Zadnik, K. (2007). Refractive error, axial length, and relative peripheral refractive error before and after the onset of myopia. *Investigative Ophthalmology and Visual Science, 48*, 2510-2519.

Mutti, D.O., Sholtz, R.I., Friedman, N.E., and Zadnik, K. (2000). Peripheral refraction and ocular shape in children. *Investigative Ophthalmology and Visual Science, 41*, 1022-1030.

Nathan, J., Kiely, P.M., Crewther, S.G., and Crewther, D.P. (1985). Disease-associated visual image degradation and spherical refractive errors in children. *American Journal of Optometry and Physiological Optics, 62*, 680-688.

Newman, E.A., and Odette, L.L. (1984). Model of electroretinogram b-wave generation: a test of the K+ hypothesis. *Journal of Neurophysiology, 51*, 164-182.

Ng, Y.F., Chan, H.H., Chu, P.H., Siu, A.W., To, C.H., Beale, B.A., Gilger, B.C., and Wong, F. (2008a). Pharmacologically defined components of the normal porcine multifocal ERG. *Documenta Ophthalmologica, 116*, 165-176.

Ng, Y.F., Chan, H.H., To, C.H., and Yap, M.K. (2008b). The characteristics of multifocal electroretinogram in isolated perfused porcine eye: cellular

contributions to the in vitro porcine mfERG. *Documenta Ophthalmologica, 117*, 205-214.

Norton, T.T., Essinger, J.A., and McBrien, N.A. (1994). Lid-suture myopia in tree shrews with retinal ganglion cell blockade. *Visual Neuroscience, 11*, 143-153.

Norton, T.T., and McBrien, N.A. (1992). Normal development of refractive state and ocular component dimensions in the tree shrew (Tupaia belangeri). *Vision Research, 32*, 833-842.

Norton, T.T., and Siegwart, J.T., Jr. (1995). Animal models of emmetropization: matching axial length to the focal plane. *Journal of the American Optometric Association, 66*, 405-414.

Ostadimoghaddam, H., Fotouhi, A., Hashemi, H., Yekta, A., Heravian, J., Rezvan, F., Ghadimi, H., Rezvan, B., and Khabazkhoob, M. (2012). Prevalence of the refractive errors by age and gender: the Mashhad eye study of Iran. *Clinical and Experimental Ophthalmology, 39*, 743-751.

Pacella, R., McLellan, J., Grice, K., Del Bono, E.A., Wiggs, J.L., and Gwiazda, J.E. (1999). Role of genetic factors in the etiology of juvenile-onset myopia based on a longitudinal study of refractive error. *Optometry and Vision Science, 76*, 381-386.

Palmowski, A.M., Allgayer, R., and Heinemann-Vemaleken, B. (2000). The multifocal ERG in open angle glaucoma--a comparison of high and low contrast recordings in high- and low-tension open angle glaucoma. *Documenta Ophthalmologica, 101*, 35-49.

Palmowski, A.M., Berninger, T., Allgayer, R., Andrielis, H., Heinemann-Vernaleken, B., and Rudolph, G. (1999). Effects of refractive blur on the multifocal electroretinogram. *Documenta Ophthalmologica, 99*, 41-54.

Paquin, M.P., Hamam, H., and Simonet, P. (2002). Objective measurement of optical aberrations in myopic eyes. *Optometry and Vision Science, 79*, 285-291.

Penn, R.D., and Hagins, W.A. (1969). Signal transmission along retinal rods and the origin of the electroretinographic a-wave. *Nature, 223*, 201-204.

Perlman, I., Meyer, E., Haim, T., and Zonis, S. (1984). Retinal function in high refractive error assessed electroretinographically. *The British Journal of Ophthalmology, 68*, 79-84.

Pierro, L., Camesasca, F.I., Mischi, M., and Brancato, R. (1992). Peripheral retinal changes and axial myopia. *Retina (Philadelphia, Pa), 12*, 12-17.

Rabbetts, R.B. (2007). Anisometropia and aniseikonia, 4th ed.

Elsevier/Butterworth Heinemann, Edinburgh. pp 275-285.

Rabin, J., Van Sluyters, R.C., and Malach, R. (1981). Emmetropization: a vision-dependent phenomenon. *Investigative Ophthalmology and Visual Science, 20*, 561-564.

Read, S.A., Collins, M.J., and Sander, B.P. (2010). Human optical axial length and defocus. *Investigative Ophthalmology and Visual Science, 51*, 6262-6269.

Rezvan, F., Khabazkhoob, M., Fotouhi, A., Hashemi, H., Ostadimoghaddam, H., Heravian, J., Azizi, E., Khorasani, A.A., and Yekta, A.A. (2012). Prevalence of refractive errors among school children in Northeastern Iran. *Ophthalmic and Physiological Optics, 32*, 25-30.

Rohrer, B., Schaeffel, F., and Zrenner, E. (1992). Longitudinal chromatic aberration and emmetropization: results from the chicken eye. *The Journal of Physiology, 449*, 363-376.

Rose, K., Smith, W., Morgan, I., and Mitchell, P. (2001). The increasing prevalence of myopia: implications for Australia. *Clinical and Experimental Ophthalmology, 29*, 116-120.

Rucker, F.J., and Wallman, J. (2009). Chick eyes compensate for chromatic simulations of hyperopic and myopic defocus: evidence that the eye uses longitudinal chromatic aberration to guide eye-growth. *Vision Research, 49*, 1775-1783.

Rudnicka, A.R., and Edgar, D.F. (1995). Automated static perimetry in myopes with peripapillary crescents--Part I. *Ophthalmic and Physiological Optics, 15*, 409-412.

Rudnicka, A.R., and Edgar, D.F. (1996). Automated static perimetry in myopes with peripapillary crescents--Part II. *Ophthalmic and Physiological Optics, 16*, 416-429.

Rudnicka, A.R., Owen, C.G., Nightingale, C.M., Cook, D.G., and Whincup, P.H. (2010). Ethnic differences in the prevalence of myopia and ocular biometry in 10- and 11-year-old children: the Child Heart and Health Study in England (CHASE). *Investigative Ophthalmology and Visual Science, 51*, 6270-6276.

Sankaridurg, P., Donovan, L., Varnas, S., Ho, A., Chen, X., Martinez, A., Fisher, S., Lin, Z., Smith, E.L., 3rd, Ge, J., and Holden, B. (2010). Spectacle lenses designed to reduce progression of myopia: 12-month results. *Optometry and Vision Science, 87*, 631-641.

Sankaridurg, P., Holden, B., Smith, E., 3rd, Naduvilath, T., Chen, X., de la Jara, P.L., Martinez, A., Kwan, J., Ho, A., Frick, K., and Ge, J. (2011). Decrease

in rate of myopia progression with a contact lens designed to reduce relative peripheral hyperopia: one-year results. *Investigative Ophthalmology and Visual Science, 52*, 9362-9367.

Sarks, J.P., Sarks, S.H., and Killingsworth, M.C. (1988). Evolution of geographic atrophy of the retinal pigment epithelium. *Eye (London, England), 2*, 552-577.

Saw, S.M., Gazzard, G., Shih-Yen, E.C., and Chua, W.H. (2005). Myopia and associated pathological complications. *Ophthalmic and Physiological Optics, 25*, 381-391.

Schaeffel, F., and Diether, S. (1999). The growing eye: an autofocus system that works on very poor images. *Vision Research, 39*, 1585-1589.

Schaeffel, F., Glasser, A., and Howland, H.C. (1988). Accommodation, refractive error and eye growth in chickens. *Vision Research, 28*, 639-657.

Schaeffel, F., Troilo, D., Wallman, J., and Howland, H.C. (1990). Developing eyes that lack accommodation grow to compensate for imposed defocus. *Visual Neuroscience, 4*, 177-183.

Schippert, R., and Schaeffel, F. (2006). Peripheral defocus does not necessarily affect central refractive development. *Vision Research, 46*, 3935-3940.

Schmid, G.F. (2003). Variability of retinal steepness at the posterior pole in children 7-15 years of age. *Current Eye Research, 27*, 61-68.

Schmid, K.L., and Wildsoet, C.F. (1996). Effects on the compensatory responses to positive and negative lenses of intermittent lens wear and ciliary nerve section in chicks. *Vision Research, 36*, 1023-1036.

Schmid, K.L., and Wildsoet, C.F. (1997). Contrast and spatial-frequency requirements for emmetropization in chicks. *Vision Research, 37*, 2011-2021.

Seeliger, M.W., Kretschmann, U.H., Apfelstedt-Sylla, E., and Zrenner, E. (1998). Implicit time topography of multifocal electroretinograms. *Investigative Ophthalmology and Visual Science, 39*, 718-723.

Seidemann, A., and Schaeffel, F. (2002). Effects of longitudinal chromatic aberration on accommodation and emmetropization. *Vision Research, 42*, 2409-2417.

Seidemann, A., Schaeffel, F., Guirao, A., Lopez-Gil, N., and Artal, P. (2002). Peripheral refractive errors in myopic, emmetropic, and hyperopic young subjects. *Journal of the Optical Society of America. A, Optics, image science, and vision, 19*, 2363-2373.

Shen, W., Vijayan, M., and Sivak, J.G. (2005). Inducing form-deprivation myopia in fish. *Investigative Ophthalmology and Visual Science, 46*, 1797-1803.

Sherman, S.M., Norton, T.T., and Casagrande, V.A. (1977). Myopia in the lid-sutured tree shrew (Tupaia glis). *Brain Research, 124*, 154-157.

Shimada, Y., Bearse, M.A., Jr., and Sutter, E.E. (2005). Multifocal electroretinograms combined with periodic flashes: direct responses and induced components. *Graefe's Aarchive for Clinical and Experimental Ophthalmology, 243*, 132-141.

Shimada, Y., Li, Y., Bearse, M.A., Jr., Sutter, E.E., and Fung, W. (2001). Assessment of early retinal changes in diabetes using a new multifocal ERG protocol. *The British Journal of Ophthalmology, 85*, 414-419.

Sieving, P.A., Murayama, K., and Naarendorp, F. (1994). Push-pull model of the primate photopic electroretinogram: a role for hyperpolarizing neurons in shaping the b-wave. *Visual Neuroscience, 11*, 519-532.

Smith, E.L., 3rd (1998). Spectacle lenses and emmetropization: the role of optical defocus in regulating ocular development. *Optometry and Vision Science, 75*, 388-398.

Smith, E.L., 3rd, Bradley, D.V., Fernandes, A., and Boothe, R.G. (1999). Form deprivation myopia in adolescent monkeys. *Optometry and Vision Science, 76*, 428-432.

Smith, E.L., 3rd, and Hung, L.F. (1999). The role of optical defocus in regulating refractive development in infant monkeys. *Vision Research, 39*, 1415-1435.

Smith, E.L., 3rd, and Hung, L.F. (2000). Form-deprivation myopia in monkeys is a graded phenomenon. *Vision Research, 40*, 371-381.

Smith, E.L., 3rd, Hung, L.F., and Harwerth, R.S. (1994). Effects of optically induced blur on the refractive status of young monkeys. *Vision Research, 34*, 293-301.

Smith, E.L., 3rd, Hung, L.F., and Huang, J. (2009). Relative peripheral hyperopic defocus alters central refractive development in infant monkeys. *Vision Research, 49*, 2386-2392.

Smith, E.L., 3rd, Hung, L.F., Huang, J., Blasdel, T.L., Humbird, T.L., and Bockhorst, K.H. (2010). Effects of optical defocus on refractive development in monkeys: evidence for local, regionally selective mechanisms. *Investigative Ophthalmology and Visual Science, 51*, 3864-3873.

Smith, E.L., 3rd, Kee, C.S., Ramamirtham, R., Qiao-Grider, Y., and Hung, L.F. (2005). Peripheral vision can influence eye growth and refractive development in infant monkeys. *Investigative Ophthalmology and Visual Science, 46*, 3965-3972.

Smith, E.L., 3rd, Ramamirtham, R., Qiao-Grider, Y., Hung, L.F., Huang, J., Kee,

C.S., Coats, D., and Paysse, E. (2007). Effects of foveal ablation on emmetropization and form-deprivation myopia. *Investigative Ophthalmology and Visual Science, 48*, 3914-3922.

Stockton, R.A., and Slaughter, M.M. (1989). B-wave of the electroretinogram. A reflection of ON bipolar cell activity. *The Journal of General Physiology, 93*, 101-122.

Stone, R.A., and Flitcroft, D.I. (2004). Ocular shape and myopia. *Annals of the Academy of Medicine, Singapore, 33*, 7-15.

Subbaram, M.V., and Bullimore, M.A. (2002). Visual acuity and the accuracy of the accommodative response. *Ophthalmic and Physiological Optics, 22*, 312-318.

Sutter, E. (2000). The interpretation of multifocal binary kernels. *Documenta Ophthalmologica, 100*, 49-75.

Sutter, E.E., Shimada, Y., Li, Y., and Bearse, M.A. (1999). Mapping inner retinal function through enhancement of adaptation components in the M-ERG, in: *Vision Science and its Applications: 1999 OSA Technical Digest Series*. Optical Society of America, Washington, DC, pp. 52-55.

Sutter, E.E., and Tran, D. (1992). The field topography of ERG components in man--I. The photopic luminance response. *Vision Research, 32*, 433-446.

Tejedor, J., and de la Villa, P. (2003). Refractive changes induced by form deprivation in the mouse eye. *Investigative Ophthalmology and Visual Science, 44*, 32-36.

Thibos, L.N., Cheng, X., Phillips, J., and Collins, A. (2002). Optical Aberrations of Chick Eyes. *Investigative Ophthalmology and Visual Science, 43*, ARVO E-Abstract 180.

Troilo, D., Gottlieb, M.D., and Wallman, J. (1987). Visual deprivation causes myopia in chicks with optic nerve section. *Current Eye Research, 6*, 993-999.

Troilo, D., and Judge, S.J. (1993). Ocular development and visual deprivation myopia in the common marmoset (Callithrix jacchus). *Vision Research, 33*, 1311-1324.

Tse, D.Y., and To, C.H. (2011). Graded competing regional myopic and hyperopic defocus produce summated emmetropization set points in chick. *Investigative Ophthalmology and Visual Science, 52*, 8056-8062.

Vera-Diaz, F.A., McGraw, P.V., Strang, N.C., and Whitaker, D. (2005). A psychophysical investigation of ocular expansion in human eyes. *Investigative Ophthalmology and Visual Science, 46*, 758-763.

von Noorden, G.K., and Lewis, R.A. (1987). Ocular axial length in unilateral

congenital cataracts and blepharoptosis. *Investigative Ophthalmology and Visual Science, 28,* 750-752.

Wachtmeister, L. (1998). Oscillatory potentials in the retina: what do they reveal. *Progress in Retinal and Eye Research, 17,* 485-521.

Wallman, J., Adams, J.I., and Trachtman, J.N. (1981). The eyes of young chickens grow toward emmetropia. *Investigative Ophthalmology and Visual Science, 20,* 557-561.

Wallman, J., Gottlieb, M.D., Rajaram, V., and Fugate-Wentzek, L.A. (1987). Local retinal regions control local eye growth and myopia. *Science (New York, N.Y.), 237,* 73-77.

Wallman, J., Turkel, J., and Trachtman, J. (1978). Extreme myopia produced by modest change in early visual experience. *Science (New York, N.Y.), 201,* 1249-1251.

Westall, C.A., Dhaliwal, H.S., Panton, C.M., Sigesmun, D., Levin, A.V., Nischal, K.K., and Heon, E. (2001). Values of electroretinogram responses according to axial length. *Documenta Ophthalmologica, 102,* 115-130.

Wiesel, T.N., and Raviola, E. (1977). Myopia and eye enlargement after neonatal lid fusion in monkeys. *Nature, 266,* 66-68.

Wildsoet, C. (2003). Neural pathways subserving negative lens-induced emmetropization in chicks--insights from selective lesions of the optic nerve and ciliary nerve. *Current Eye Research, 27,* 371-385.

Wildsoet, C.F., and Pettigrew, J.D. (1988). Kainic acid-induced eye enlargement in chickens: differential effects on anterior and posterior segments. *Investigative Ophthalmology and Visual Science, 29,* 311-319.

Wolsley, C.J., Saunders, K.J., Silvestri, G., and Anderson, R.S. (2008). Investigation of changes in the myopic retina using multifocal electroretinograms, optical coherence tomography and peripheral resolution acuity. *Vision Research, 48,* 1554-1561.

Wong, T.Y., Foster, P.J., Johnson, G.J., and Seah, S.K. (2003). Refractive errors, axial ocular dimensions, and age-related cataracts: the Tanjong Pagar survey. *Investigative Ophthalmology and Visual Science, 44,* 1479-1485.

Wu, P.C., Chen, Y.J., Chen, C.H., Chen, Y.H., Shin, S.J., Yang, H.J., and Kuo, H.K. (2008). Assessment of macular retinal thickness and volume in normal eyes and highly myopic eyes with third-generation optical coherence tomography. *Eye (London, England), 22,* 551-555.

Wu, S.Y., Nemesure, B., and Leske, M.C. (1999). Refractive errors in a black adult population: the Barbados Eye Study. *Investigative Ophthalmology and Visual Science, 40,* 2179-2184.

Yap, M., Wu, M., Liu, Z.M., Lee, F.L., and Wang, S.H. (1993). Role of heredity in the genesis of myopia. *Ophthalmic and Physiological Optics, 13*, 316-319.

Yinon, U., Rose, L., and Shapiro, A. (1980). Myopia in the eye of developing chicks following monocular and binocular lid closure. *Vision Research, 20*, 137-141.

Zadnik, K. (1997). The Glenn A. Fry Award Lecture (1995). Myopia development in childhood. *Optometry and Vision Science, 74*, 603-608.

Zeng, G., and McFadden, S.A. (2010). Regional Variation in Susceptibility to Myopia From Partial Form Deprivation in the Guinea Pig. *Investigative Ophthalmology and Visual Science, 51*, ARVO E-Abstract 1736.

Zhong, X., Ge, J., Smith, E.L., 3rd, and Stell, W.K. (2004). Image defocus modulates activity of bipolar and amacrine cells in macaque retina. *Investigative Ophthalmology and Visual Science, 45*, 2065-2074.

Zhu, X., Park, T.W., Winawer, J., and Wallman, J. (2005). In a matter of minutes, the eye can know which way to grow. *Investigative Ophthalmology and Visual Science, 46*, 2238-2241.